Research and Development of Heat Pipe and Its Application to PC Cooling

March 2002

Masataka Mochizuki

Contents

Nomenclature

A	: Activation energy of the reaction	(J)
A_c	: Heat transfer area of condenser	(m^2)
A_e	: Heat transfer area of evaporator	(m^2)
A_0	: Accelerated factor	
A_p	: Footprint area of the heat sink base plate	(m^2)
A_s	: Footprint or contact area of the heat source	(m^2)
D_i	: Inside diameter of heat pipe	(m)
D_w	: Wire diameter	(m)
Δt	: Temperature difference, $= T_{el}-T_o$	(°C)
F	: Response parameter	
$F(T)$	: Shift factor	
h_c	: Heat transfer coefficient in condenser	($W/m^2 \cdot °C$)
h_e	: Heat transfer coefficient in evaporator	($W/m^2 \cdot °C$)
k	: Boltzmann's constant	(J/K)
k_b	: Thermal conductivity of the heat sink base plate	(W/m•°C)
K_{HP}	: Effective thermal conductivity of heat pipe	(W/m•°C)
K_0	: Heating time	(h)
L_{60}	: Predicted life time in case of operation at 60°C	(h)
L_a	: Length of adiabatic section	(m)
L_c	: Length of condenser	(m)
L_e	: Length of evaporator	(m)
L_{eff}	: Effective heat transfer distance	(m)
M	: Mass generation rate	(Kg/s)
N_b	: Number of bent corner	
N_l	: Wick layer number	
N_w	: Number of wire	
Q_{max}	: Maximum heat transfer rate	(W)
$Q_{max\text{-}fact}$	: Factor of maximum heat transfer rate	(W-m)
q_e	: Heat flux at evaporator of heat pipe	(W/m^2)
R_b	: Spreading thermal resistance of heat sink base plate	(°C/W)
R_c	: Thermal resistance of bent corner	(°C/W)
R_0	: Average heat sink thermal resistance	(°C/W)
R_{hp}	: Thermal resistance of heat pipe	(°C/W)
$R_{hp,t}$	: Total thermal resistance of MHP	(°C/W)
R_{sa}	: Thermal resistance between heat sink and ambient air	(°C/W)

R_t	: Total thermal resistance	(°C/W)
T	: Absolute temperature	(K)
t	: Time	(s)
T_{ain}	: Inlet temperature of cooling air	(°C)
t_b	: Thickness of heat sink base plate	(m)
T_{el}	: Elevated heating temperature	(°C)
T_{hpe}	: Evaporator temperature of heat pipe or vapor chamber	(°C)
T_o	: Normal operating temperature	(°C)
ΔT	: Temperature difference	(°C)

Research and Development of Heat Pipe and Its Application to PC Cooling

Masataka Mochizuki

Abstract

This paper describes the development of the cooling systems for the laptop Personal Computer (PC), as well as the Miniature Heat Pipe (MHP) structure and its performance in relation to cooling the Micro Processor Unit (MPU) assembled in the laptop PC. Described also are developments in the heat sink with heat pipe technology for cooling the desktop PC, server, and workstation. The paper consists of 9 chapters.

Chapter 1 describes the background of this research, progressing to the MPU with its higher heat generation and the demand of PC's. Recently, since there has been rapid progress of the PC and of its performance, the development of advanced cooling systems has been required for PC MPU's with high heat generation. Since the Pentium processor's (trade mark by Intel Corp.) release for practical use in 1995, it was necessary to cool MPU due to increasing heat generation. Developments of advanced cooling systems, with passive cooling provided by MHPs of 3 to 4 mm diameter, were applied to cooling MPU in laptop PCs.

Chapter 2 describes the structure of the MHP, its manufacturing method, thermal performance, and some functions. There are several main types of wick structure used in heat pipes such as fiber wicks, sintered powder, screen mesh and axial grooves. This research is concerned with the optimization of wick design, maximum heat transfer rate of MHP (Q_{max}), thermal resistance (R_{hp}), and the influence of heat pipe orientation through experiment. For practical use, most heat pipes will be formed into a flattened shape of 2 mm thickness and with several bends, so that it is necessary to examine the change in heat transfer characteristics after flattening and bending. A MHP has an optimal quantity of filling charge of working fluid, being 0.1 gram due to the its small internal volume. Therefore, it is very important to keep the maximum filling error within $\pm 5\%$ of the total volume, and careful filling techniques and processes are needed. The present paper also covers the optimal filling ratio of working fluid.

Chapter 3 describes the development of a heat pipe with fine fiber wicks by conducting an experimental study in order to improve performance.

Chapter 4 describes another development of thinner heat pipes and sintered wire heat pipes. There has been a trend to use thin notebook PC's of A-4 and B-5 size, particularly in Japan. The thermal performance of thinner heat pipes of 2.0mm and 1.5mm was investigated. Although heat pipes thinner than 1.0 mm is possible to be

fabricated, it is impractical if it cannot work very well with feasible heat transfer rate. Also, investigations to improve the thermal performance by wetability of container and wick materials were undertaken. Additionally, we have developed a sintered wire heat pipes which can achieve lower thermal resistance while maintaining a higher maximum heat transfer rate from higher capillary force, suitable for applications of the increasing MPU power.

Chapter 5 describes the reliability issues of long term MHP operation. The accelerated life test was carried out using the Arrhenius model, and frozen start-up was also examined experimentally.

Chapter 6 describes the various kinds of cooling systems with MHPs assembled into laptop PC's. Also, for a higher heat thermal solution of 30 to 40 watts, a system level analysis by thermo-fluid dynamic computer simulation was performed and thermal interface material was sought. Before 1994, the laptop PC was cooled by ventilation and natural convection cooling using a small heat sink or an aluminum spreader plate, as the heat of the MPU was lower than 3 watts. After the Pentium processor appeared, a thermal spreader plate with a MHP was developed and quickly expanded to practical use. The thermal resistance between the chip junction and the ambient air was approximately 6 to 10 K/W. As the individual thermal resistance of a MHP needs to be below 1 K/W, larger thermal resistance remains for other thermal parts. In particular, it is estimated to reduce contact thermal resistance between a heat pipe, the MPU, and heat sink. The use of soldering, thermal epoxy, etc., can create the thermal solution to reduce the contact thermal resistance. Normally Thermal Interface Material (TIM) like silicon or boron-nitride base thermal pad, thermal grease, or Phase Change Material (PCM) may aid installation by lowering thermal resistance when the MPU is assembled into the PC. A forced cooling system called a Remote Heat Exchanger (RHE) was developed in 1998 for applications of increasing MPU heat generation of over 10 watts. A RHE consists of a block to attach to the MPU, a heat pipe to carry the heat, and a heat exchanger with a miniature fan to exhaust heat to the ambient air. The present paper describes the design concept and an experimental study on thermal performance issues. On the other hand, designers are still interested in passive thermal solution, even if the MPU power increases, because the consumption of energy with active thermal solutions is not preferred particularly in a battery mode operation. Therefore, a hinged heat pipe cooling system has been developed that is capable of cooling the system without consuming electrical energy. A primary heat pipe transfers heat from the MPU to the hinged parts, and a secondary heat pipe can take over to transfer heat to the back panel of the Liquid

Crystal Display (LCD) where the temperature is the lowest because of lower heat-generating parts than the bottom skin area on the laptop PC. The LCD area also provides a very wide heat dissipation surface area to the ambient air. A thermal hinge, which is different from a mechanical torque hinge, should provide thermal resistance lower than 1 K/W with good reliability for long term operation, at least 30,000 open and close cycles. In addition to the ever increasing MPU power there are many other parts that generate heat (such as HDD, memory, and so on), total thermal solutions are needed. Here, the paper describes the system level thermal design using a computer thermo-fluid dynamics simulation.

Chapter 7 describes a heat sink with heat pipe technology for a desktop PC, server, and workstation applications. There exists a large demand for an advances in heat pipe cooling technology. The cooling of MPU by a combination of a heat sink and a fan has been widely used for desktop PC. Meanwhile, various heat sinks, such as extrusion, die-cast heat sink, etc., are used in conjunction with a system fan for server and workstation applications. The frequency of MPU has been increasing rapidly to over 1 GHz, and the heat generated is from 70 to 100 watts. Although the heat generation by the MPU is exponentially increasing, its die size is designed using the same size. The size of the circuit board has decreased from 0.25 μm to 0.18 μm, and is continuing to decrease even further. Contrary to this, the size of the heat sink will almost linearly depend on the heat generation of the MPU, so that it is difficult to reduce its size. Since non-uniform temperature distribution occurs at the base of the traditional aluminum heat sink, its surrounding area is decreasing to a lower temperature than the heat source. A heat sink combined with a two dimensional heat pipe structure may solve this problem because a heat pipe can provide temperature uniformity to the heat sink base. A plate heat pipe, which is called a Vapor Chamber (VC) is necessary to handle 50 W/cm^2 of an evaporator heat flux. In addition, it is required to be less than 5 mm thick. The wick structure, which consists of sintered copper powder, has been chosen for easy fabrication on any configuration and geometry. A VC should work very well at any orientation without capillary limitation. The present paper describes fundamental test and thermal performance experiment on the VC. In parallel, it is very important to reduce contact thermal resistance between heat sink and VC. The best method of attachment would be to use metallic bonding like soldering or brazing. The VC is not actually almighty in any case of design, so that estimation method whether VC is effective or not is needed and requested. The modeling and testing of the VC has been considered in this paper.

Chapter 8 describes future cooling systems. New cooling systems for future PC

having much larger heat generation are proposed. The more improved heat pipes capable of enhancing the maximum heat transfer rate and lower thermal resistance and an Opened Brayton Air Cooler could be developed and applied to the system as one of new systems soon.

As the concluding remark. Chapter 9 describes how heat pipe technology is very helpful and important in cooling down the chip temperature of computers.

1. Introduction

1.1 Progressing chips with increasing power

Recently, there have been rapid progress in the development of Personal Computers (PC) and of its performance. It has therefore been necessary to develop advanced cooling systems for PC applied Micro-Processor Unit (MPU) with high heat generation. Since the Pentium processor's (trade mark by Intel Corp.) release for practical use in 1995, more attention was necessary in cooling the MPU due to the increased heat generation. Specifically, the MPU for laptop PC's needs an advanced cooling system with a passive solution which can be provided by a miniature heat pipe of 3 to 4 mm in diameter (called a micro heat pipe, MHP), which has been immediately developed and applied to the system. The cooling apparatus with heat pipes has been progressing, so that currently most laptop PC's are being equipped with heat pipe cooling parts inside. This paper discusses what performance is required in cooling the PC and to clarify the performance of the MHP. Figure 1-1 shows historical trends of increased frequency on various chips and the expected frequency to the 2015.

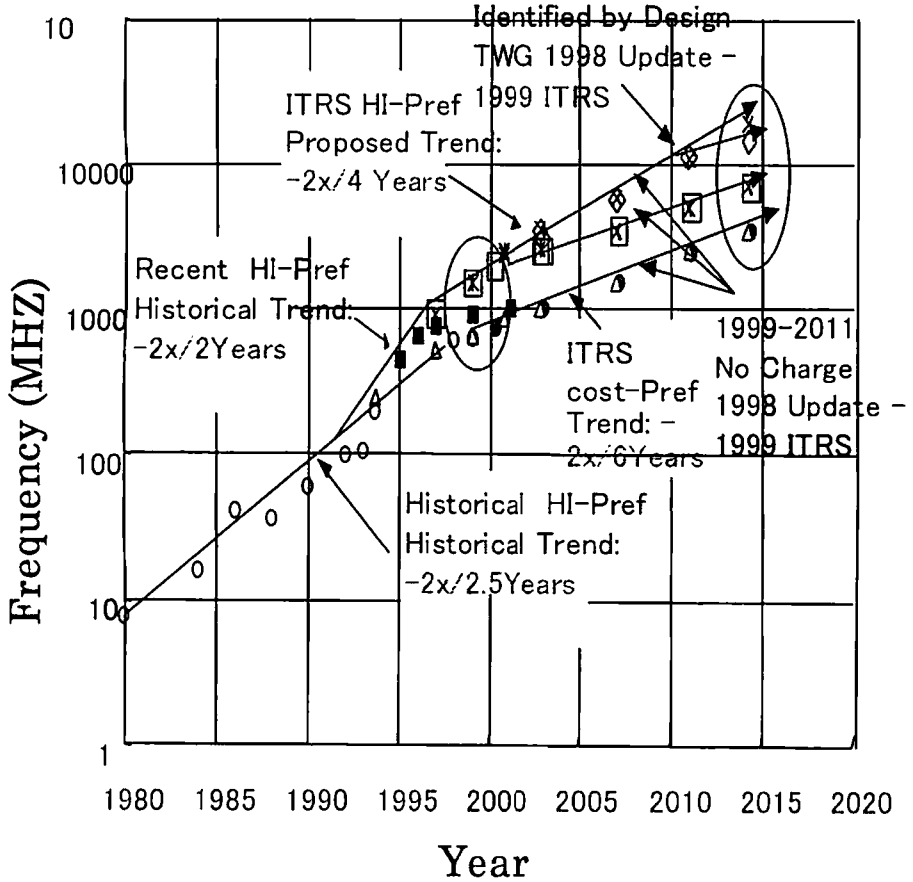

Fig. 1-1 Historical and expected tendency of increasing frequency on chips [1-1]

As per Moor's expectation, the frequency of chips had increased at 10 times the rate in the 10 years from 1980 to 1990, and has continued to increase in the years since then. We already have 1 GHz MPU in 2001. The frequency is expected to reach 10 GHz level after 10 years, in the year 2010 at maximum.

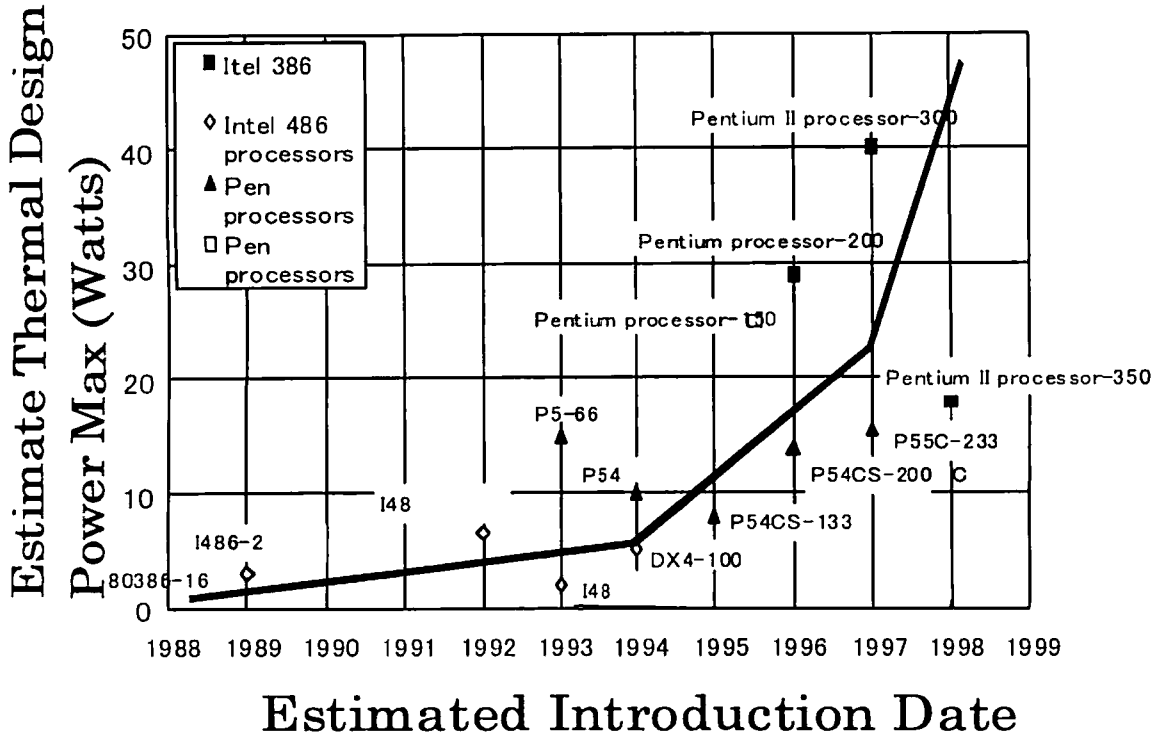

Fig. 1-2 Increasing thermal design power of chips [1-1]

After 1995, the Pentium™ processor was born, and the power of the MPU increased exponentially. Designers need thermal solutions to handle 30 Watts for laptop PC's and 70 Watts for Desktop PC's in 2001. According to a recent announcement by Intel, a chip will struggle with power consumption. Of course, chip manufacturers intend to reduce the power consumption for performance by means of new architecture and chip design. It is expected that a 10GHz MPU needs finer CMOS transistor technology by 0.03 μm. It evident that the progress of the MPU developments for the last 30 years trends towards the prediction by Moor's expectation. For instance, it is correct that the ratio of the increasing number of transistors has doubled for the last 2 years. Meanwhile, the size of the MPU die has been just enlarged by 14 %. This means that the die will doubled in size for the next 10 years. One of the reasons was that it was possible to manufacture many large sized chips on silicon wafers by reducing the defect ratio. The frequency has doubled in pace for the latest 2 years. Since transistor

technology was changed from Bipolar to CMOS in 1980, the clock speed had rapidly increased [1-2].

For the last 10 years, the chip manufacturing process has shrunk from 1 μm to 0.18 μm, after that clock speed had increased 50 times. The performance of the MPU had improved substantially (75 times in capacity) during the last 10 years with the increase in frequency and the development of micro-architecture and chip design. As an expectation for the next 10 years, the MPU will continue to progress to 0.03 μm, for example 0.13 μm in 2001, 0.10 μm in 2003, 0.07 μm in 2005, and 0.05 μm in 2007. As a result, it can be expected that the number of transistors in an MPU will increase to 200 million pieces after 5 years, and then 1 billion pieces after 10 years. Assuming that the MPU developments follow a trend doubly increasing in transistors and enlarging the die size 14% over 2 years, the following die size will be expected using wiring width of 0.13 μm technology for the next generation architecture.

28 mm square (784 mm^2) in 2003
32 mm square (1,024 mm^2) in 2005
36 mm square (1,296 mm^2) in 2007
41 mm square (1,681 mm^2) in 2009

If this estimation is correct, the thermal power of the MPU will reach several kWs within 10 years. However, processor melt down will occur due to the high thermal power level. This thermal issue should be avoided without enlarging die size. It is clear that the power consumption of an MPU is a major headache with regard to MPU progress. The power density of the MPU is the next barrier. The thermal power density of the MPUs had surpassed that of a hot plate level and will reach the level of a nuclear power reactor and rocket engine in 2010 and then close to the sun's surface in 2015. As a more accurate expectation of the thermal power, it may be approximately 600 watts in 2010, which generates the same heat as an electric heater. The video chips will also generate a great deal of heat, so that electric power consumption will become a very challenging issue. It is quite true that only new advanced MPUs with appropriate cooling technology can achieve practical use status. The thermal budget which is the temperature difference between the MPU case and atmosphere divided by power is shown in the following example.

Maximum MPU case temperature : 90℃
Atmosphere : 40℃
Power : 200 Watts

The thermal budget of (90-40)/200=0.25 ℃/W is required, which is equal to the thermal resistance of a satisfactory thermal solution. A 0.25 ℃/W thermal network,

comprising of a heat sink for heat dissipation to the atmosphere, and a secure air flow in an air cooling system on a PC.

Figure 1-3 shows the expected heat generation of new MPUs with the 32 bit processor base for desktop, server, and workstation. From the year 2000, a chip will be designed by 0.18 μ m technology and the heat generated will have reached 80 watts and then close to 100 watts in 2002. Instead of a traditional aluminum extrusion heat sinks, a new heat sink using folded fins and stacked fins providing very large heat transfer area will be applied and heat pipe technology can assist in reducing the thermal resistance of these heat sinks.

Figure 1-4 shows a similar tendency of 64 bit MPU technology for NT servers and high-end desktop PC's. In 2002, it is expected that 0.13 μ m technology will be applied to the 64 bit chip and the heat reached will be 150 watts. It is expected that 64 Bit chips will need vapor chamber (flat heat pipe) heat sinks.

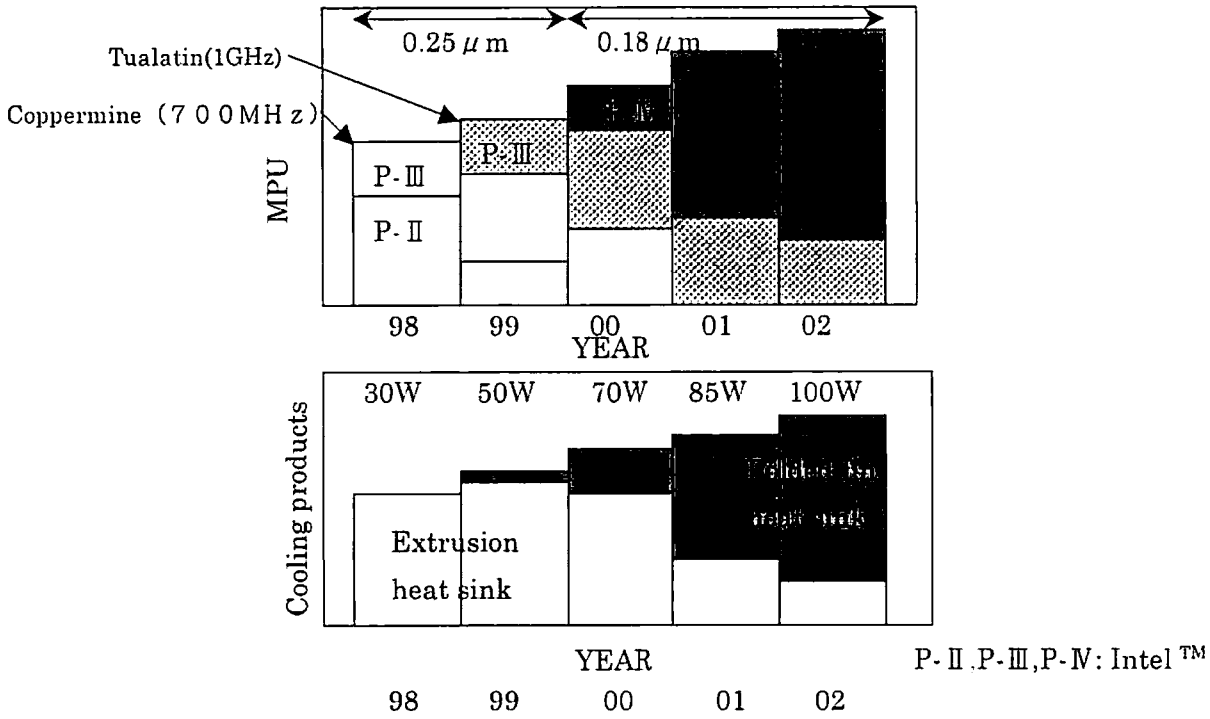

Fig. 1-3 New processor and heat sinks for 32 Bit MPU for desktop PC

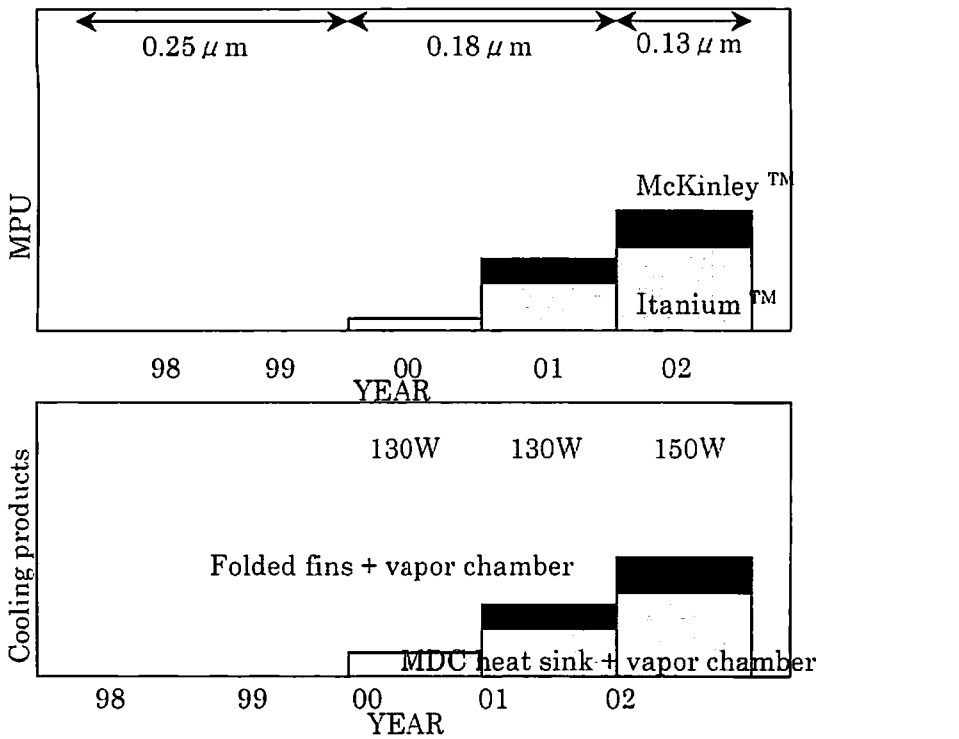

Fig. 1-4 Heat generation from 64 Bit MPU for NT server and high-end desktop PC

1.2 Demand for personal computers [1-3]

Figure 1-5 shows the demand of increasing shipments of PC's. Approximately 130 Million PC's were manufactured and shipped into the market in 2000. The APEC region has in particular shown an increase in the demand of PC's in Fig. 1-6.

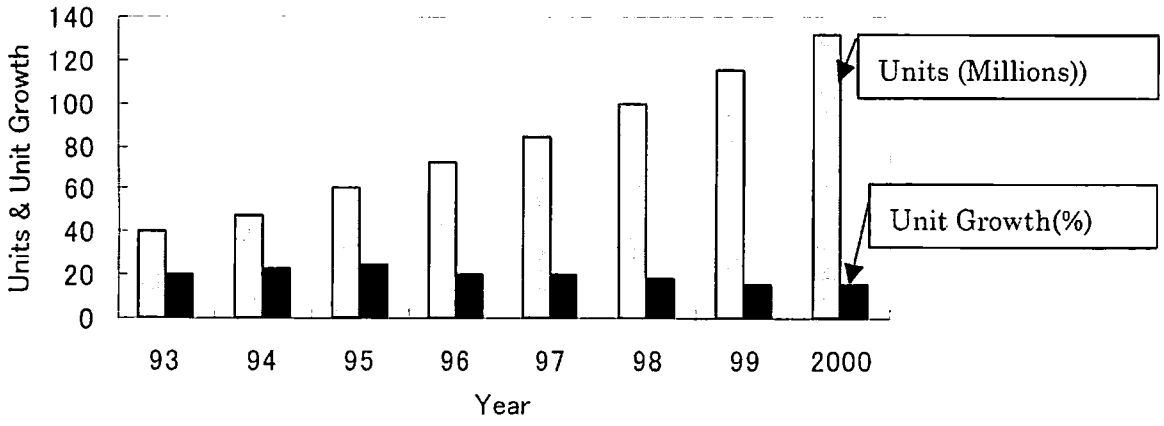

Fig. 1-5 Shipment record of personal computers in the world (Source: Dataquest)

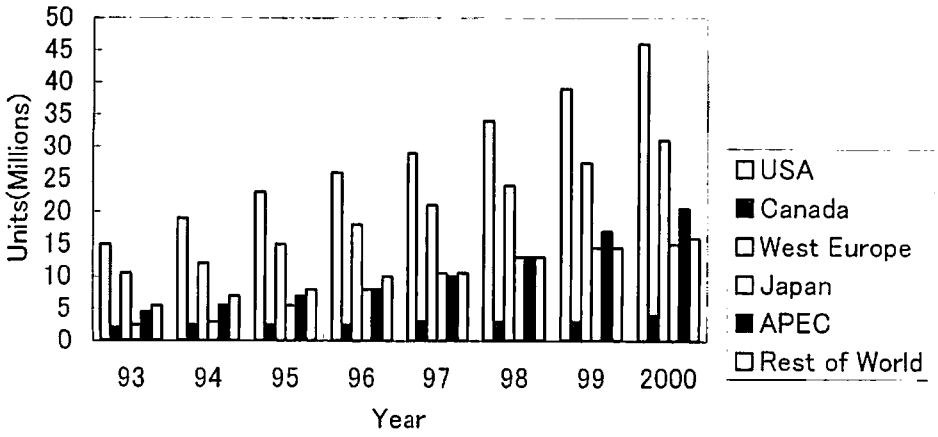

Fig. 1-6 Shipment of personal computers to each region (Source: Dataquest)

Figure 1-7 shows the data of shipments for desktop PC's that gross per unit is still increasing but when the ratio of expansion has reached a stable condition. 70 million desktop PC's were delivered into the world wide market in 2000. Approximately 20 million laptop PC's had been provided for the market in 2000 as shown in Fig. 1-8.

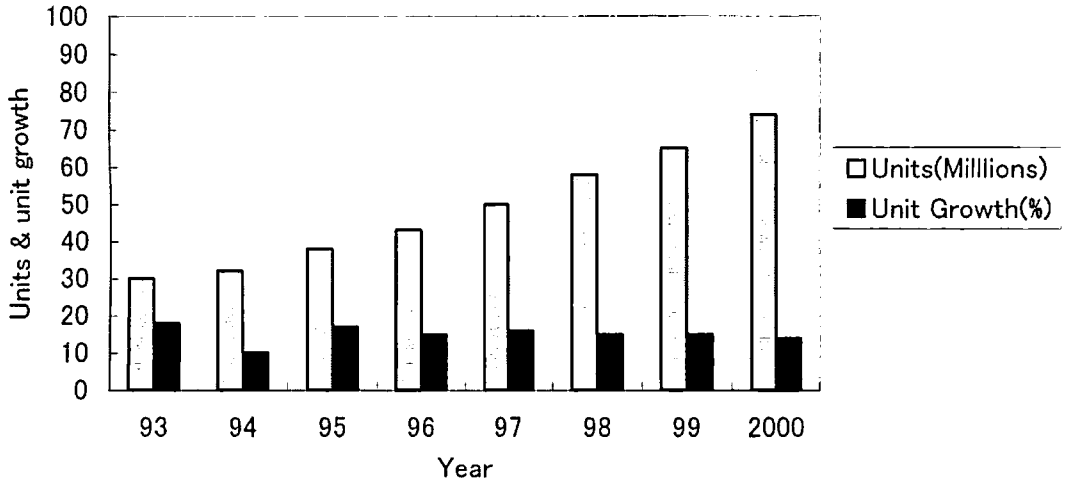

Fig. 1-7 Shipment of desktop personal computers (Source: Dataquest)

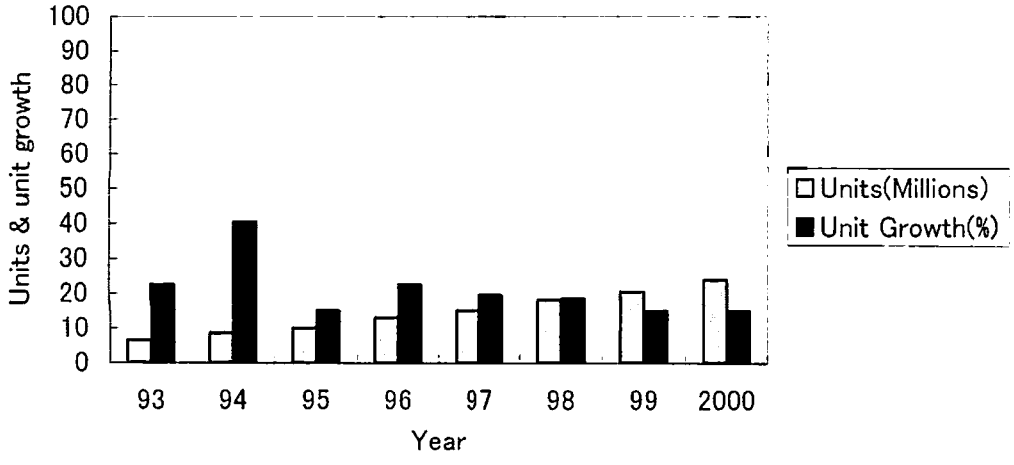

Fig. 1-8 Shipment of laptop personal computers (Source: Dataquest)

References

(1-1) Kaveh Azar, " *The history of power dissipation*", Electronics cooling, vol. 6, No. 1, Jan. 2000, pp. 42 - 48.

(1-2) H. Goto, PC watch home page, February 6, 2001.

(1-3) Internet news, Daetaquest Co., Jan. 2001

2. Structure and thermal performance of the miniature heat pipe [2-1]

2.1 Various structures and features of miniature heat pipes

The heat pipe was invented and named by Dr. Grover in 1960, to apply space craft in particular temperature control of electronics devices. Heat pipes have been used for many application such as heat exchanger for heat recovery, snow melting system, electronics and electric system, etc.

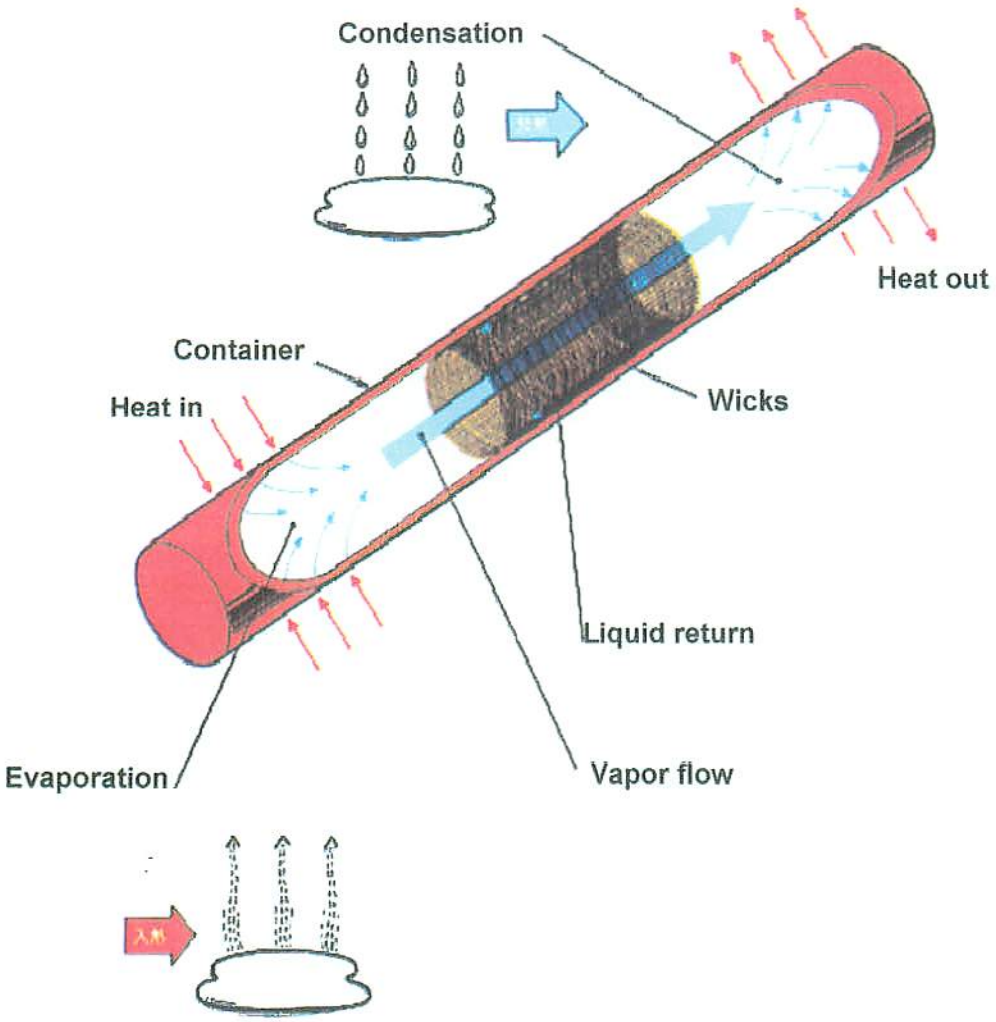

Fig. 2-1 The structure of heat pipe with wicks[2-1]

Figure 2-1 shows the structure of a typical heat pipe with wick structure. There are several kinds of wick structure such as metal fiber bundle, screen mesh, sintered metal powder, and axially grooved heat pipes as shown in the following Fig. 2-2. A heat pipe with wicks capable of generating capillary force basically works at any orientation

by vaporizing at the evaporator, moving vapor from the evaporator to the condenser section, condensing the vapor at condenser, and moving liquid back to the evaporator by means of capillary force. This phenomenon is continuously repeated as a closed system. As a heat pipe utilizes phase change phenomenon, the circulating flow rate of working fluid can be approximately 100 to 500 times as small as a mass heat transfer systems like single phase liquid cooling. Therefore, a 3 or 4 mm miniature heat pipe may be need in the cooling of a MPU.

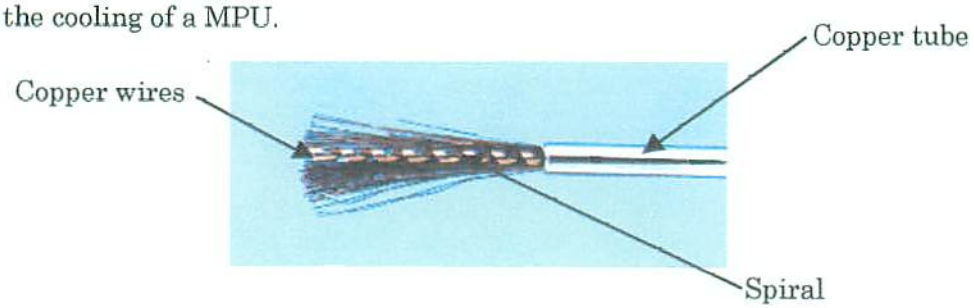

Wire bundle wick

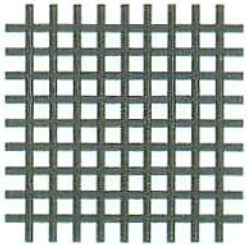

Screen mesh wick

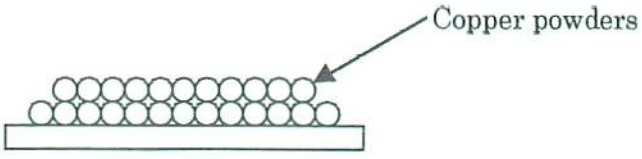

Sintered powder wick

Axially grooved

Fig. 2-2 Various type of wick for heat pipe

Listed below are some requirements of MHP for laptop PC cooling.

1) Larger Q_{max}. (Over 10 W in 3mmOD MHP)
2) Lower thermal resistance. (Approx. below 1 K/W)
3) Stable performance at any orientation.
4) Stable performance when bent and flattened.

Table 2-1 Comparison between various heat pipes

Type of heat pipe	Wire bundle	Screen mesh	Sintered powder	Axially grooved
Q_{max} (3mm Round)	Excellent (13watts)	Good (10watts)	Excellent (12watts)	Poor (5watts)
Thermal resistance (Horizontal)	Good (0.7K/W)	Good (0.8K/W)	Good (0.7K/W)	Excellent (0.5K/W)
Top heat performance (L_{eff}:200mm)	Good (1.5K/W)	Good (5K/W)	Excellent (1.5K/W)	Poor (No work)
Performance in bent & flattened	Excellent	Poor	Poor	Poor

Table 2-1 shows the features of the various types of heat pipes. Actually, there is no almighty heat pipe for general requirements of higher Q_{max}, lower R_{hp}, operation able at top heat mode, and stable performance when bent and flattened. Wire bundle and sintered powder wick heat pipes have basically larger Q_{max} due to higher capillary force. On the other hand, an axially grooved heat pipe gives the lowest thermal resistance due to the larger unobstructed vapor space. From the top heat mode operational point of view, a higher capillary heat pipe provides much better performance. As stable performance is required when a heat pipe is bent and flattened, a flexible wick heat pipe with wire bundle wicks is preferred. This may suggest that the wick should continue without a pin point fault like the water pipe line.

2.2 Manufacturing method of the miniature heat pipe

Figure 2-3 shows the manufacturing flow chart of the miniature heat pipe. Instead of the vacuum process, evacuation and degassing are very useful for high volume production of miniature heat pipes.

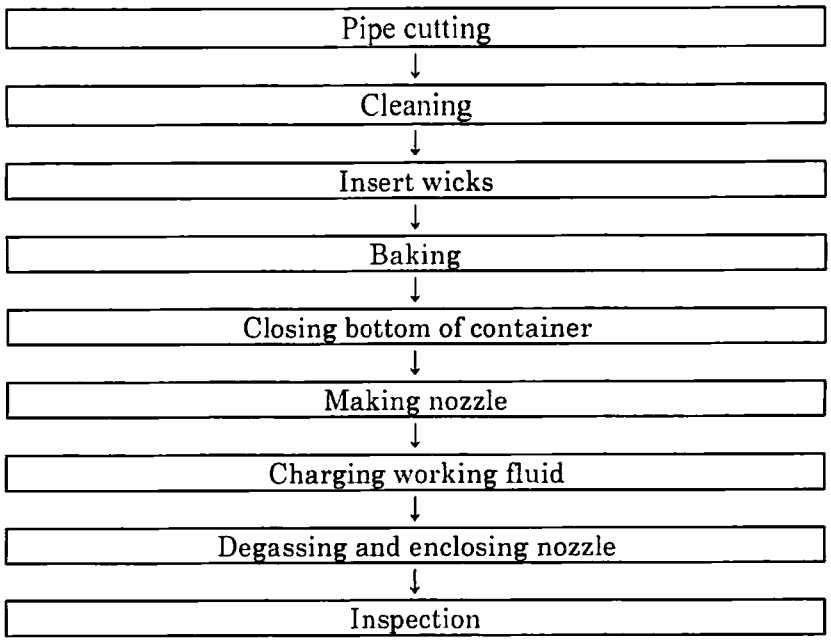

Fig. 2-3 Manufacturing method of the miniature heat pipe

It is better to select an oxygen free copper (C-1020) for the tube and wick materials in order to avoid the non-condensable gas generation that can degrade the thermal performance of a MHP. The baking process at high temperatures approximately 500 ℃ is very important as well as the cleaning process. It is recommended to reduce the both ends by using a spinning roller or squeezing machine instead of an end plate welding because of greater cost reduction, suitable for high volume production, and obtaining a tighter pressure vessel at both ends. Water is used as the general working fluid of heat pipes. Most heat pipes used for laptop PC's are actually copper-water because of the good performance by higher Merit number of the working fluid, better operating temperature and internal pressure range, easy manufacturing cost, environmental requirements, and so on. Distilled water is used in the industry but the degassing process is necessary in the heat pipe manufacturing process. The seasoning process at 180 to 200 ℃ is a convenient process to evacuate non-condensable gas in order to obtain a more reliable heat pipe. In fact, after closing both ends of the heat pipe by completely welding, a micro leakage check is necessary.

2.3 Thermal characteristics of miniature heat pipe [2-1]

2.3.1 Geometry and dimension of typical miniature heat pipe

There are two key factors, maximum heat transfer rate (Q_{max}) and thermal resistance (R_{hp}) for miniature heat pipes. The heat transfer rate of a heat pipe which is calculated by thermal resistance and temperature difference of both ends should be smaller than Q_{max}. Figure 2-4 shows the configuration and dimension of standard MHP, round and flattened MHP for industrial use.

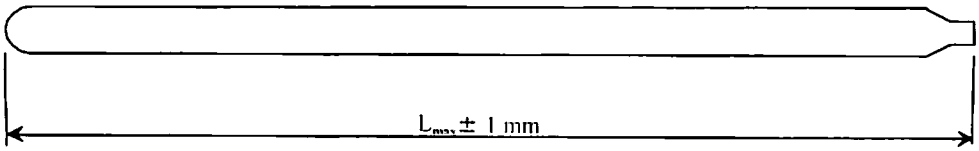

Round Heat Pipe

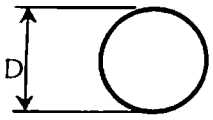

D±0.1 mm	L_{max} mm
3	300
4	350
5	400
6	800
8	800
9.5	800

Flat Heat Pipe

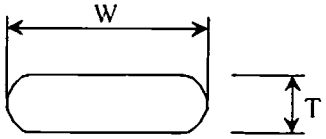

Wmm	T±0.1mm	Original OD
3.6	2.0	3
5.2	2.0	4
6.2	3.0	5
7.8	3.0	6
10.9	3.0	8
13.3	3.0	9.5

Fig. 2-4 Standard MHP for round and flattened geometry.

2.3.2 Maximum heat transfer rate of heat pipe (Qmax)

There are typically 5 limiting factors in the heat transfer phenomenon of heat pipes;

1) Capillary limit
2) Entertainment limit or flooding limit in thermosyphon
3) Boiling limit
4) Sonic limit
5) Viscous limit

The measured data of $Q_{max\text{-}fact}$ is 2 W-m at 50℃ as operating temperature, and at horizontal orientation in 3mm round heat pipe with wire bundle wick. Therefore, actual maximum heat transfer rate can be estimated by equation (2-1), when length of heat pipe is known.

$Q_{max}=(Q_{max\text{-}fact}) / L_{eff}$ (2-1)

L_{eff}: Effective heat transfer distance (m)

$L_{eff}=L_e/2 + L_a + L_c/2$ (2-2)

L_e: Length of evaporator (m)

L_a: Length of adiabatic section (m)

L_c: Length of condenser (m)

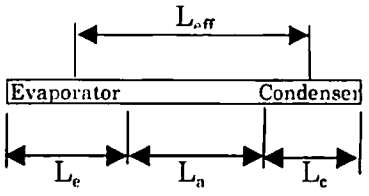

For example, Q_{max} of wire wick 3mm OD heat pipe at L_e=50mm, L_c=250mm, L=300mm). and L_{eff}=150mm is estimated in the following.

Q_{max} = (2 W-m) / (0.15 m)

= 13 watts

As a reference of Q_{max}, for axially grooved heat pipe is just 4.6 watts through experimental testing. Since it is clear that $Q_{max\text{-}fact}$ of axially grooved heat pipe is 0.7W-m, it is found that a wire wick heat pipe is approximately three times larger Q_{max} than an axially grooved heat pipe. As the heat transfer limitation of the MHP is normally restricted by capillary limit, wick design of MHP is important. The values shown below outline the maximum heat transfer rate of copper-water heat pipe having copper wire bundles as wicks, in the case of 300 mm long, 150mm as effective heat transfer distance (L_{eff}), 50 ℃ of operating temperature, and horizontal orientation.

OD	Q_{max}
3mm	13 watts
4	25
5	40
6	60
8	110
9.54(3/8")	150

The Q_{max} of flattened heat pipe which is pressed from round heat pipe is shown in the following table.

Width	Thickness	Original OD	Q_{max}
6mm	2mm	3mm	10 watts
5.2	2	4	15
6.2	3	5	27
7.8	3	6	35
10.9	3	8	48
13.3	3	9.54(3/8")	57

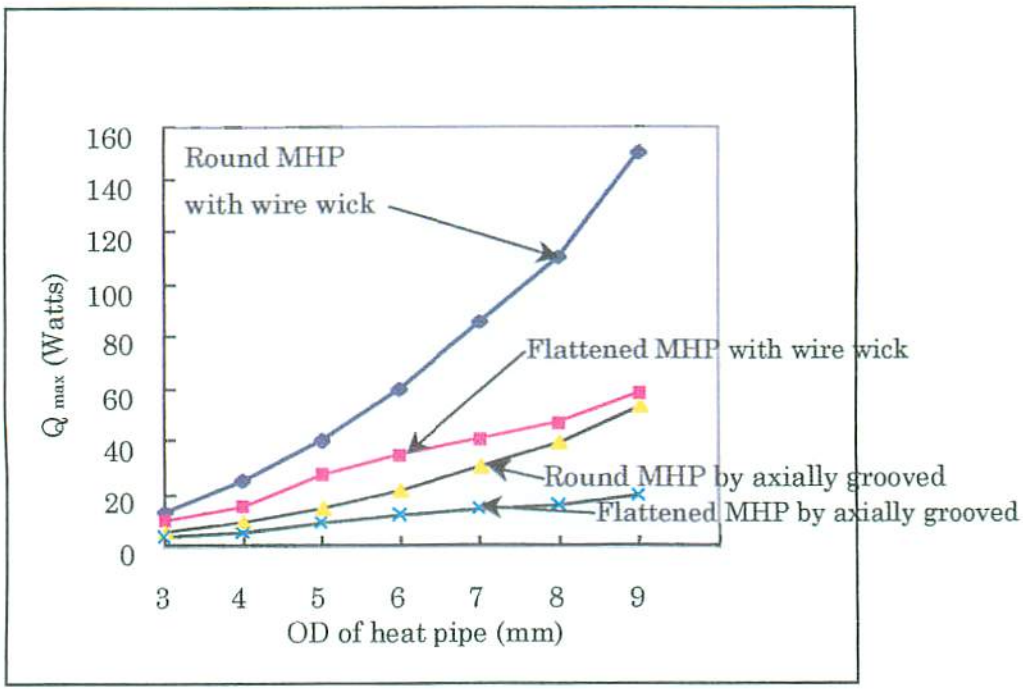

Fig. 2-5 Maximum heat transfer rate (Qmax) of MHP

Figure 2-5 shows the relation between Q_{max} vs. heat pipe size in wire wick and axially groove heat pipe.

2.3.3 Thermal resistance of heat pipe (R_{hp})

The thermal resistance of a heat pipe can be estimated by equation (2-3) with negligible effects of the thermal conductivity of wick and container.

$$R_{hp} = 1 / (h_e \cdot A_e) + 1 / (h_c \cdot A_c) \quad K/W \quad (2\text{-}3)$$

	Round heat pipe	Flattened heat pipe (2mm thick)
h_e: Heat transfer coefficient in evaporator	6,000 $W/m^2 \cdot K$	4,000 $W/m^2 \cdot K$
h_c: Heat transfer coefficient in condenser	6,000 $W/m^2 \cdot K$	4,000 $W/m^2 \cdot K$
A_e: Heat transfer area of evaporator	$\pi \cdot D_i \cdot L_e$ m^2	$\pi \cdot D_i \cdot L_e$ m^2
A_c: Heat transfer area of condenser	$\pi \cdot D_i \cdot L_c$ m^2	$\pi \cdot D_i \cdot L_c$ m^2
D_i: Inside diameter of heat pipe		

For example:

R_{hp} of round heat pipe for OD=3mm, L=300mm, L_e=50mm, L_c=250mm, D_i=2.4mm,

R_{hp}= 1 / (6,000 · 0.0024 · π · 0.05) + 1 / (6,000 · 0.0024 · π · 0.25)

= 0.53 K/W

Another example:

R_{hp} of flattened heat pipe for thickness=2mm, width=3.6mm, L=300mm, L_e=50mm, L_c=250mm, (Original OD=3mm, D_i=2.4mm round heat pipe)

R_{hp}= 1 / (4,000 · 0.0024 · π · 0.05) + 1 / (4,000 · 0.0024 · π · 0.25)

= 0.80 K/W

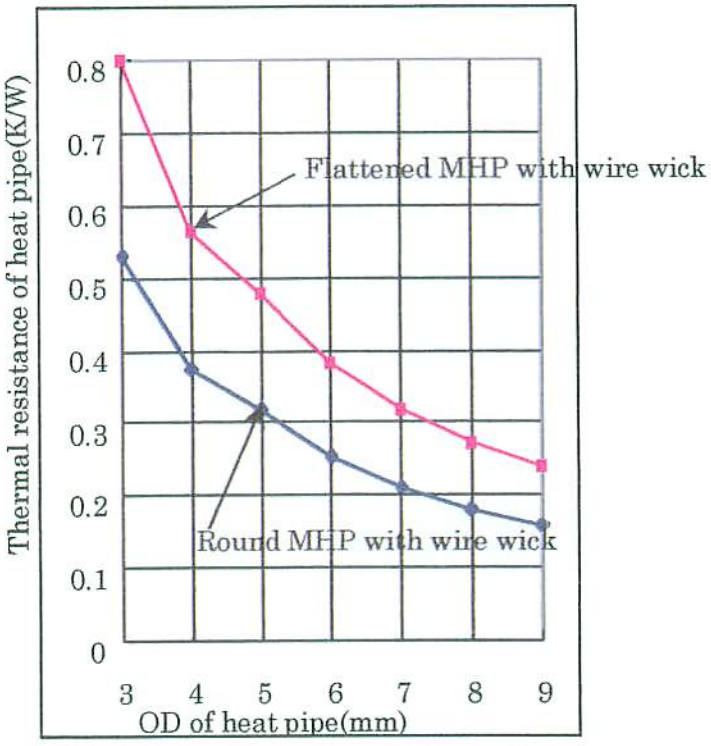

L_e=50mm, L_c=250mm, Orientation: Horizontal

Fig. 2-6 Thermal Resistance of Round and Flattened MHP

Figure 2-6 shows the thermal resistance of round and 2mm flattened MHP. For example, a 4 mm round MHP has 0.38 K/W × 10 watts = 3.8 ℃ as temperature difference between evaporator and condenser when input power is 10 watts. This temperature difference will be acceptable on total thermal design of laptop PC's.

When a heat pipe is bent, a temperature drop occurs, which is caused by vapor and liquid pressure loss. The bending resistance (R_c), tabulated below may be added to the fundamental heat pipe resistance. The allowable radius should be kept to over 3 times of OD.

Original OD	R_c of round heat pipe	R_c of flattened heat pipe
3 mm	0.2 K/W	0.26 K/W
4	0.15	0.20
5	0.12	0.16
6	0.1	0.13
8	0.08	0.10
9.54	0.06	0.08

The total thermal resistance with bend($R_{hp,t}$) is shown by equation (2-4). A bent corner of heat pipe increases thermal resistance.

$$R_{hp,t} = R_{hp} + N_b \cdot R_c \qquad (2\text{-}4)$$

N_b: Number of bent corners

2.3.4 Design of wire wicks

Optimization of wire wick design is needed. Here, it assumes that a vapor space of 80% of the total internal space is appropriate. Equation (2-5) shows the balance between wick number and vapor space.

$$(\pi/4) \cdot D_i^2 \cdot (1\text{-}0.8) = (\pi/4) \cdot D_w^2 \cdot N_w \qquad (2\text{-}5)$$

D_i : Inside diameter of tube (2.4mm in case of 3 mm OD)

D_w : Wire diameter (0.1 mm)

N_w : Number of wire

Equation (2-6) shows the relation for the number of wick layers (N_l) and the calculated number of wick layers are shown in the following table for the various heat pipe sizes:

$$N_l = (D_w \cdot N_w) / (\pi \cdot D_i) \qquad (2\text{-}6)$$

OD (D_i)	Wire size(D_w)	Wire number(N_w)	Wick layer number (N_l)
3mm (2.4mm)	0.1mm	115 pieces	1.53
4 (3.4)	0.1	231	2.16
5 (4.2)	0.1	353	2.68
6 (5.0)	0.1	500	3.18
8 (7.0)	0.1	980	4.46
9.54 (8.54)	0.1	1,459	5.44

2.3.5 Criteria of pure water as working fluid

In general, water is one of the best working fluids for heat pipes in the temperature range of electronics cooling, but the content of water must be controlled using following criteria. The check of electro-conductivity is used at the industrial level.

Table 2-2 Water impurity contents for working fluid

Contents	Unit	Measurable lower limit by	ion-exchange water	distilled water	Tap Water
			For working fluid	Commercial goods	General
Mg	mg/L	0.1	<0.1	<0.1	6.3
Na	mg/L	0.1	<0.1	<0.1	20.4
K	mg/L	0.1	<0.1	<0.1	1.1
Ca	mg/L	0.1	<0.1	<0.1	9.2
Cl -	mg/L	1	<1	<1	30.2
F +	mg/L	0.08	<0.08	<0.08	<0.08
SO_4 -	mg/L	1	<1	<1	13
SiO_2	mg/L	2	<2	<2	19
Fe	mg/L	0.03	<0.03	<0.03	<0.03
Al	mg/L	0.02	<0.02	<0.02	<0.02
PO_4 -	mg/L	0.04	<0.04	<0.04	<0.04

2.4 Influence of filling ratio on miniature heat pipe performance

The internal volume of a MHP is very small, so that the performance of a MHP sensitively depends on the amount of working fluid. For example, the filling ratio should be controlled within 0.1 gram ± 5%. Figure 2-7 shows the general influence when MHP is over-filled or under-filled in heat pipe.

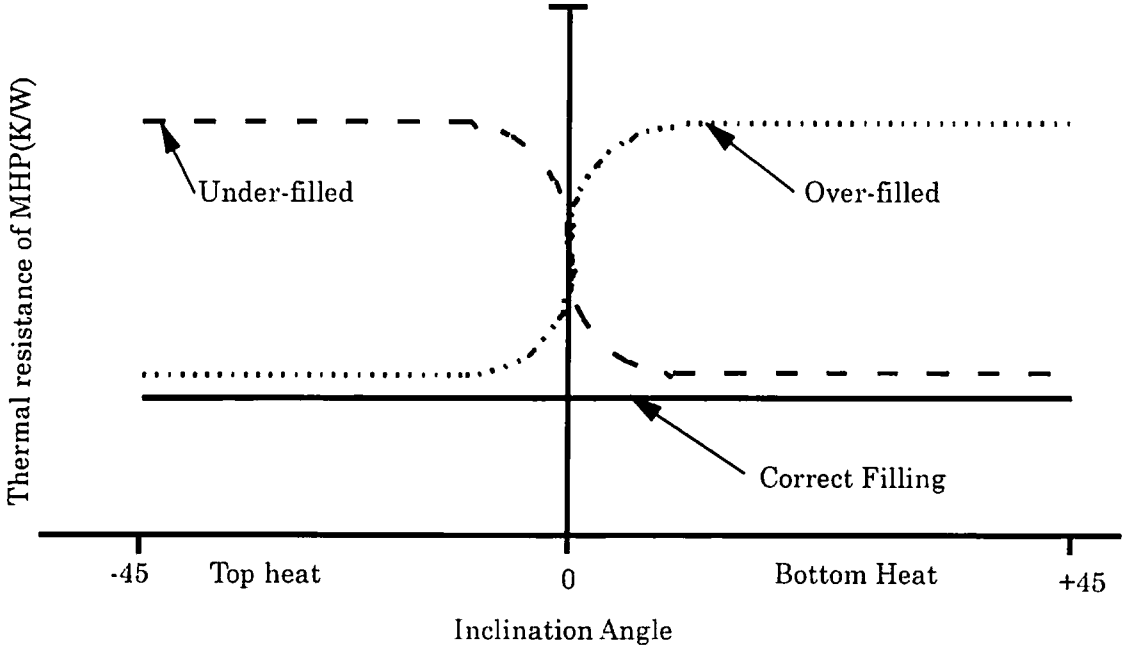

Fig. 2-7 Influence of thermal resistance when filling ratio is changed.

In the case of an over filled heat pipe, the thermal resistance tends to be lower at top heat mode orientation and higher at bottom heat mode orientation. On the other hand, the thermal resistance tends to be larger at top heat mode and smaller resistance at bottom heat mode in the case of under-filled heat pipes.

Figure 2-8 shows a general curve of the relation between filling ratio and thermal resistance in horizontal mode. It is very important to find the optimum filling ratio of the working fluid.

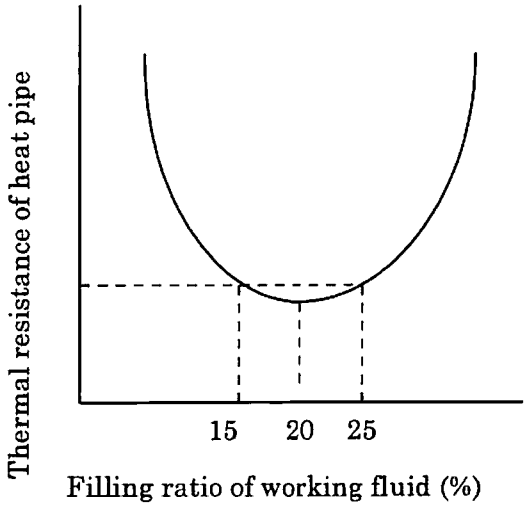

Fig. 2-8 Thermal resistance vs filling ratio

Reference

(2-1) Fujikura heat pipe catalogue, "*Thermal solution of cooling MPU*", HD 2000.03.2000

3. Development of heat pipe by improved wire wick [3-1], [3-8], [3-9]

3.1 Necessity of improved wire wick

Higher heat fluxes associated with electronics cooling require heat pipes with high maximum heat transfer at any inclination. Therefore, improved wick structures are needed. In particular, the operation at top heat mode (vertical orientation) is required by most of the notebook manufacturers with a decrease in 30% to 40% of the thermal resistance compared with conventional systems. The wick structure has been modified, with additional capillary channels but with small effects on the heat pipe permeability. Using this new design criterion, which balances the permeability and capillary needs, heat pipes with wire bundle as a wick structure were developed.

The diameter of the wire were varied from 0.05 mm to 0.1 mm and the maximum input power is about 16 Watts. It was found that the vapor space vs. liquid space ratio is an important parameter for this type of heat pipe. Also, the test results show that the thermal resistance is a strong function of the orientation. We have obtained heat pipes, with 2 to 5 times lower thermal resistance than the previous conventional heat pipes when they were used in the top heat mode operation. A comparison with other types of wick structures is also presented. Thermal resistances as low as 0.5 K/W at top heat mode and 0.2 K/W at horizontal mode were obtained. The application of heat pipes with this new wick structure to electronics cooling has been successful, especially in notebook applications.

With the demand for closing of the performance gap between desktop and laptop PC's, increased MPU performance has been developed for use in laptop PC's. Higher performance processors will have larger heat generation. This creates a challenge in providing a thermal solution in laptop PC's since high performance processors and additional features such as more Caches, more DRAM, larger HDD, PCMCIA and CD-ROM leads to higher total power dissipation. It is even more of a challenge to provide the thermal solution without compromising the computer's size, cost and weight. The total heat generated by the current MPU and other components as previously mentioned can be in excess of 20 to 25 W. With this amount of heat, the traditional cooling using a fin heat sink and or fan may not be a viable solution. In searching for an alternative cooling solution, the heat pipe seemed to offer the most promising means of solving the heat problem. Nowadays more than 80% of notebook Pc's require the use of heat pipes in the cooling solution. Most of the cooling solutions are custom designed and therefore the heat pipe specifications are different from one project to another. The ultimate goal for any thermal solution is "the lowest thermal resistance at any heat pipe orientation". Since the performance of the heat pipes depend mainly on the wick

structure and each heat pipe is custom designed, the wick structure should be custom designed for most of the applications. In addition to this, the fill charge must also be optimized for each application. This presents quite a challenge for the designers and for the mass production process. The heat pipes to be used for such applications should have:

- Higher maximum heat transfer performance (Q_{max} >16 Watts to 20 Watts)
- Medium wick capillary radius (heat pipe length approximately from 100mm and 300 mm)
- Lower thermal resistance at any orientation (especially top heat mode)
- Smaller diameter (approximately 3 to 6 mm)

These requirements show that there is a need for a wick structure which has high permeability (therefore higher heat transport capability) and medium capillary radius (therefore medium capillary height). These two parameters are somehow contradictory, because a small capillary radius means lower permeability, or high flow resistance. Therefore, in most cases the thermal engineer must compromise between these competing factors. The most common used wick structures used in heat pipes for notebook computers cooling application are mesh, groove, sintered wick, fiber bundle and called "super fiber wick".

3.2 Balancing the permeability and capillary pumping

Figure 3-1 shows the variation of the permeability and capillary pumping for different wick structures. It can be seen that each individual wick structure has its own advantages and disadvantages. Therefore, many options are available for the thermal designer in electronics cooling design. Also, it can be said that most researchers[3-2] highly recommend that experiments conducted in order to establish the most appropriate wick structure for each particular application. Despite many experimental studies[3-2]~[3-7], the general thermal theory is not used very much in heat pipes design (3 to 6 mm diameter). It is arguable that heat pipe theory is well supported by experimental works. mainly in explaining the heat transfer phenomena in the wick structure and in the boiling section. Therefore, most of the heat pipe design is based on empirical data and the "know how" of each heat pipe manufacturer.

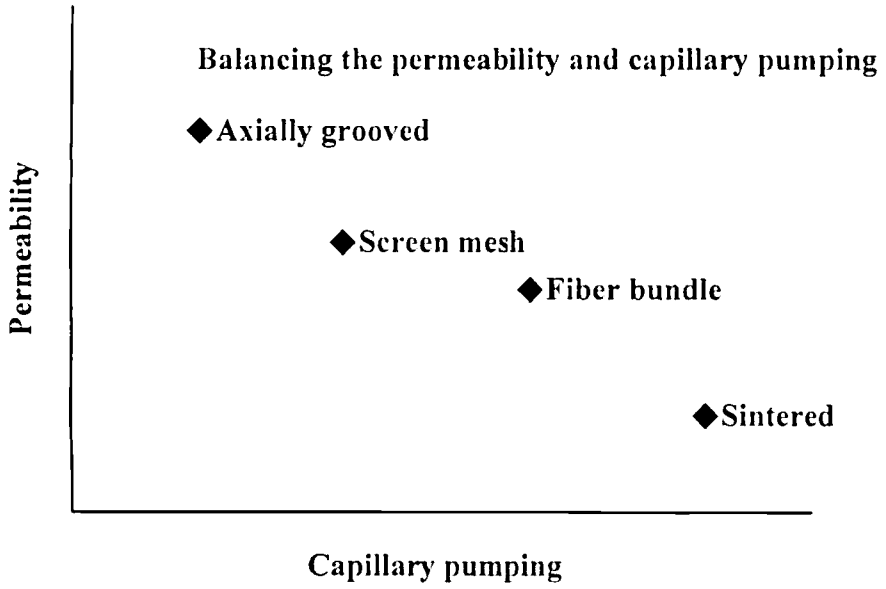

Fig. 3-1 Variation of permeability versus capillary pumping for different wick structures

Conceivably the top heat mode operation may show the differences between different types of wicks. In addition to this, the top heat mode operation can decide the best heat pipe performance for each particular application. To meet this requirement, we have developed a new design that led to the fabrication of the called super fiber wick heat pipe. Using statistical data, we considered that the performance of the fiber bundle heat pipe is a function of the vapor space and number of wires. We have found that the diameter of the wick and the number of wires is mainly a function of the following:

1) Heating mode (top heat, horizontal or inclined)
2) Final configuration of the heat pipe (flat or round)
3) Thermal resistance specifications

The wire diameter ranges from 0.1 mm to 0.05 mm or even less. Obviously, the use of a larger size wire diameter is not recommended for the top heat mode operation. The use of many wires of a smaller diameter provided better results for the top heat mode operation. Figure 3-2 presents the general criterion in choosing the super fiber wick structure.

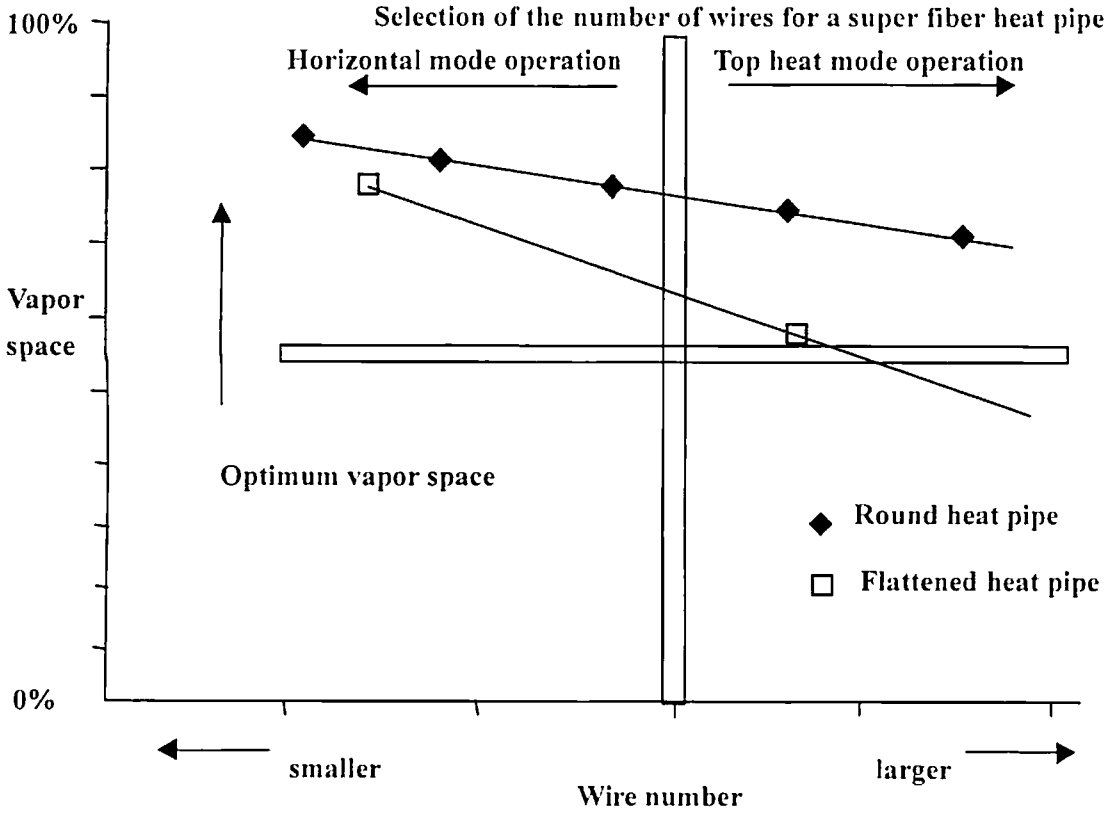

Fig. 3-2 Super fiber wick criterion : vapor space versus the wire numbers

3.3 Test setup

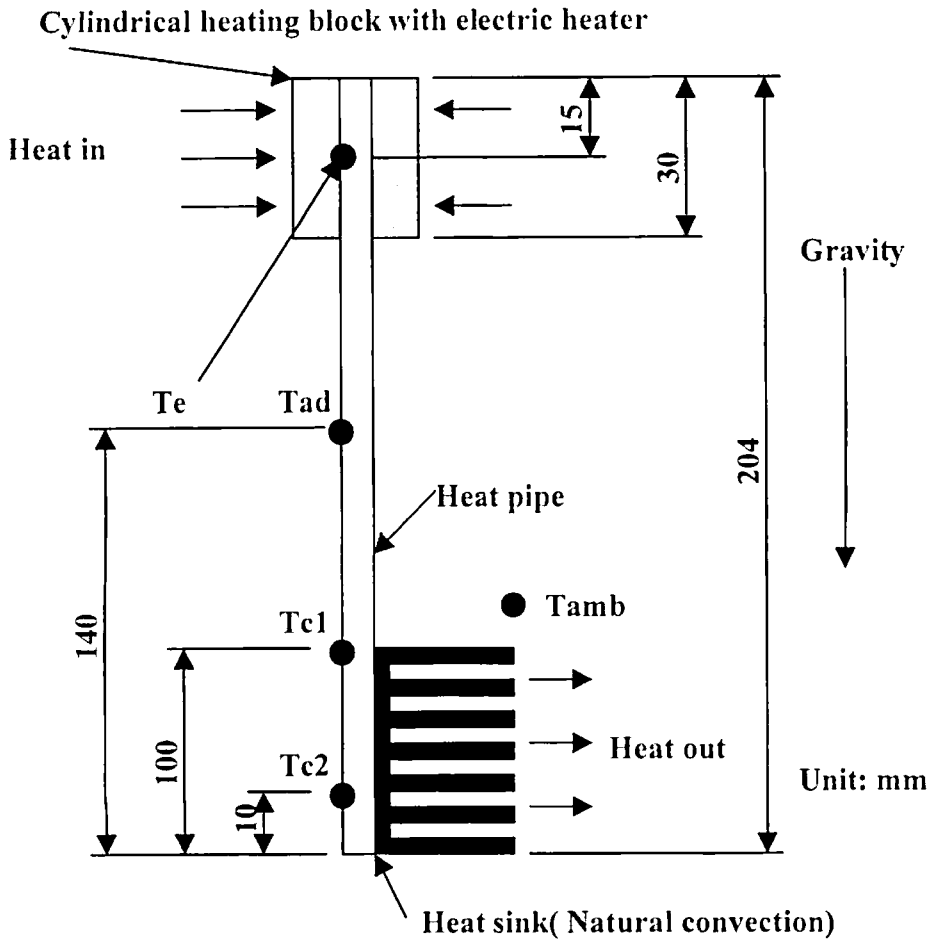

Fig. 3-3 Test setup and location of the thermocouples

The test setup is shown in Fig. 3-3. An electric heater was attached to the top end of the heat pipe (evaporator) using thermal grease over a length of 30 mm. The other end of the heat pipe (condenser) was cooled by a heat sink, which was attached using a thermal interface material over a length of 100mm. A stable power supply was used to generate the heat input into the heater, with power consumption measured by an ammeter and a voltmeter. The heat pipe was arranged at 90 degree inclination of top heat mode operation for all tests, except horizontal tests. The whole test setup was put into an acrylic box with a ventilating port for simulating natural convection at the condenser section of the heat pipe. The temperatures were measured and continuously recorded. The data was recorded under steady state condition. Approximately 1 hour of testing was performed for each increment of heat input. The location of the temperature measurement points are shown in Fig. 3-3. The tested heat pipe

configuration is presented in Table 3-1. The container is made of copper and the working fluid was distilled water.

Table 3-1 Heat pipe configuration for testing

Evaporator length	Condenser length	Outside diameter	Total length
30	100	4	204

Unit: mm

3.4 Discussion of the test results

Figure 3-4 shows the comparison between a normal fiber bundle wick and a super fiber wick heat pipe. It can be seen that by increasing the number of wires by a factor of 6 to 7 the thermal resistance can be decreased by as much as sixteen times. This can be explained by the fact that the number of capillary channels increases and the vapor space has been kept constant for both heat pipes.

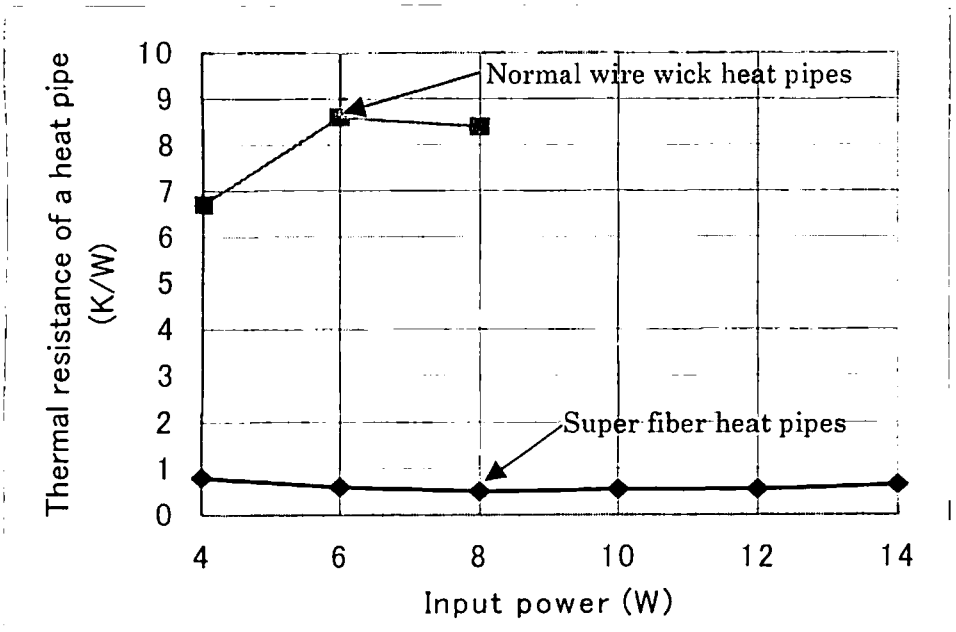

Fig. 3-4 Comparison between the normal and super fiber bundle wick structures (4mm OD MHP, L=204mm, Top heat mode)

Figure 3-5 shows the comparison between the horizontal and vertical top heat operation for the super fiber bundle heat pipe. It can be seen that there is no significant difference between the horizontal and vertical operation at lower power inputs.

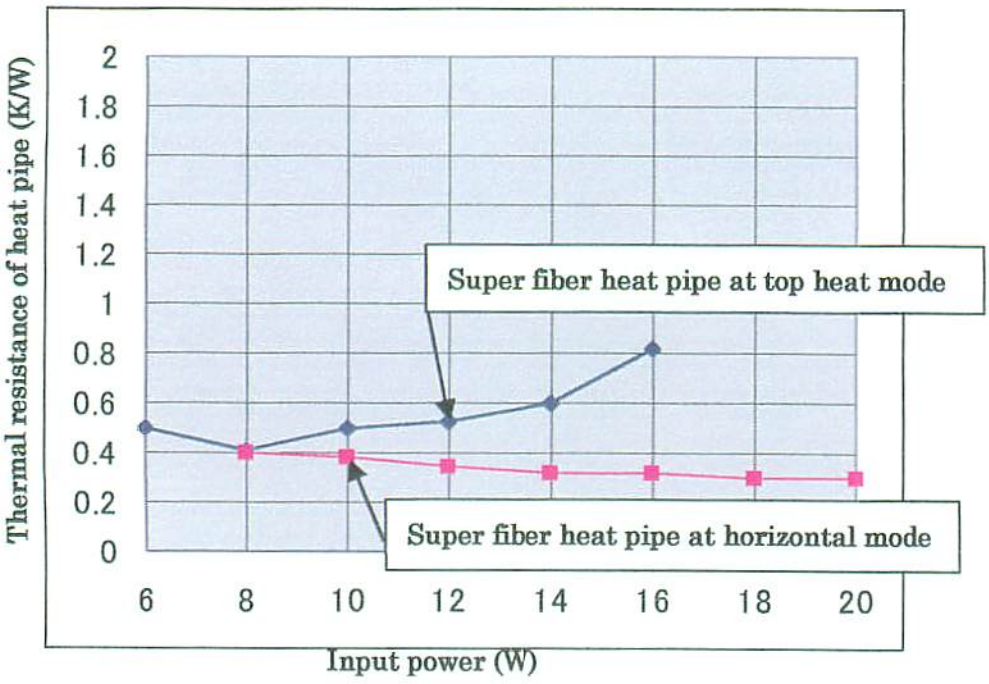

Fig. 3-5 Comparison between the horizontal and vertical operation for the super fiber bundle heat pipe, 4mm OD, L-204mm.

As the power increases the thermal resistance at top heat mode increases linearly. On the other hand, horizontal operation is almost constant up to more than 20 watts.

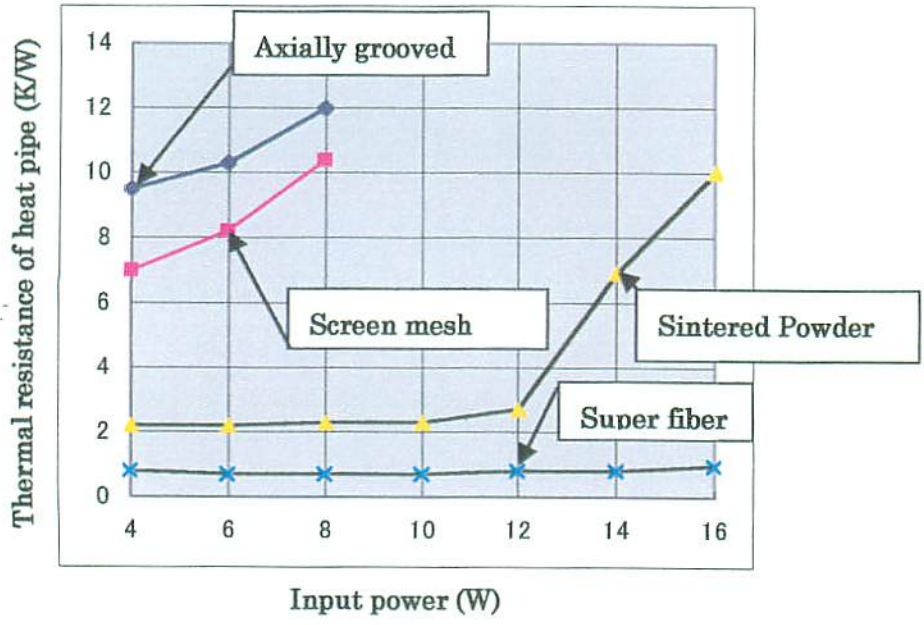

Fig. 3-6 Comparison between different types of wick structures at top heat mode

Figure 3-6 shows the thermal resistance of the different wick structures versus heat input. Even at low power input, the heat pipes show quite different characteristics. It can be seen that the grooved heat pipe had the highest thermal

resistance for the top heat mode operation. This is because the capillary force was small and the capillary limit was very low. The poor heat transfer performance of the mesh heat pipe was probably caused by the dry out phenomena due to high flow resistance and low permeability of the wick. Another consideration is that the mesh may not have been very well attached to the heat pipe internal wall. It can be seen from Fig. 3-6 that the sintered heat pipe and the super fiber heat pipe are the suitable wick structures for applications with high input power at top heat mode operation. The sintered heat pipe had a thermal resistance of more than 2 K/W. In this case, the flow resistance was quite high, because of the small capillary radius and of the random size of the sintered particles. It can be seen that the thermal resistance increased abruptly when the power input was greater than 12 W. On the other hand, the super fiber heat pipe had much lower and more stable thermal resistance even though input power increases over 12 watts. This superior performance may be explained by the fact that the wire wick heat pipe has a low flow resistance and high permeability, and that the capillary force is adequate to transport the liquid from condenser to evaporator. With the use of normal fiber bundle wick structure, we have found out that we can not reduce the thickness of the heat pipe lower than 1.5 mm. The results of this study have been applied for the fabrication of the 1.4 mm thick super fiber heat pipe, originally with an outside diameter of 3 mm. Experiments are under way to reduce the thickness of the heat pipe even lower than 1.4 mm without significant reduction of thermal performance. The thermal performance of the 3 mm OD heat pipe which was flattened to 1.4 mm thickness was also measured.

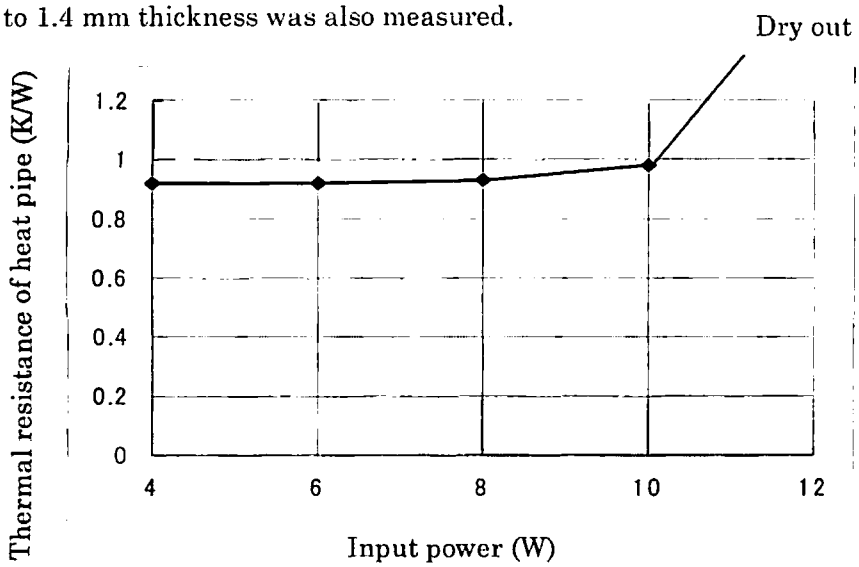

Fig. 3-7 Variation of the thermal resistance for the 1.4 mm thick heat pipe, 3 mm original OD, with super fiber wick, at horizontal orientation

Figure 3-7 shows the test results. It can be seen that it is possible to fabricate a 1.4 mm thick heat pipe with a thermal resistance of about 1 K/W. This result shows the improvement which can be obtained by using a super fiber wick structure for heat pipes used in electronic cooling applications. It may be concluded that:

·The vapor space and the number of wires affect the performance of the heat pipe with a fiber bundle wick structure.

·For top heat mode operations a smaller diameter wire and increased number of wires should be used.

·The super fiber wick has a much lower thermal resistance than other wick structures.

At top heat mode operations:

·The thermal resistance is much higher at top heat mode operation than horizontal operation.

·Further work is needed in developing a super fiber wick heat pipe with a thickness lower than 1.4 mm.

References

(3-1) Ioan sauciuc, Masataka Mochizuki, Kouichi Mashiko, Yuji Saito, Thang Nguyen, and Jeff Lev, *"The design and testing of an improved wick structure to be used in heat pipes for electronics cooling applications"*, Proceeding of the 11th International Heat Pipe Conference, pp.447-451, Tokyo, Septembr 1999.

(3-2) A. Faghri, *"Heat Pipe Science and Technology"*, Taylor and Francis Ltd, 1995.

(3-3) H. Xie, M. Aghazadeh, W. Lui and K. Haley, *"Thermal Solution to Pentium Processors in TCP in Notebooks and Sub-Notebooks"*, IEEE, Transaction on Components and Packaging and Manufacturing Technology, Part A, Vol. 19, No. 1, pp.201-210, March 1996.

(3-4) P. D. Dunn, D. A. Reay, *"Heat Pipe"*, Pergamon Press Ltd., 3 rd edition, 1982.

(3-5) T. Nguyen, M. Mochizuki, K. Mashiko, Y. Saito and K. Goto, *"Cooling CPU Using Hinged Heat Pipe"* , Proceedings of the 5th International Heat Pipe Symposium , pp.218-222, Melbourne, Australia, 1996.

(3-6) The Heat Transfer Engineering Data Book, (the 4th edition revision), JSME, p.46.

(3-7) Nguyen, T., M., Mochizuki, K., Mashiko, Y. Saito, I. Sauciuc, and R. Boggs, *"Advance Cooling System Using Miniature Heat Pipes in Mobile PC"*, Proceedings of the 6th ITHERM'98 Conference, pp.507-511, Seattle, USA, 1998.

(3-8) I. Sauciuc, M. Mochizuki, K. Mashiko, T. Nguyen and A. Akbarzadeh *"Enhancement of boiling heat transfer in heat pipes for use in electronics cooling applications"*, Proceedings of the 5th JSME-ASME joint Thermal Engineering Conference, AJTE99-6307, pp.1-5, San Diego, CA, USA, March 1999.

(3-9) I. Sauciuc, M. Mochizuki, K. Mashiko, Y. Saito, and T. Nguyen, *"The Design and Testing of the Super Fiber Heat Pipes for Electronics Cooling Applications"*, Proceeding of the 16th Annual IEEE Semiconductor Thermal Measurement and Management Symposium, pp.27-32, San Jose, CA USA, March 2000.

4. Development of thinner heat pipe and sintered wire heat pipe[4-1), (4-2)]

4.1 Request of thinner and high performance heat pipe

The thickness of most heat pipes used in general purpose laptop PC's is still 2 to 3 mm. With the advent of thinner laptop PC's, the demand for a thinner heat pipe with below 2mm has arisen. However, heat pipe has a limitation with regard to thickness due to the minimum requirement of the fluid flow passage. It is tough in trailing thinner heat pipe than 1.4 mm in this experiment. It is also essential to obtain smaller thermal resistance and to keep higher Q_{max}.

4.2 1.4mm thinner heat pipe

The thermal performance of a 1.4mm thick heat pipe by 3mm OD was measured and preliminarily discussed in chapter 3. However, that was approximately 10 watts as maximum heat transfer rate at horizontal mode. Here, a bigger size and thinner heat pipes were fabricated and measured to meet the large heat generated by the MPU, which was greater then 16 Watts. Figure 4-1 shows a typical test set up to measure thermal resistance and Q_{max} of heat pipe. The evaporator was attached to the heating block with electric heater and a condenser had forced a cooling heat sink with a miniature fan.

Unit : mm

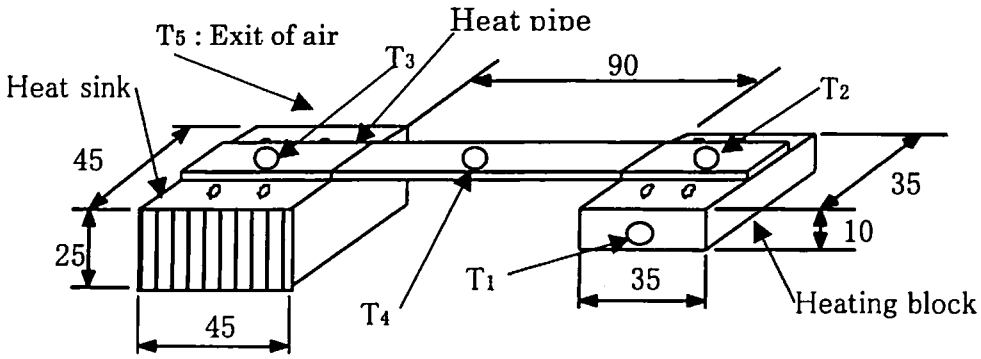

Fig. 4-1 Test setup to measure thermal resistance and Q_{max} of a heat pipe

In this experiment, a heat pipe was used in the following dimension.

Outside Diameter (OD)	6 mm original
Length of heat pipe (L)	170 mm
Thickness of Heat pipe(T)	1.4 mm
Width of heat pipe (W)	8.7 mm

0.05mm OD wires were used to form the wick structure. Temperature measuring points are shown in Fig. 4-1.

T_1 : Temperature of a heating block

T_2 : Temperature of heating area on a heat pipe

T_3 : Temperature of cooling area on a heat pipe

T_4 : Temperature of adiabatic section on a heat pipe

T_5 : Atmospheric temperature

$\Delta T=T_2-T_3$: Temperature difference of heat pipe

The thermal resistance of heat pipe can be calculated from equation (4-1).

$$R_{hp}=\Delta T / Q \quad (°C/W) \qquad (4\text{-}1)$$

Q: Heat input (watts)

Table 4-1 shows the measured thermal resistance with varying heat input in horizontal orientation.

Table 4-1 1.4mm thick heat pipe thermal resistance

Heat input [W]	T_1 [°C]	T_2 [°C]	T_3 [°C]	T_4 [°C]	T_5 [°C]	ΔT [°C]	R [°C/W]
4.01	65.1	61.7	49.9	56.0	29.2	11.8	2.94
6.13	79.1	74.7	62.0	66.6	30.8	12.7	2.07
8.11	93.3	87.6	74.4	77.4	33.5	13.2	1.63
10.2	106.1	98.9	84.6	87.1	35.2	14.3	1.40
11.9	118.6	110.3	93.6	94.8	35.7	16.7	1.40
14.0	130.4	121.0	102.4	102.7	36.6	18.6	1.33
16.2	142.3	131.7	110.8	110.0	37.2	20.9	1.29

Figure 4-2 shows the relation between ΔT and input power. This still reflects stable performance of a 1.4 mm thick heat pipe without limitation of heat transfer. In this experiment, Q_{max} was not found, because the temperature of T_1 became too high when input power was increased to over 16 watts.

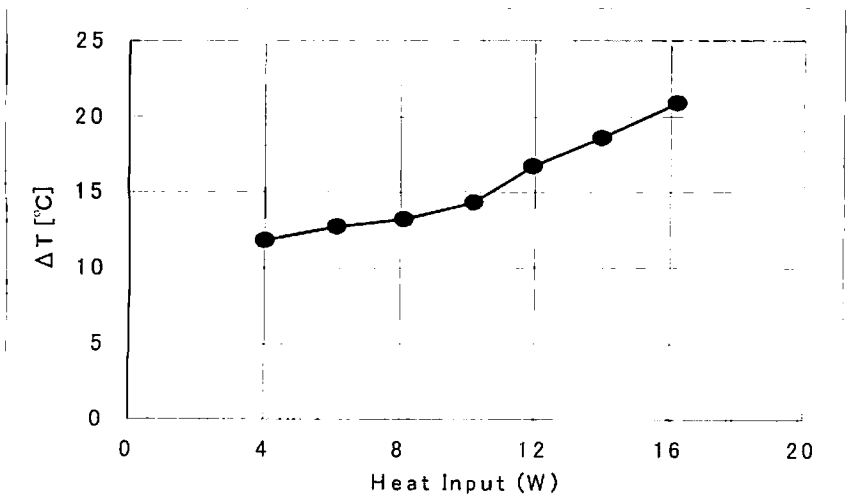

Fig. 4-2 The relation between ΔT and input power in 1.4 mm thick heat pipe

The heat flux of evaporator at 5.3 W/cm ^{2} input was obtained from equation (4-2).

q_e = 16.2 W / (3.5cm × 0.872cm) (4-2)

= 5.3 W / cm^2

At this time, thermal resistance of the heat pipe is Rhp=1.29 K/W.

On the other hand, thermal resistance of a traditional heat pipe with wire wick is shown in Fig. 2-6. These data were obtained by heating both surfaces with 50 mm long. If the condenser effect was omitted, the thermal resistance may be changed. The thermal resistance of 0.39 K/W was obtained in the case of 50mm long surrounded evaporator, two side heating, original OD 6mm, and 2 mm thick heat pipe, as shown in Fig. 2.6. Meanwhile, the test described above was conducted by one side heating. Therefore, it will be estimated to be doubled of 0.39 K/W when we use a one side heating block as occurs in real MPU heating.

0.39 K/W × 2 × 50mm / 35mm = 1.1 K/W

The above value after converting to the same geometry of 1.4mm thick and test sample has almost the same measured resistance. This is the minimum thickness of wired wick heat pipes. Figure 4-3 shows a method of making a thinner heat pipe.

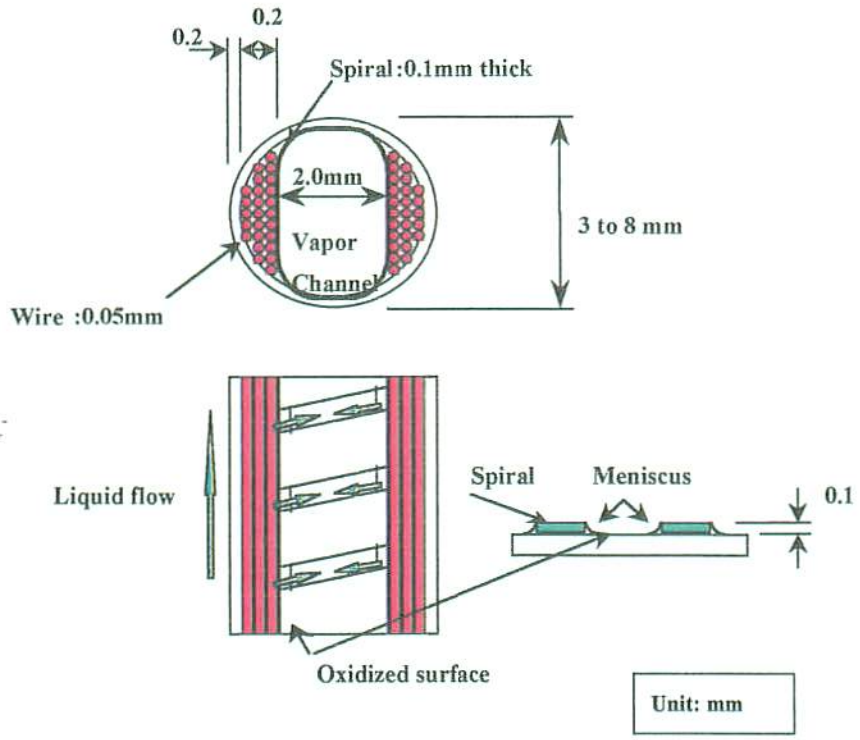

Fig. 4-3 Local wire bundle heat pipe

Firstly, two pieces of wire bundle are inserted into the tube with a spiral. A spiral

should push wires onto the inside of the tube. Recommended spiral size is perhaps 0.3 mm width and 0.1 mm square flat wire made of phosphor-bronze. The objective of wires at both sides is to feed working liquid straight from end to end which is able helped by secondary liquid feeding caused by meniscus between the spiral in contact with the internal copper surface. Also, it would be helpful to use copper surface with oxidization. Pure copper surface does not have good wet-ability. A very thin 1 to 2 Mm layer of cupric oxide (Cuo) may help to improve the wetting of the surface. The Cuo layer is black color. However, CuO may cause chemical reactions with vapor inside of heat pipe. Therefore, it is necessary to include a pre-oxidization treatment as follows:

1) 150 to 250 ℃ heating in oven by atmosphere for 1 to 2 hours.
   Surface of copper can be changed to black CuO.
2) 500℃ heating by N_2 or N_2 + 3%H_2 gas purge for 1 to 2 hours.
   Surface of CuO will be changed to Cu_2O which color is salmon-pink.

Cu_2O is more stable against vapor or water atmosphere inside the heat pipe and of course good wet-ability with water.

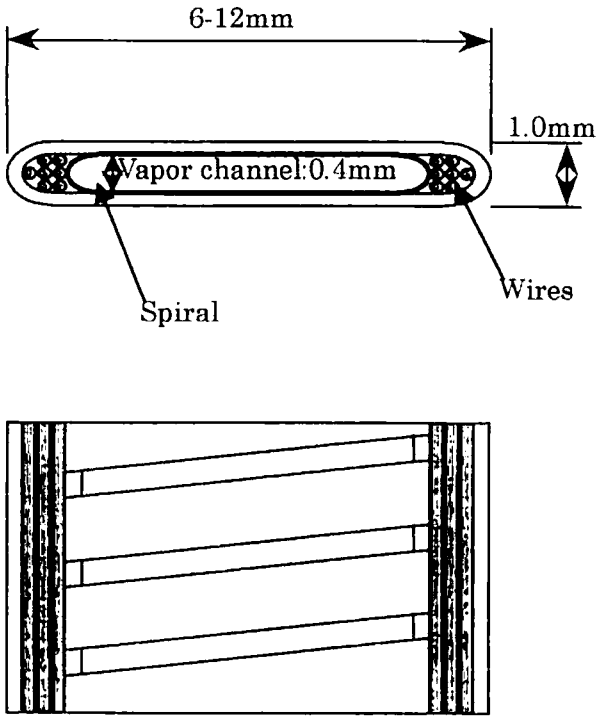

Fig. 4-4 Thinner flattened heat pipe with local wire bundle

Figure 4-4 shows an example of thin heat pipe of 1 mm thick made by the local wire bundle wick design. It can work well but it is was found that maximum heat flux at the evaporator is limited to approximately below 5 W/cm^2.

4.3 Sintered wire wick heat pipe

4.3.1 How to reduce thermal resistance of heat pipe

Compared to grooved heat pipes, wire wick heat pipes provide higher capillary force, but the thermal resistance of such a heat pipe is larger than with the grooved heat pipe because the wick is floating on the heat transfer surface. This chapter introduces sintered wire wick heat pipe which is an improvement because of lower thermal resistance. As shown in equation (4-1), the thermal resistance of a heat pipe depends on the heat transfer coefficient and the heat transfer area at the evaporator and condenser. A bottleneck occurs at the evaporator in the case of most PC cooling. The heat transfer area can be enlarged while maintaining the high capillary force. This author investigated the sintering of the wires onto the copper tube. As a result, all of heat input can be transferred directly to the wire wick.

4.3.2 Testing sample and setup

Here, a the sintered wire wick heat pipe sample was fabricated with the following specifications:

1) Size : Original OD 6mm, t=0.4mm, flattened to 2.5mm
2) Wick : 0.05 mm wire × 400 pieces
3) Length : 172 mm long

After wire wicks with a spring is inserted into a copper tube, it put into the continuous furnace at 1050 ℃ for 1 hr. with nitrogen + 3% hydrogen atmosphere. The wires can be sintered with internal copper tube.

4.3.3 Test data

Figure 4-5 shows the test setup. Cooling of the condenser section was provided by a heat sink with a miniature fan. Also, Figure 4-6 shows a photo of the test setup. Figure 4-7 shows the thermal resistance of three types of heat pipes: conventional wire (0.05 mm × 400 pieces), axially grooved (0.1mm square grooved), and sintered wire (0.05 mm × 400 pieces) when L_{eff} is set up at 84.5mm. ΔT between T_e and T_c were lower than 2 ℃ in three types, and then thermal resistance was lower than 0.15 K/W. From Q_{max} point of view, there is no indication of any dry-out even at an input power of 50 watts. Figure 4-8 shows the thermal resistance of heat pipes in L_{eff}=109.5mm. Axially grooved heat pipe has started to dry-out after being heated up to 40W. Axially grooved heat pipe showed the dry-out phenomenon at 20W when L_{eff} is 127mm in Fig. 4-9. Sintered wire heat pipes can achieve lower thermal resistance even at higher Q_{max} values.

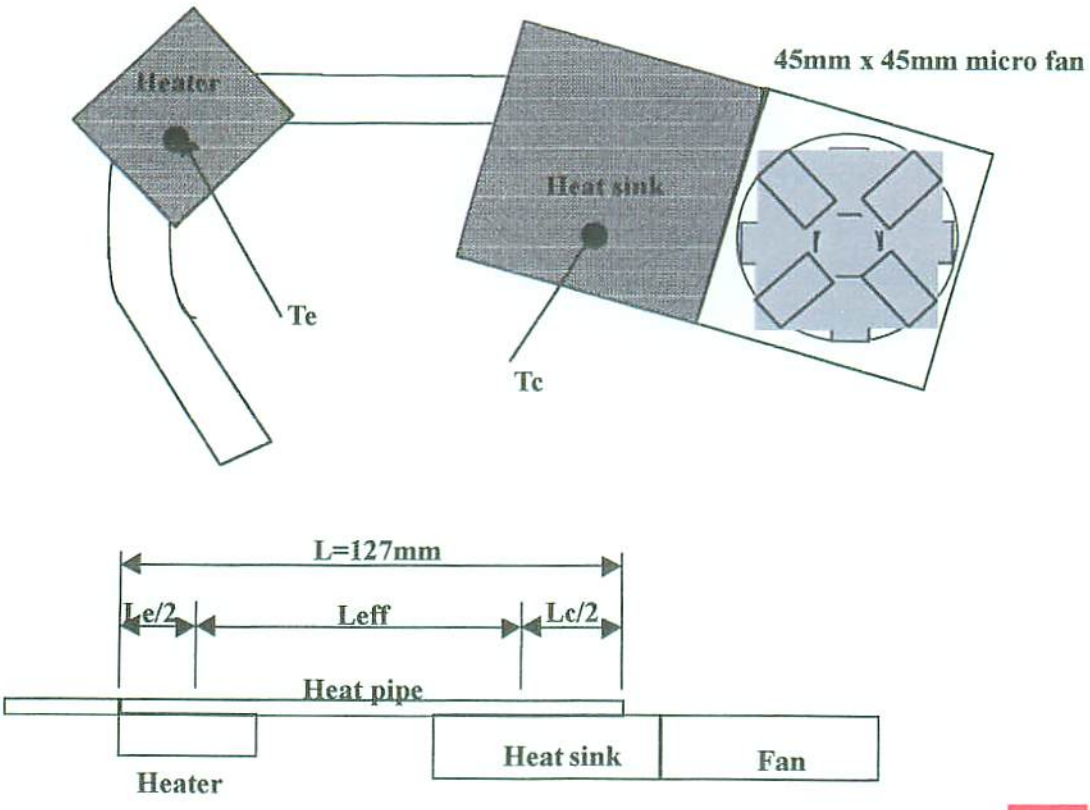

Fig. 4-5 Test setup

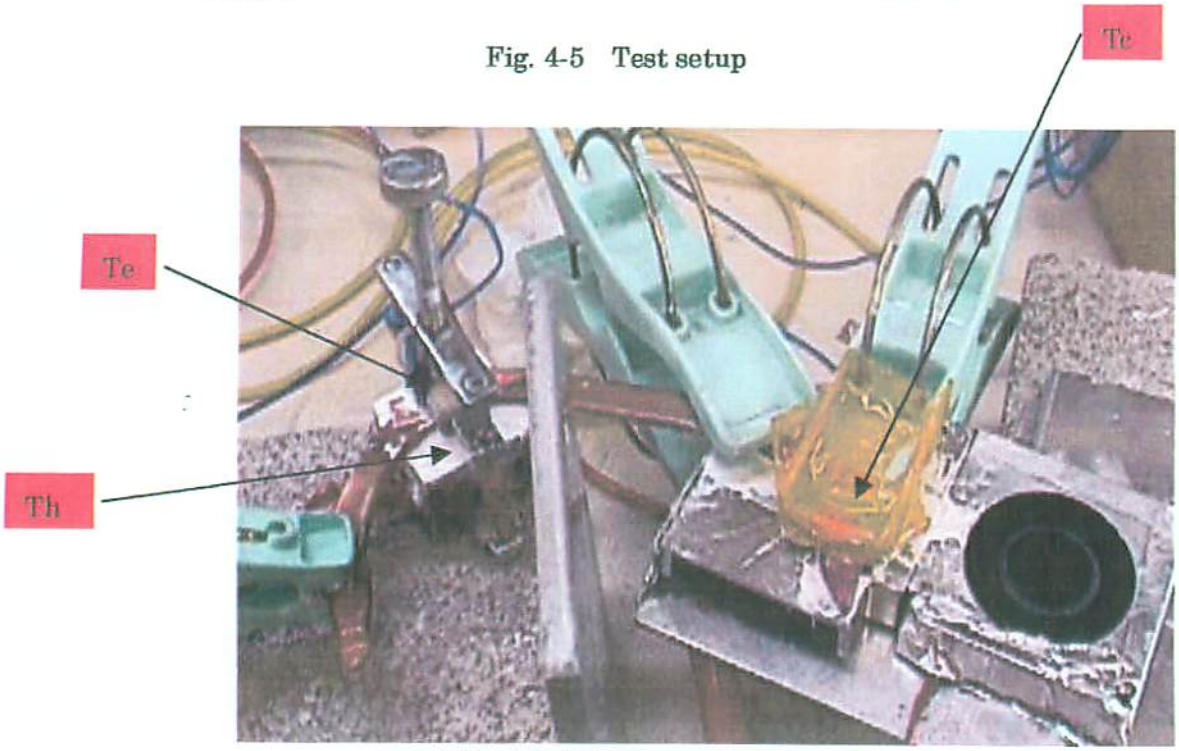

Fig. 4-6 A photograph of test setup

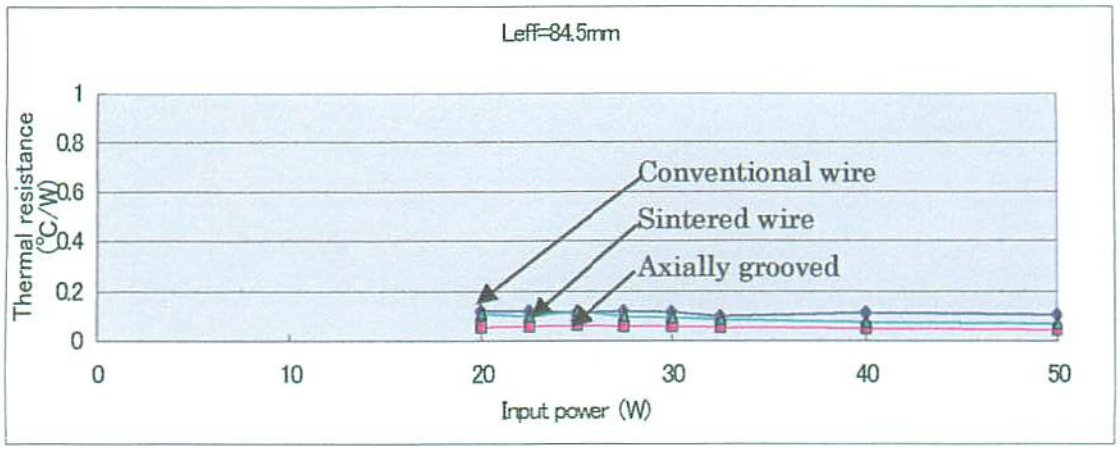

Fig. 4-7 Thermal resistance of heat pipes at L_{eff}=84.5mm

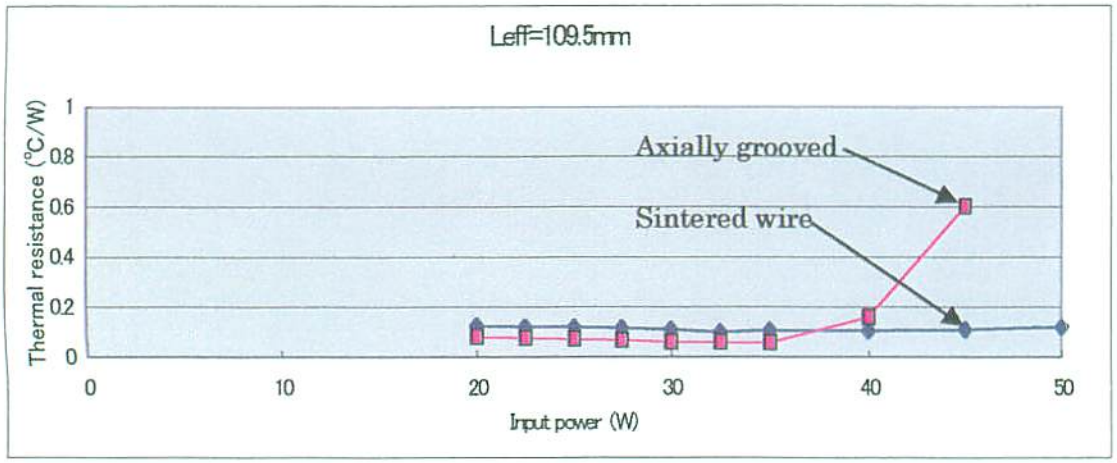

Fig. 4-8 Thermal resistance of heat pipes at L_{eff}=109.5mm

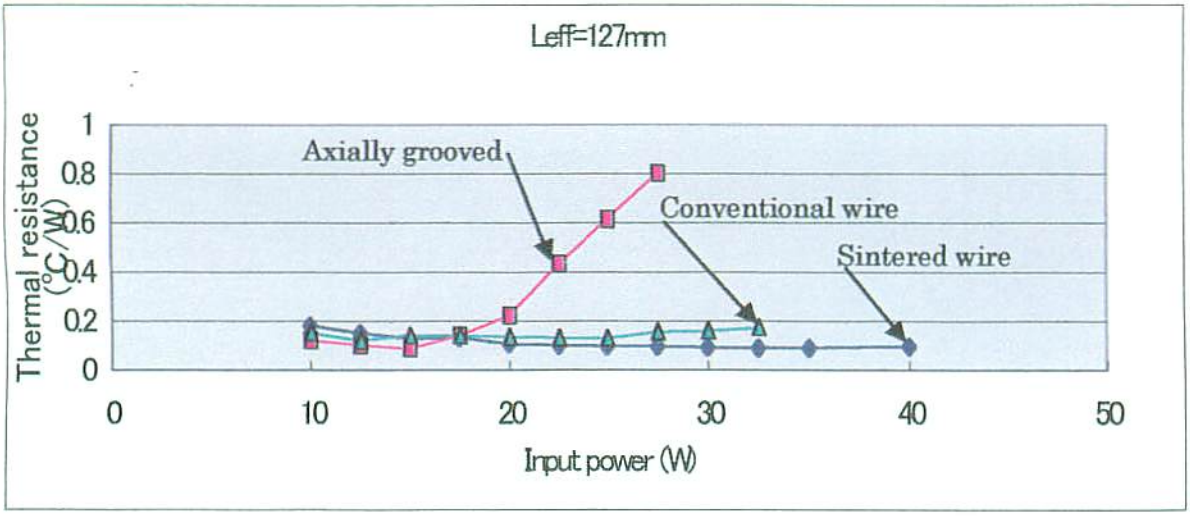

Fig. 4-9 Thermal resistance of heat pipes at L_{eff}=127mm

Figure 4-10 shows the measured data at 15 degrees inclination of top heat mode in the case of L_{eff}= 84.5 mm. In axially grooved heat pipe, dry-out took place at over 17W. Wired and sintered pipes do not have any dry-out problem even at high heat input over 30 W.

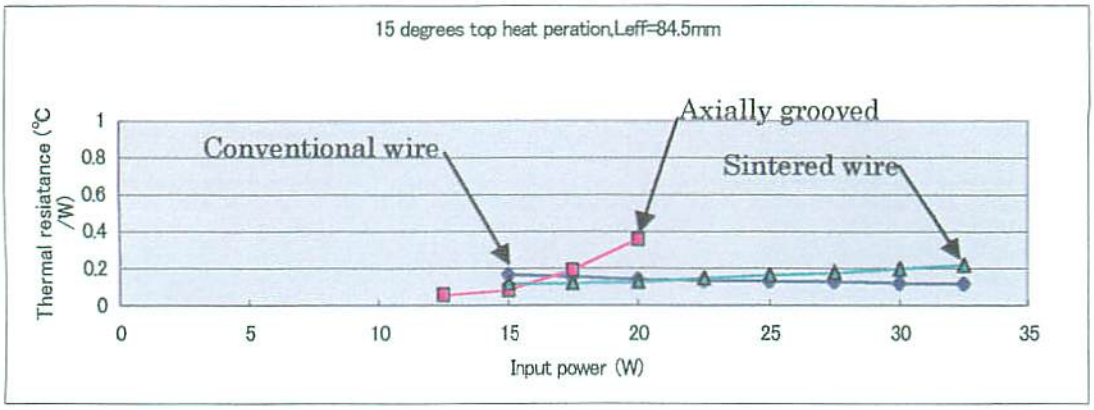

Fig. 4-10 Thermal resistance of heat pipes at 15 degrees top heat mode and L_{eff}=84.5mm

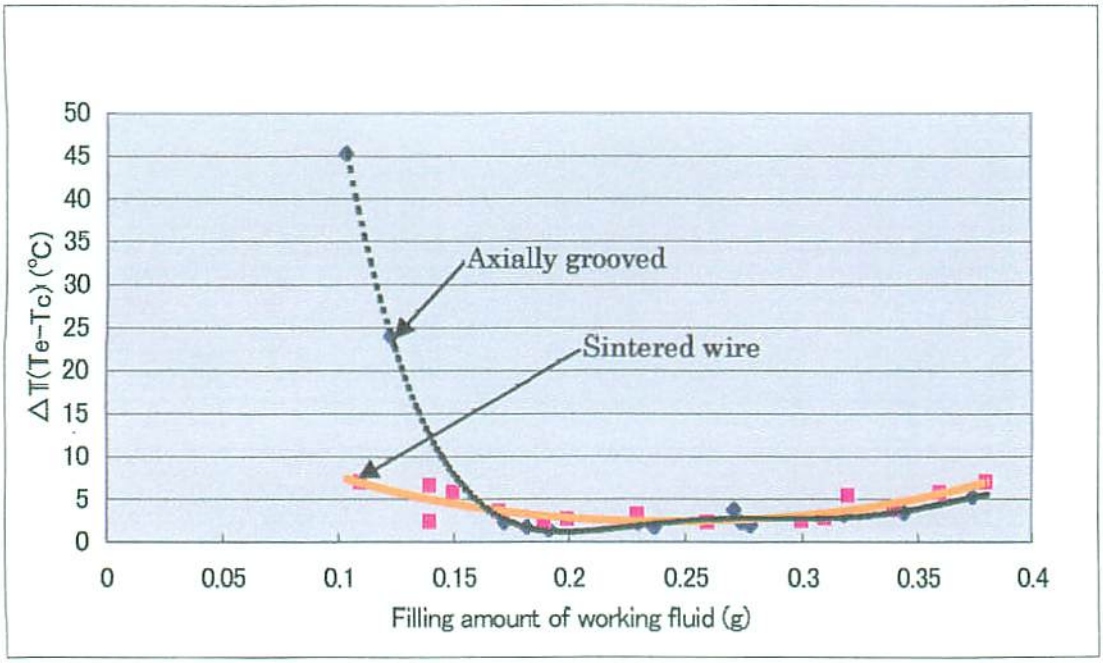

Fig. 4-11 The relation between ΔT and filling amount of working fluid

Figure 4-11 shows the relation between ΔT (T_e-T_c) and filling amount of working fluid. It was found that lower filling amount for the axially grooved heat pipe resulted in larger thermal resistance. On the other hand, the sintered wire heat pipe can have wider range of lower thermal resistance.

References

(4-1) M.Mochizuki, Y. saito, I. Sauciuc, and Y. Kawahara, *" Thermal Characteristics of Fine Fiber Wicks Heat Pipe"*, Pre prints of 37th Japan Symposium of Heat Transfer, A-154, pp.43-44, 2000

(4-2) K. Eguchi, M. Mochizuki, K. Mashiko, K. Goto, Y. Saito, Y. Nagaki, A. Takamiya, T. Nguyen, and I. Sauciuc, " Micro Heat Pipe for Cooling CPU ", Fujikura Technical Review No.27, pp.63-67, 1998.

5. Reliability of heat pipe

5.1 Required item of reliable heat pipe

A heat pipe is a typical passive heat transfer element without movement, filled with working fluid and sealed under vacuum condition. Reliability is therefore an issue of concern and the following items were tested and discussed.

1) Long term performance by accelerated life test.

2) Industrial level quick evaluation

3) Frozen startup

5.2 Prediction of long-term performance of miniature heat pipes by accelerated life tests [5-1 ~5-5]

5.2.1 Necessity of heat pipe reliability

Due to the limited space, most PC's and telecommunication systems place constraints on the size of heat pipes, so that normally heat pipes of a diameter 3 or 4 mm and length less than 400 mm are preferred. For heat pipes of this size the available internal volume is generally low, usually less than 1 cm^3. Therefore, if any non-condensable gases remained or generated after heat pipe fabrication, the heat transfer capabilities of the heat pipes are influenced, and in turn cause a degradation in the cooling performance of the designed thermal solutions. Normally, the reliability requirement of heat pipes is a minimum of 10 years without appreciable degradation in performance. Heat pipe technology is relatively new, and reliability and life test information is quite scarce. Therefore, the purpose of this study was to determine if the Arrhenius model can predict non-condensable gas generation in heat pipes from the accelerated life tests. Many failure mechanisms in heat pipes involve similar chemical reactions by metal and working fluid, after which the Arrhenius model can often be applied to the life test data. Mechanisms that change with time often fits this model, for example, corrosion, oxidation, diffusion and creep mechanisms. In these cases, a logarithmic plot of the response parameter against the reciprocal of the absolute temperature shows a straight line relationship. In this study, the author did not measure the non-condensable gas, but it was assumed that the amount of non-condensable gases generated in the heat pipe were proportional to the temperature drop in the heat pipe. At present, heat pipes are widely used in computer, telecommunication and other various electronic equipment. It is estimated that more than 75% of high performance notebook computers have integrated heat pipes as thermal solutions today. It is therefore crucial to carry out life tests as well as accelerated life tests to determine the performance reliability of heat pipes. Most of the heat pipes used in the computer industry are copper-water heat pipes because water is a safe environmental fluid, and it is also the best heat transport fluid in the medium

operating within a temperature range of 50 to 150 °C for computers.

Usually, the main cause of heat pipe degradation is the generation of non-condensable gases, which accumulate in the heat pipe condenser.[5-3~5-4] Heat pipe performance degrades as a result of (1) chemical reaction that generates non-condensable gases or (2) corrosion and erosion of the container and wick. Although heat pipes rarely undergo catastrophic failure, the amount of non-condensable gases that accumulate in the condenser with time, will form a diffusion barrier to vapor flow and will reduce the available condenser area. Corrosion and erosion of the container and wick can be manifested as a change in the wetting angle of the working fluid as well as the permeability, porosity, or capillary pore size of the wick. Solid precipitation resulting from corrosion and erosion are transported by the flowing fluid to the evaporator region where they are deposited when the fluid vaporizes. This leads to increased resistance to fluid flow in the evaporator, resulting in a decrease in the heat transport capacity of the heat pipe. Most literature describes that copper is compatible with water but little or no life test data is available. Most efforts in obtaining life test data are concentrated on steel-water heat pipes. Murakami et al.[5-1~5-2] provided life test data and life estimation for phosphorous deoxidized copper-water heat pipe and oxygen-free copper-water heat pipe. They tested heat pipes which were of a grooved type, 6.35 mm in diameter and 200 mm long. They found that the phosphorous copper-water heat pipe generated an appreciable amount of non-condensable gas, while the oxygen-free copper-water heat pipe generated a slight amount of non-condensable gas. The non-condensable gas was mainly composed of CO_2, O_2, H_2, and N_2. They predicted that the oxygen-free copper-water heat pipe would degrade about 5 °C in 20 years under the operating temperature of 60 °C. The primary objective of the present author is (1) to carry out life tests on copper-water heat pipe, (2) to perform accelerated tests on heat pipes at elevated temperatures and (3) to use a simple Arrhenius plot to predict long-term heat pipe performance.

5.2.2 Experimental setup

16 samples of commercially available oxygen-free copper-water heat pipes were used for the accelerated life test. They were round heat pipes with fine fibers as wicks in contact with the inside wall of the pipe. A thin spiral coil inserted centrally along the pipe and provided a radial force to pushing the fiber wicks against the container. The spiral coil also acted partially as a flow separator between vapor and liquid. The container, fiber wicks and spiral coils were all oxygen-free copper. All 16 heat pipes tested were 3 mm in diameter and 250 mm in length. The 16 heat pipes were divided

into 4 sets of 4 heat pipes. Each set was tested at a fixed constant accelerated temperature. The accelerated temperatures were 40, 70, 100 and 130 °C. Figure 5-1 shows the test set up. Each set of heat pipes is placed in a separated copper block that was heated by use of an AC electric heating element which is regulated to maintain the block at constant set temperature. The block is fully insulated. The evaporator and condenser lengths are about 65 mm and 130 mm respectively. Cooling is controlled by natural air convection from the surface of the heat pipe condenser to the ambient air.

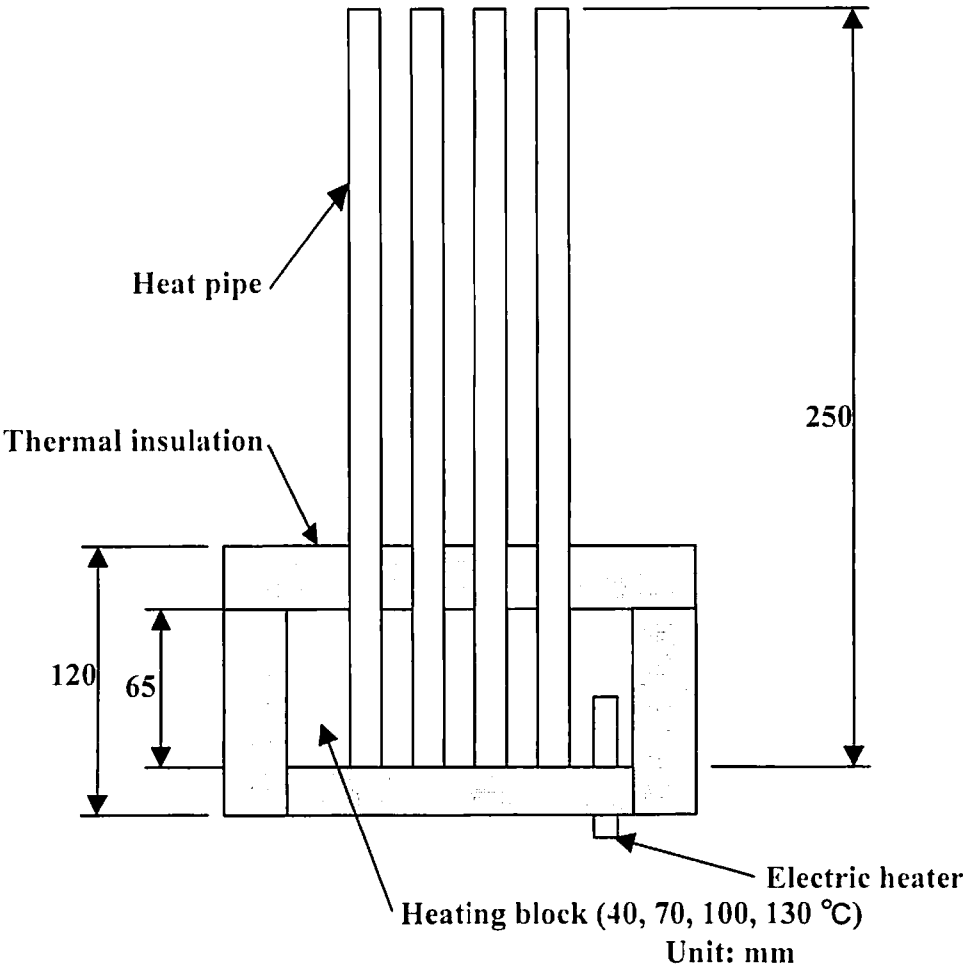

Fig. 5-1 Accelerated life test set up

Each set of heat pipes was heated constantly at the set temperatures for a long period of time. The tested heat pipes were removed from elevated temperatures and tested at 40 °C and the temperature drop ($\triangle T$) of the heat pipes were measured as shown in Fig. 5-2. After these temperature drops were measured, the heat pipes were placed in

their original test set up.

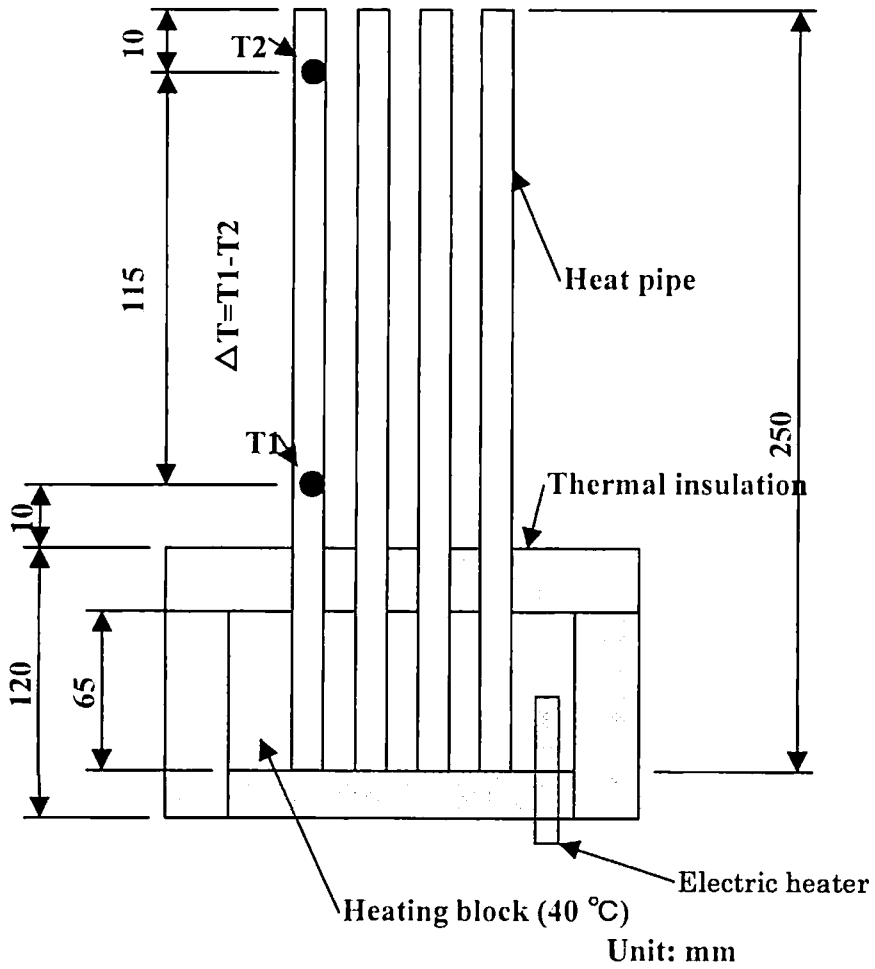

Fig. 5-2 Test setup to measure heat pipe performance temperature difference (△T)

5.2.3 Analysis of data by the Arrhenius model

Figure 5-3 shows the raw data of accelerated life tests for elevated temperatures of 70, 100 and 130 °C for more than 350 days. The 40 °C data set was not included because generally it showed no degradation in heat pipe performance during the tested. When many failure mechanisms are involved in an activation process, the Arrhenius model can often be applied to life-test data. Mechanisms that involve rate processes such as corrosion, oxidation, diffusion and creep, often fit this model. In these cases a logarithmic plot of the response parameter (F) against the reciprocal of the absolute temperature is a straight line relationship. In general, the model can be described by the equation (5-1).

$$F = \text{const} \cdot \exp(A/kT) \qquad (5\text{-}1)$$

where,

A = Activation energy of the reaction (J),

k = Boltzmann's constant (J/K),

T= Absolute temperature (K)

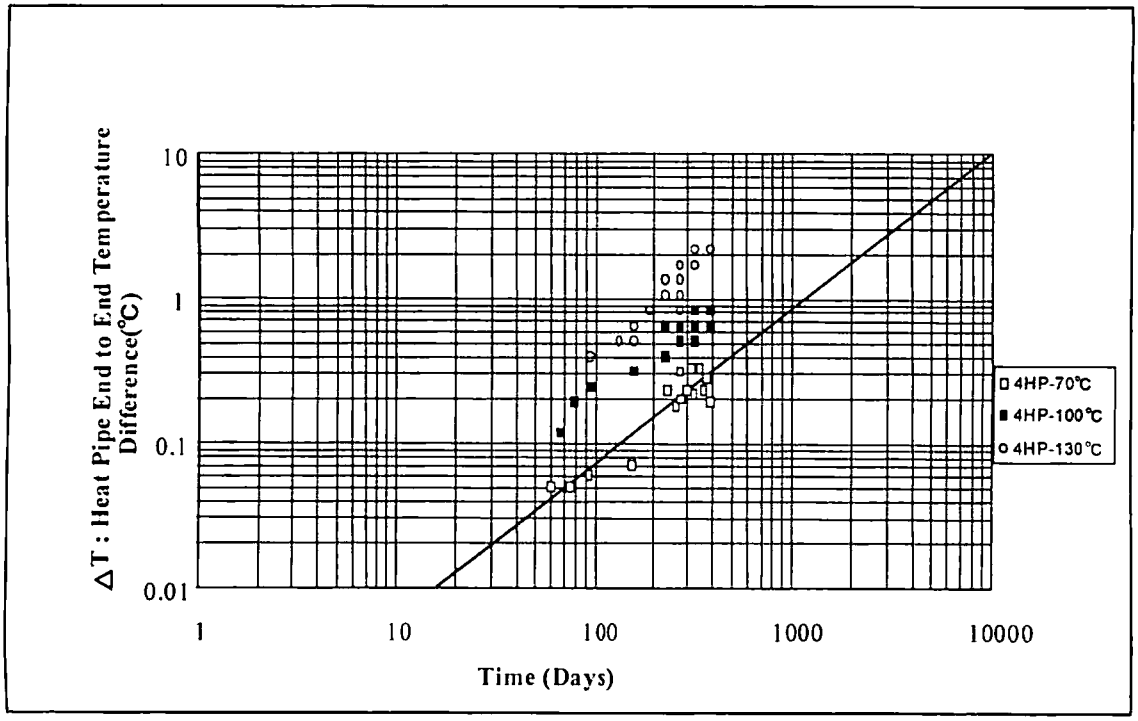

Fig. 5-3 Raw data of heat pipe temperature difference vs. elapsed time

It is assumed that the amount of the non-condensable gas generation can be expressed by equation (5-2).

$M(t,T) = f(t)*F(T)$ (5-2)

where,

M = Mass generation rate

t = Time

Since the non-condensable gas volume was not measured, it was therefore assumed for the sake of simplicity that the amount of non-condensable gases was directly proportional to the heat pipe performance temperature drops as indicated by equation (5-3):

$\triangle T(t,T) = f(t)*F(T)$ (5-3)

where $\triangle T$ is the heat pipe performance temperature drop and F(T) is the shift factor, which was given by the Arrhenius relationship in equation (5-1). If this is the case, it shifts the temperature drop in Fig. 5-3 along the time scale to establish a universal

curve as shown in Fig. 5-4. The factor by which each set of data is shifted is the shift factor F(T). Finally, the shift factors were plotted on an Arrhenius plot as shown in Fig. 5-5, which shows that the shift factors do fall on a straight line on an Arrhenius plot and fit the Arrhenius model depicted by equation (5-1).

Foe example, let's assume that the allowable heat pipe degradation is 5 °C at operating temperature of 70 °C. In this situation, the universal curve in Fig.5-4 results in the product of time and shift factor being equal to 5,500 days. Since the shift factor for 70 °C equals 1, the predicted time required for the heat pipe to degrade 5 °C is 15 years.

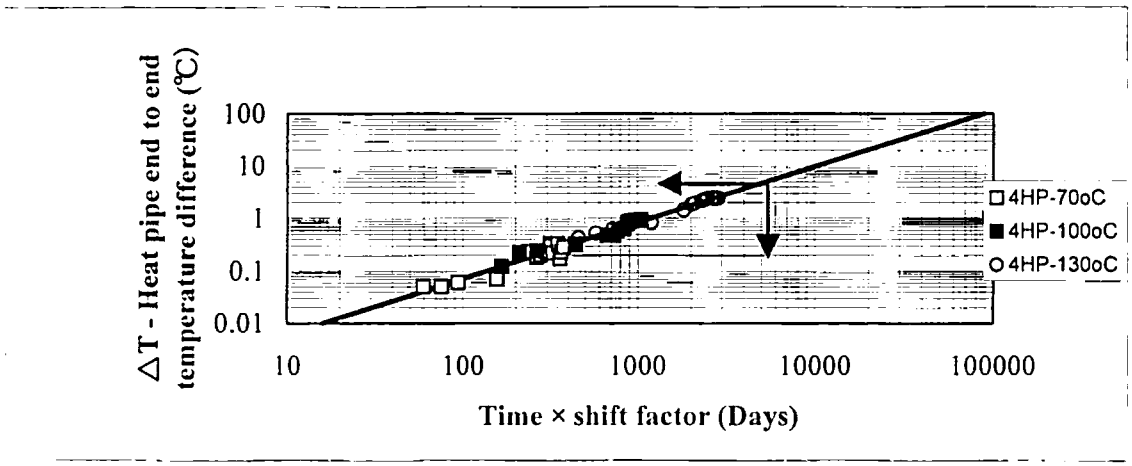

Fig. 5-4 Universal curve

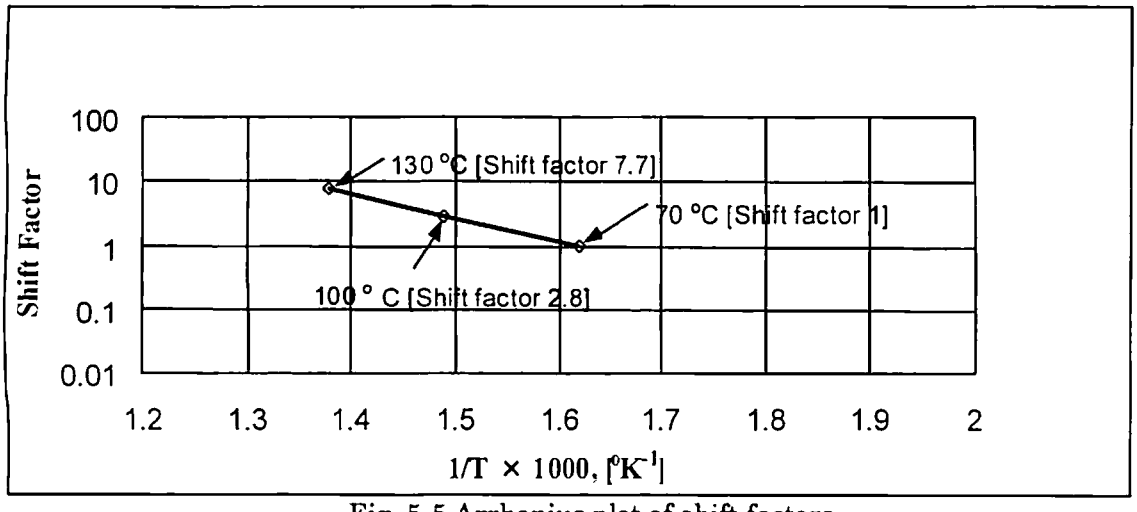

Fig. 5-5 Arrhenius plot of shift factors

5.2.4 Discussion

(1) Data obtained for the accelerated life tests did fit the Arrhenius model. Therefore, the above analysis is valid and can be used to predict the heat pipe performance

temperature drop ($\triangle T$) at various operating temperatures over longer periods than actually tested.

(2) The predicted period for a heat pipe to degrade is approximately 5 °C is over 15 years of continuous operation at a temperature of 70 °C.

(3) It is essential to continue the acceleration life tests for a longer period of time to validate the model further.

(4) Easy evaluation at industrial level check

In general, the speed of a chemical reaction can be estimated by the simple Arrhenius model. For instance, it will accelerate at twice the rate when the operating temperature increases 10 °C .

Assuming this, it can be shown, as in equation (5-4), that

$$L_{60} = K_0 \cdot A_0^{(\Delta t/10)} \qquad (5\text{-}4)$$

where, A_0 : Accelerated factor

K_0 : Heating time (hours)

L_{60} : Predicted life time in case of operation at 60°C (hours)

Δt : Tel-To (°C)

T_{el} : Elevated heating temperature (°C)

T_o : Normal operating temperature (°C)

When the accelerated heating temperature of the heat pipe is assumed to be 180°C (T_{el}) for 20 hours, the predicted life time at 60°C (To) can be estimated as follows.

$$L_{60} = 20 \cdot 2^{(120/10)}$$

$$= 20 \cdot 4096$$

$$= 8,1920 \text{ hours}$$

$$= 10 \text{ years}$$

Fig. 5-6 shows a hot water heating test for a heat pipe. The temperature of the bath is controlled at 50°C, which ideally should be lower than 60°C due for checking of the temperature drop of the expanded non-condensable gas. Before the acceleration test, T_1 and T_2 of the heat pipe are measured through the hot water dipping test.

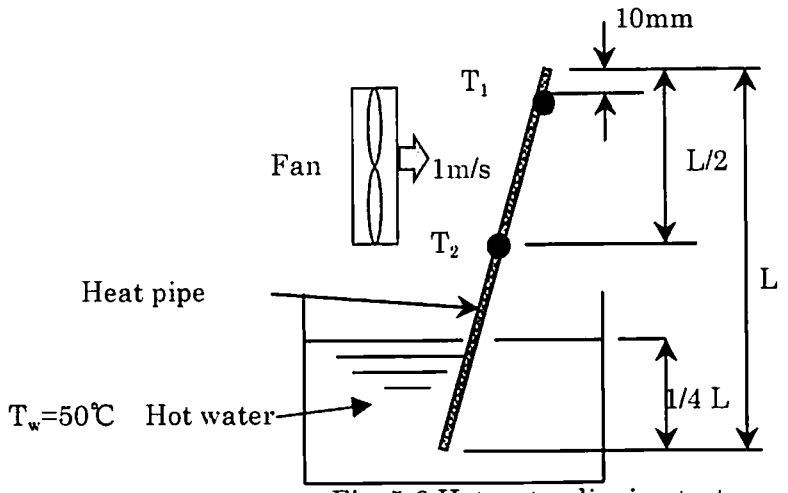

Fig. 5-6 Hot water dipping test

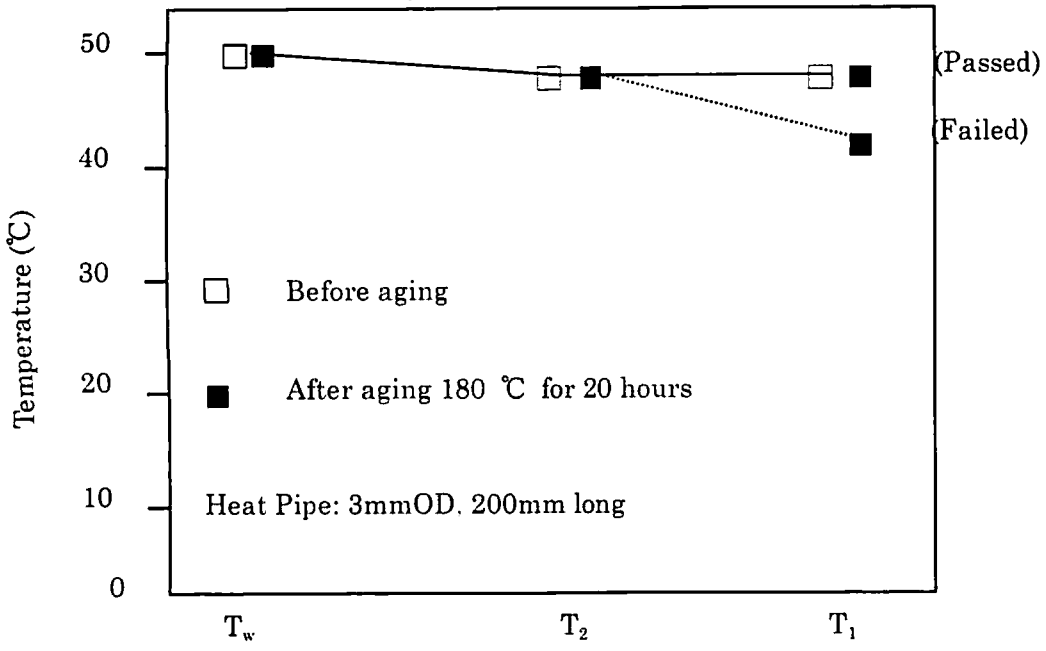

Fig. 5-7 Temperature distribution of passed and failed heat pipe after acceleration

After an aging test of 180℃ for 20 hours, the heat pipe will be checked for T_1 and T_2. If non-condensable gas generation does not take place through heat pipe aging, $\triangle T=T_2-T_1$ will be within 2 ℃ and T_2 should be the same temperature level. Figure 5-7 shows the temperature distribution of both types of heat pipe. When non-condensable gas was generated, the heat pipe showed a temperature drop of T_1.

5.3 Long-term operation test

As a simple life test, heat pipes are operated on a long-term basis. Heat pipes were heated at horizontal mode operation for 12,500 hours. The samples of heat pipe used were 4mm OD × 256mm long copper-water heat pipe with copper wire. The evaporator was heated by an 80 mm long electric heater block and the condenser was cooled by natural convection air. Figure 5-8 shows the temperature change of T_1(10mm from top) and T_2 (just center of the heat pipe at adiabatic section). Insignificant changes in temperature drops were recorded through out the 12,500 hours heating. The actual temperature differences between T_2 and T_1 were within 2 or 3℃.

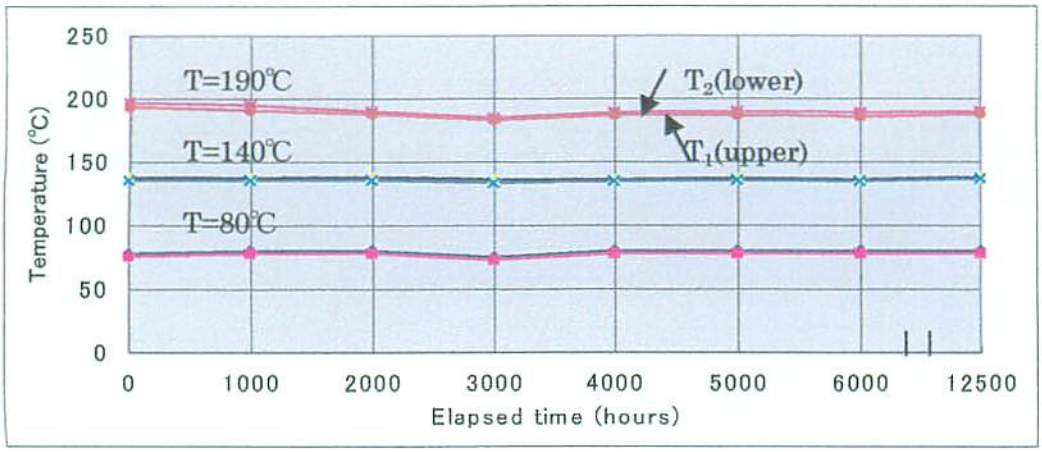

Fig. 5-8 Long term operation test of heat pipes at horizontal mode

Figure 5-9 shows long term heating test data of the same size heat pipe in the case of a top heat mode operation. Neither the top heat mode nor the long-term operation resulted in the occurrence of any major change.

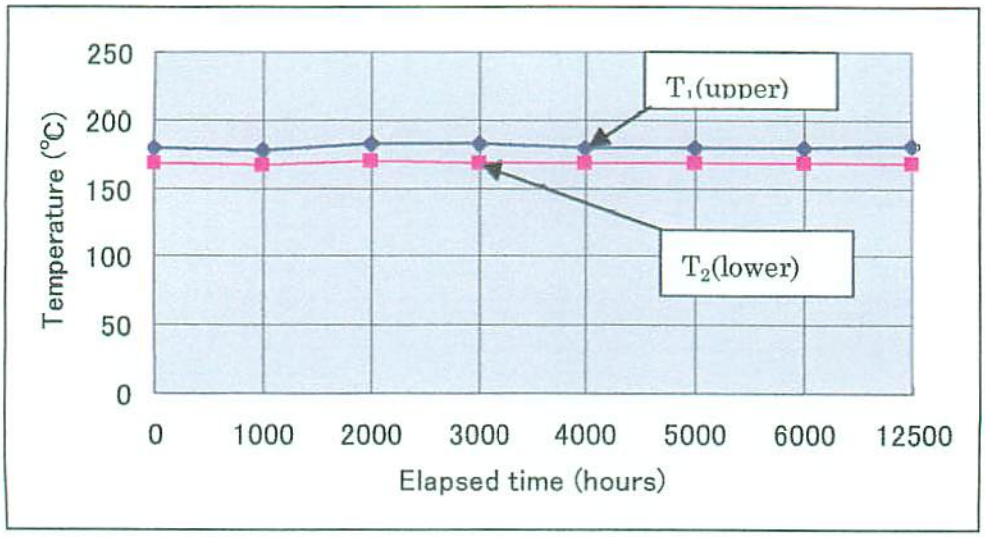

Fig. 5-9 Long term operation test of heat pipes at top heat mode

5.4 Frozen test of heat pipe

As a PC is being transported by airplane and stored at a warehouse, the ambient temperature will on occasion go below 0℃. Here, a frozen cycle test of the water heat pipes was carried out. Figure 5-10 shows a schematic of the experimental set up of a frozen cycle.

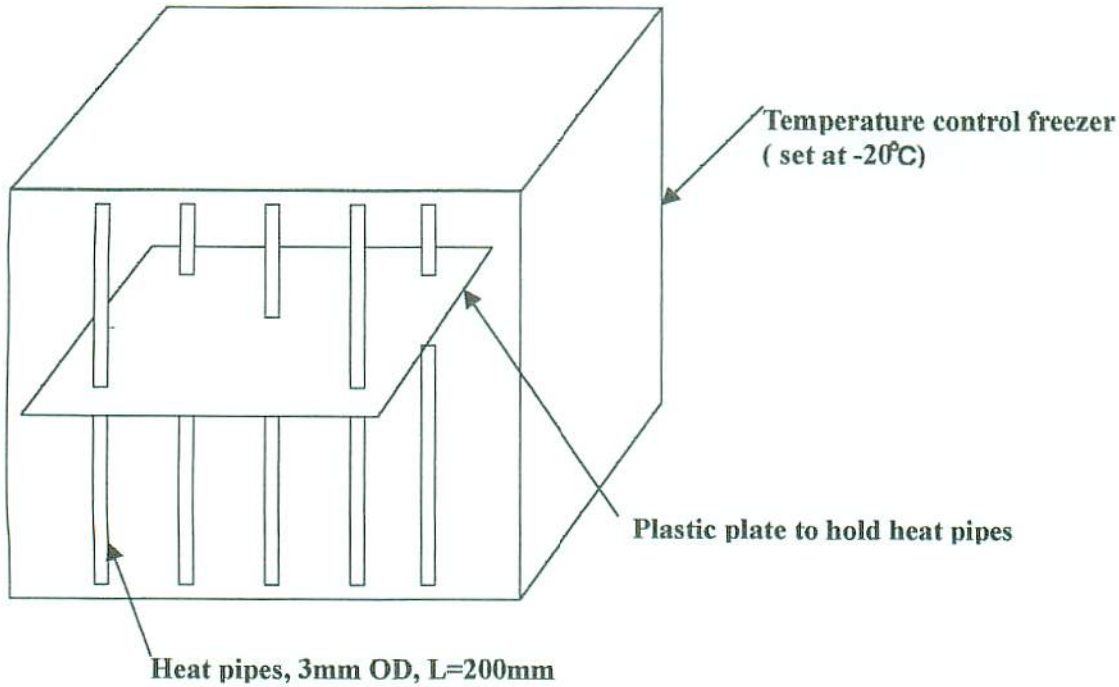

Fig. 5-10 Schematic of experimental set up of frozen cycle

Five pieces of 3 mm heat pipe were supported vertically by means of a plastic plate. The heat pipes were then frozen in a refrigerator.

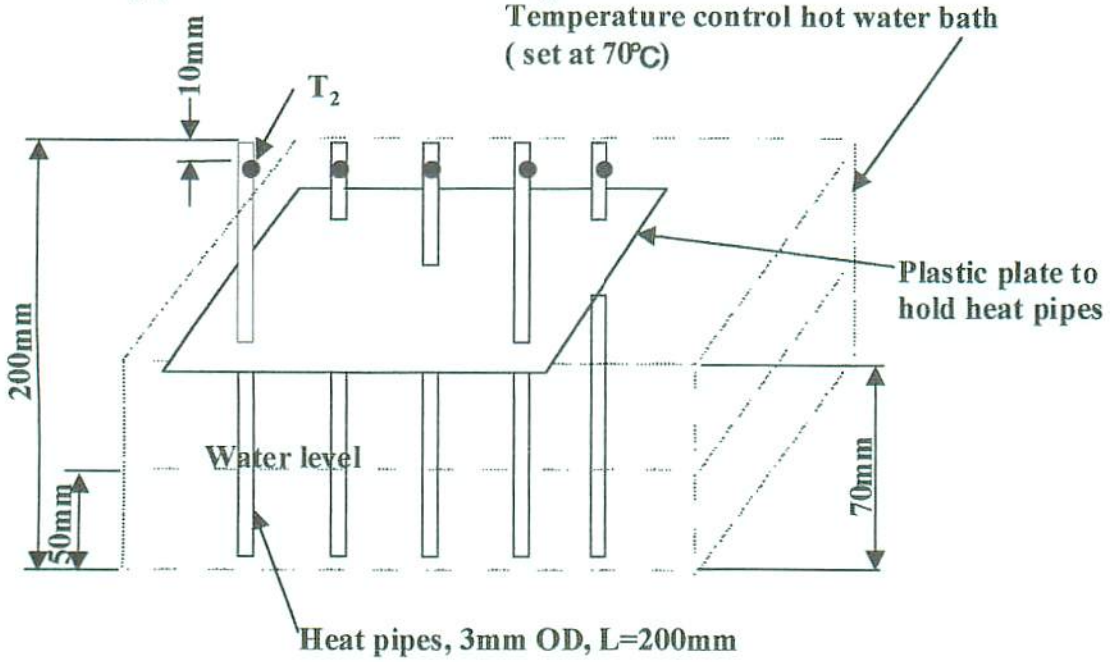

Fig. 5-11 Schematic of experimental set up of defrosting

After the heat pipes were frozen at –20℃, they were dipped into a 70℃ hot water bath. T_2 located 10mm from the top of the heat pipes was continuously measured through frozen to defrost processes.

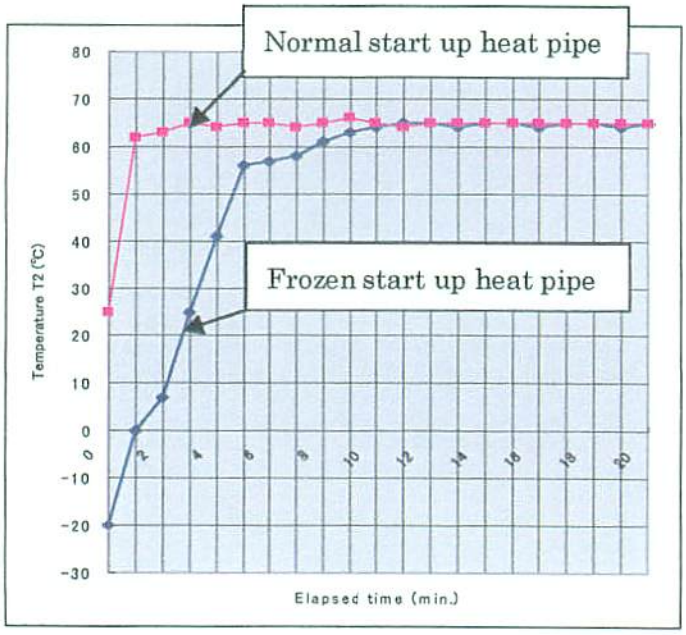

Fig. 5-12 Frozen start up property of heat pipe

Figure 5-12 shows the measured temperature T_2 when the heat pipe was started up from –20℃ compared with the normal startup from the ambient temperature.
A frozen heat pipe has a slow thermal response, but after 10 minutes it achieved almost the same performance as under normal conditions. Five cycles were continued for each 5 pieces of heat pipes. There were not any big difference amongst them. Usually, a heat pipe with wicks can start up very well from a frozen sate. However thermosyphons with water sometimes crack due to the expansion of the ice. This means that the wick can distribute water uniformly to help in the prevention of the frozen crack problem.

References

(5-1) M. Murakami, K. Arai, Y. Kojima, " *Statistical Prediction of Long-Term Reliability of Copper-Water Heat Pipes from Accelerated Test Data* ", Proceedings of 6th International Heat Pipe Conference Vol. II , pp.269-274, Grenoble, France, May 1987.

(5-2) Yasushi Kojima and Masahide Murakami, " *A Statistical Treatment of Accelerated Heat Pipe Test Data (2)*", Proceedings of 7th International Heat Pipe Conference Vol. II , pp.33-37, Minsk, USSR, 1990.

(5-3) Petrick, S.W., "*Hydrogen Gas Generation in Water/Stainless Steel Heat Pipe* ", ASME Paper 72-WA/HT-37, November 1972, New York.

(5-4) T. Anderson, " *Hydrogen Evolution in Nickel-Water Heat Pipes*", AIAA 8th Thermophysics Conference, Palm Springs, California, July 1973.

(5-5) Dunn, P.D., Reay, D.A., "*Heat Pipes* ", 4th edition, 1994, Pergamon Press.

(5-6) Faghri, A., "*Heat Pipe Science and Technology* ", 1995, Taylor and Francis.

(5-7) Thang Nguyen, Masataka Mochizuki, Akihiro Takamiya, Mitsuru Kamimori, and Renya Ikeda, *"Prediction of long term performance of miniature heat pipes from accelerated life tests"*, Proceeding of the 11th International Heat Pipe Conference, pp.230-233, Tokyo, Japan, September 1999.

6. Cooling System for laptop PC using heat pipe[6-1, 6-2, 6-3, 6-4, 6-6, 6-7, 6-8]

6.1 Progress of cooling system of Laptop PC

In the demand for closing the performance gap between desktop and laptop PC's, more and more powerful performance processors have been developed for use in laptop PC's. The drawback in the higher performance processor is that they exhibit higher heat generation. This creates a challenge in providing a thermal solution since high performance processors and additional electronics parts such as more Cache, more DRAM, larger HDD, PCMCIA and CD ROM lead to higher total power dissipation. It is even more challenging to provide a thermal solution without compromising the notebook's size and weight. Currently, the heat generated from the CPU is approximately 16 to 20 watts. It is expected that this power will rise from 20 to 30 watts in by 2002. The processor's die surface where most heat is generated is usually small, approximately 10 mm × 10 mm.

For effective cooling, the heat must spread over a larger surface area and be away from the processor, as there is no space available in the vicinity of the processor. Heat must be transferred to a remote location where there is space available for cooling, usually in the corners or on the sides of the laptop PC. In computer applications, the operating temperatures are normally between 50 to 100 °C. In this temperature range water is the best working fluid.

This section describes various cooling solutions using heat pipes for cooling of laptop PC's as follows:

(1) Heat pipe with heat spreader plate: In this method, the heat pipe is used to spread the heat of the processor onto metal plates which can be placed under the keyboard or on the chassis of the notebook. Heat is transferred from the metal plates through the keyboard and chassis and cooled by natural convection. In this method with the use of the heat pipe, heat dissipation can increase 2 to 3 times more than the case of no heat pipe. It is evident that the larger the spreading plate the more effective it is to use heat pipe.

(2) Remote heat exchanger (RHE): In this system, the heat pipe is used to transfer heat from the processor to a heat sink in a remote location, usually in the corners or on the sides of the laptop PC. An axial fan or blower is used to blow air through the heat sink for cooling. In general, the processor's temperature limit is less than 100 °C and the ambient air is about 45 °C. If one uses a solid copper rod to transfer heat from the processor to the heat sink, one may expect the temperature of the copper rod at the heat sink to be close to the ambient air, so that there will not be

effective cooling. However, if a heat pipe is used, the temperature drop from one end of the heat pipe to the other end is quite small and generally it is less than 5 °C for 10 watts of heat input.

(3) Hinged heat pipe system: This system consists of two heat pipes and a hinge connector. The primary heat pipe is fixed and is in contact with the processor, transferring heat to a secondary heat pipe via a hinge connector that joins the two heat pipes together. The second heat pipe is used to transfer heat onto a metal plate located at the back of LCD display. The purpose of the connector is to transfer heat from the first to the second heat pipe and to allow the second heat pipe to rotate when opening and closing the laptop PC's lid.

6.2 Heat pipe with heat spreader plate[6-5]

A heat pipe commonly is used to transfer heat from the processor to a heat spreader plate which is usually made of aluminum and is installed under the keyboard or on the chassis of the laptop PC as shown in Fig. 6-1 and Fig. 6-2 respectively.

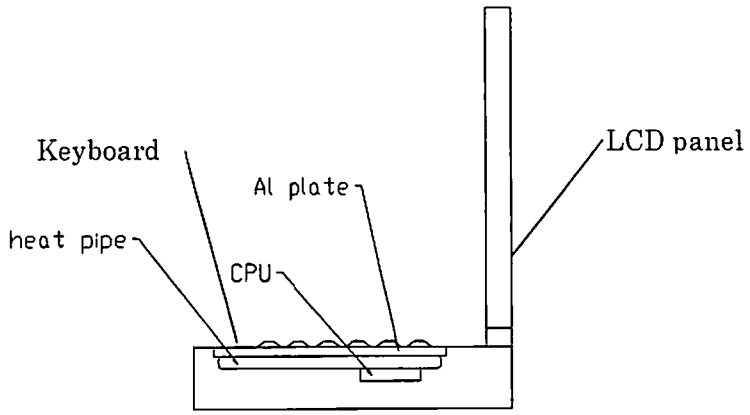

Fig. 6-1 Heat spreader plate with a heat pipe under keyboard

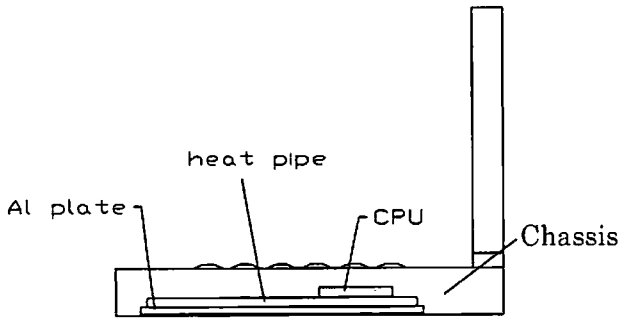

Fig. 6-2 Heat spreader plate with a heat pipe on chassis

An example of this system consisted of a rectangular heat spreader plate made of aluminum placed on the chassis of the laptop PC. The dimensions of the plate are approximately 0.6 mm thick, 190 mm long and 100 mm width. The heat pipe is a 3 mm round that is pressed into an elliptic cross section of dimensions approximately 2 mm × 3.6 mm × 200 mm (height × width × length) to accommodate it for the height constraint in the laptop PC. The heat pipe is mechanically attached to the heat spreader plate with rivets. The heating and cooling sections of the heat pipe are approximately 30 mm and 170 mm respectively. The test results of this system are shown in Fig. 6-3.

The total thermal resistance R_t is calculated as follows:

R_t $=\triangle T/Q$ where,

Q = Heat input (W)

R_t = Total thermal resistance (°C/W)

$\triangle T$ = Temperature difference between the processor surface temperature and the atmosphere (°C)

If the maximum allowable surface temperature of the processor is set at 95 °C (maximum 100 °C) and the ambient temperature is 45 °C, from Fig. 6-3, one can estimate that this system can dissipate approximately 6W. Xie et al.[6-4] conducted tests of similar configuration and obtained similar results.

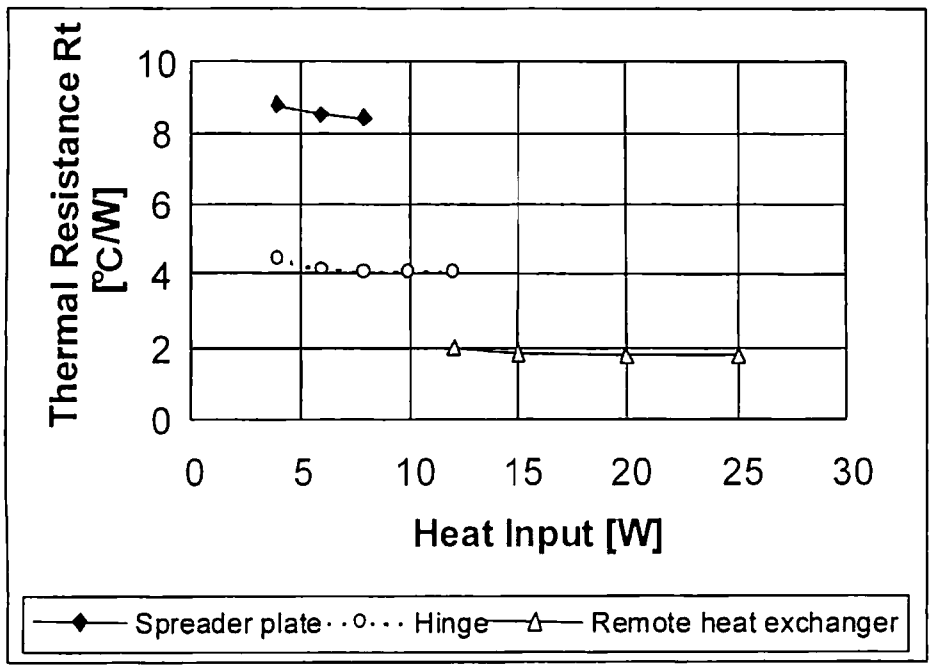

Fig. 6- 3 Test results of heat spreader with a heat pipe, hinged heat pipe, and RHE

Figure 6-4 shows an example of a products which consist of heat spreader plate or

heat sink with heat pipe for cooling of laptop PC's. In most cases, the heat spreader plate is pure aluminum (A-1100) is preferred due to its light weight, high thermal conductivity (220 W/m·K), easy stamping, and low cost. The heat pipe is assembled to the heat spreader plate by mechanical clamping with or without thermal grease. The purpose of the thermal grease is to minimize the thermal contact resistance between heat pipe and spreader plate. An example of heat pipe installed in the die cast heat sink with thermal grease as interface material is shown in the bottom left corner of photograph in figure 6.4.

Fig. 6-4 Various real products of passive cooling part consisting of heat spreader with heat pipe

6.3 Remote heat exchanger system (RHE)

This system is a combination of two heat pipes, channeled plate aluminum heat sink and fan as shown in Fig. 6-5. One end of the heat pipe was soldered to an aluminum block (or copper block), and the other end was soldered to the base of the heat sink. The heat sink was fully ducted for air flow. Approximate dimensions (in mm) of the system are as follows;

- Heat pipe: 2 × 3.6 × 200 (height × width × length)
- Plate heat sink: 2.5 × 7.5 × 60 × 35 × 0.4 × 1.2 × 49 (base × fin height × width × length × fin thickness × pitch × number of fins).
  Total fins surface area was approximately 250 cm^2.
- Heat block : 30 ×30 × 3 (width × length × thickness)

- Heat source : A processor thermal die of 1 cm^2 .
- Fan: 50 × 50 × 10 (width × height × thickness); 4 CFM (ft^3/min.) (0.113m^3/min.) free airflow and 8 mmH_2O static pressure.

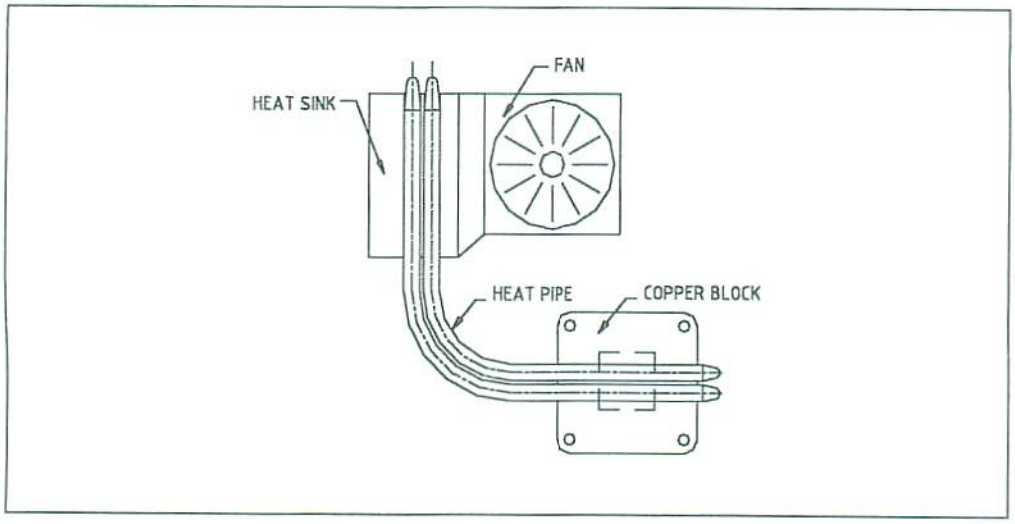

Fig. 6 –5 Schematic presentation of RHE

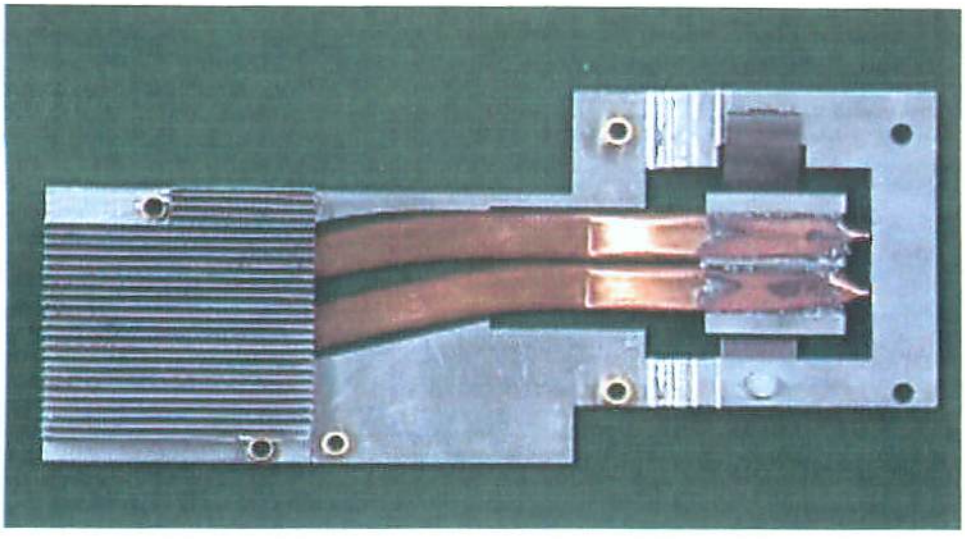

Fig. 6-6 Typical high performance RHE

Figure 6-6 shows the current product of a high performance cooling part which has two 4mm OD flattened heat pipes. It is able to dissipate approximately 25 watts by forced air cooling. The heat pipes directly placed onto the MPU with a thermal interface material between the mating surfaces. Heat pipes and MPU are held tight in contact under compression load of the spring bar. A certain level of compression load is required to maintain the contact thermal resistance to a minimal, but not too high load that may caused damage to the surface of the MPU. For further reduce the thermal contact resistance heat pipes are metallic bonded to aluminum block by soldering.

6.4 Hinged heat pipe [6-5]

For the hinged heat pipe system, the heat from the processor is routed onto the aluminum heat spreader plate located on the back screen of the display as shown in Fig. 6-7. Basically this system consists of two heat pipes and a hinge connector. The primary heat pipe is fixed and is in contact with the heat source, transferring heat to the secondary heat pipe via a hinge connector that joins the two heat pipes together. The second heat pipe is used to transfer heat onto the aluminum heat spreader plate. The purpose of the connector is to transport heat from the first to second heat pipe and to allow the second heat pipe to rotate when the notebook's lid is opened and closed. The approximate dimensions of the system are as follows.

- First heat pipe : 4mm × 130mm (OD × length)
- Second heat pipe: 4mm × 250mm (OD × length)
- Hinge connector : 7mm × 25mm × 16.8mm (width × length × height); material copper C-1020.
- Heat spreader plate: 174mm × 250mm × 0.4mm (width × length × thickness); material A1050.
- Heat block : 30mm × 30mm × 3mm (width × length × thickness); material A1050.
- Heat source : 133 MHz processor (TCP) TCP: Tape Carrier Package

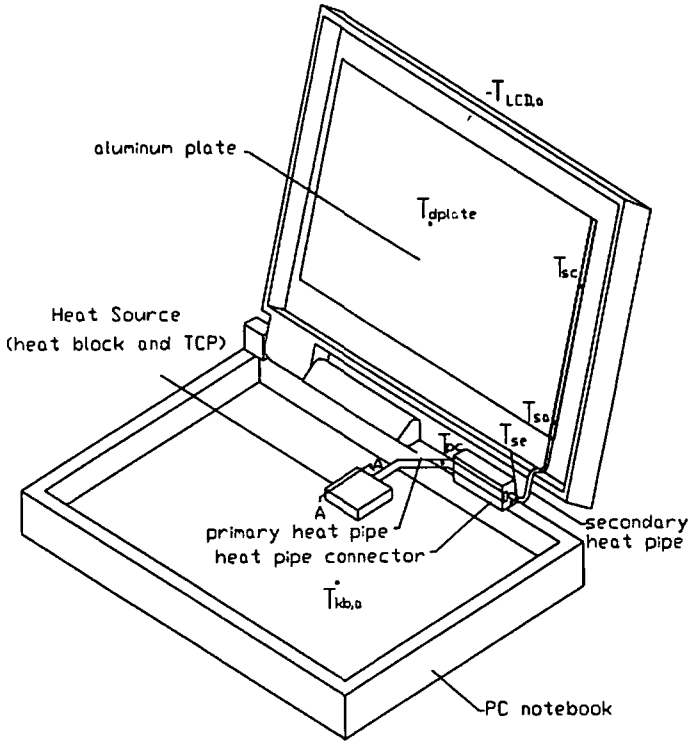

Fig. 6-7 Schematic of hinged heat pipe system

As shown in Fig. 6-3, the total thermal resistance R_t of the hinged heat pipe system was about 4.1 °C/W at heat input of approximately 10 watts. Based on the temperature constraint of the MPU temperature of 95 °C and ambient of 45 °C, this system can be used to dissipate about 12 watts. At 12 watts heat input and the ambient air of 22 °C, the temperature measured at the back of the LCD and the plastic skin (T_{LCD}) was about 45 °C. The test results of the PC thermal simulation test with a MPU and other thermal parts is shown in Table 6-1. The total thermal resistance R_t was calculated in the following:

$R_t = (T_1 - T_{19}) / Q$

$= (69.4 - 28.5) / 9.5$

$= 4.31$ °C/W

If the MPU surface temperature is limit to a limited temperature of 95 °C and the ambient air of 35 °C, this system can be used to dissipate 13.9 watts.

$Q = (T_{cpu} - T_a) / R_t$

$= (95 - 35) / 4.31$

$= 13.9$ W

Table 6-1 Test result of hinged heat pipe

Power : 26 W MPU(9.5W); Memory(9W); HDD(3.5W); PCMCIA(2.2W); Battery(2.2W)	Temperature (°C)
T_1 – CPU	69.4
T_2 – CPU	64.7
T_3 – Primary heat pipe	66.8
T_4 – Primary heat pipe	66.1
T_5 – Hinge part	60.4
T_6 – Secondary heat pipe	55.9
T_7 – Secondary heat pipe	54.3
T_8 – LCD heat spreader plate	42.5
T_9 – LCD heat spreader plate	41.7
T_{10} – LCD heat spreader plate	42.6
T_{11} – Back of LCD	34.4
T_{12} – Under keyboard	52.1
T_{13} – Heat spreader plate	67.0
T_{14} – Inside ambient	31.7
T_{15} – Memory	72.7
T_{16} – HDD	57.9
T_{17} – PCMCIA	60.0
T_{18} – Battery	45.4
T_{19} – Outside ambient	28.5

Figure 6-3 shows Rt=4.1 °C/W in case of the thermal hinge heat pipe, and on the other hand the PC thermal simulation test with a MPU and other thermal components registered in 4.31 °C/W. This means other electronics components influence 0.2 °C/W of additional thermal resistance.

Figure 6-8 shows a thermal hinge part which was developed. Copper was chosen as the heat transfer element material and the geometry was a "C" shape ring with a slightly larger phosphor bronze " C" ring joined with the copper "C" ring to keep spring force. A lubricant was charged into two grooves inside the copper "C" ring. The hinge part was separated into two pieces for easy assemble and installation. The main purpose of the thermal hinge is to provide heat transfer from MPU to the back of the display, however the thermal hinge can also be utilized as mechanical to hinge to support the notebook's lid.

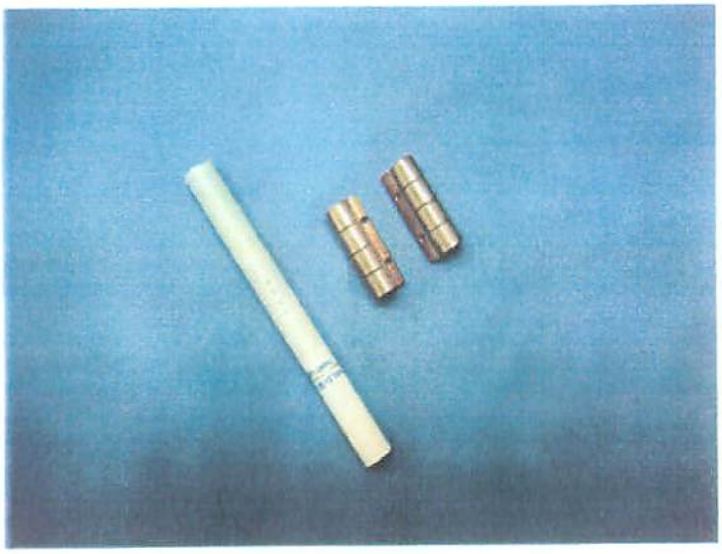

Fig. 6-8 Thermal hinge part

Fig. 6-9 Reliability test equipment of thermal hinge heat pipe

The testing equipment used for a reliability of the thermal hinge heat pipe is shown in Fig.6-9. The hinge rotates for 90 degrees under the motion of opening for 1 second, stopping for 1 second, closing for 1 second, and stopping for 1 second, and then it was repeated for 30,000 cycles.

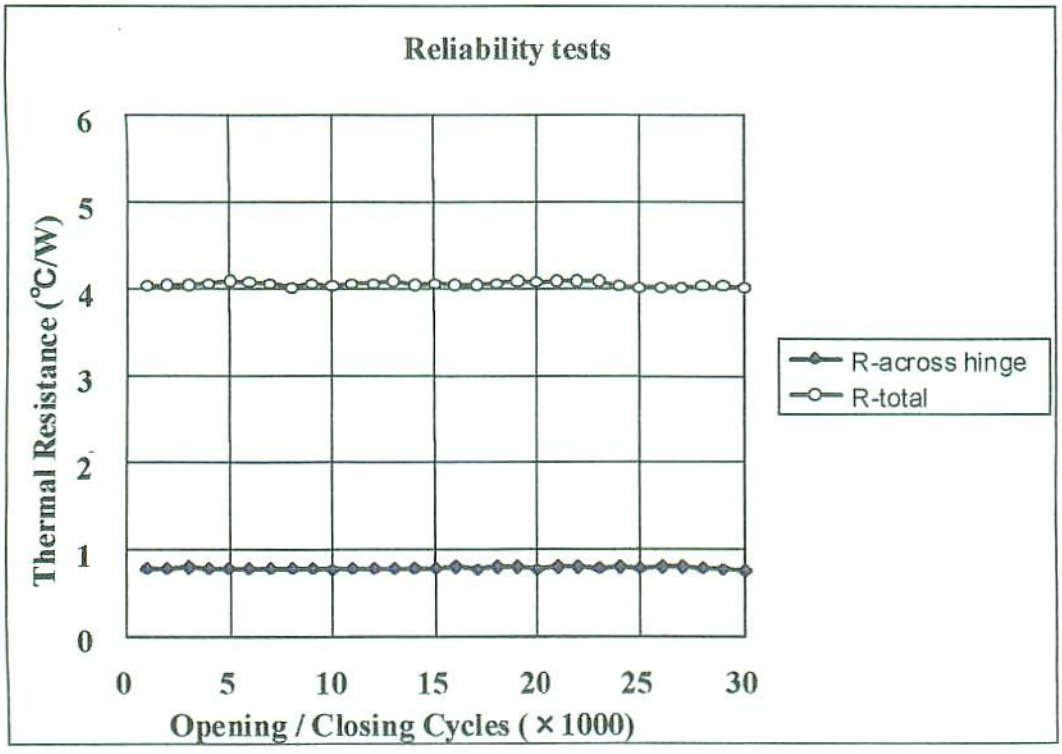

Fig. 6-10 Reliability test data of thermal hinge heat pipe

Figure 6-10 shows the reliability data for 30,000 cycles of the opening and closing process. "R-across hinge" means thermal resistance between the primary heat pipe and the secondary heat pipe including evaporator resistance of the primary MHP and

the condensing resistance of the secondary MHP. Results showed "R-across hinge" remained constant at 0.8 K/W. Total thermal resistance was remained constant at 4 K/W. Figure 6-11 shows the practical product of a combination between the thermal hinge and the mechanical hinge for cooling a laptop PC. Since the copper heat pipe is soft, the thermal hinge not capable to withstand the mechanical torque of the notebook'lid. Therefore, the thermal hinge should be located between two mechanical torque hinges to avoid mechanical damage and stress to the heat pipe as illustrated in Fig. 6-11.

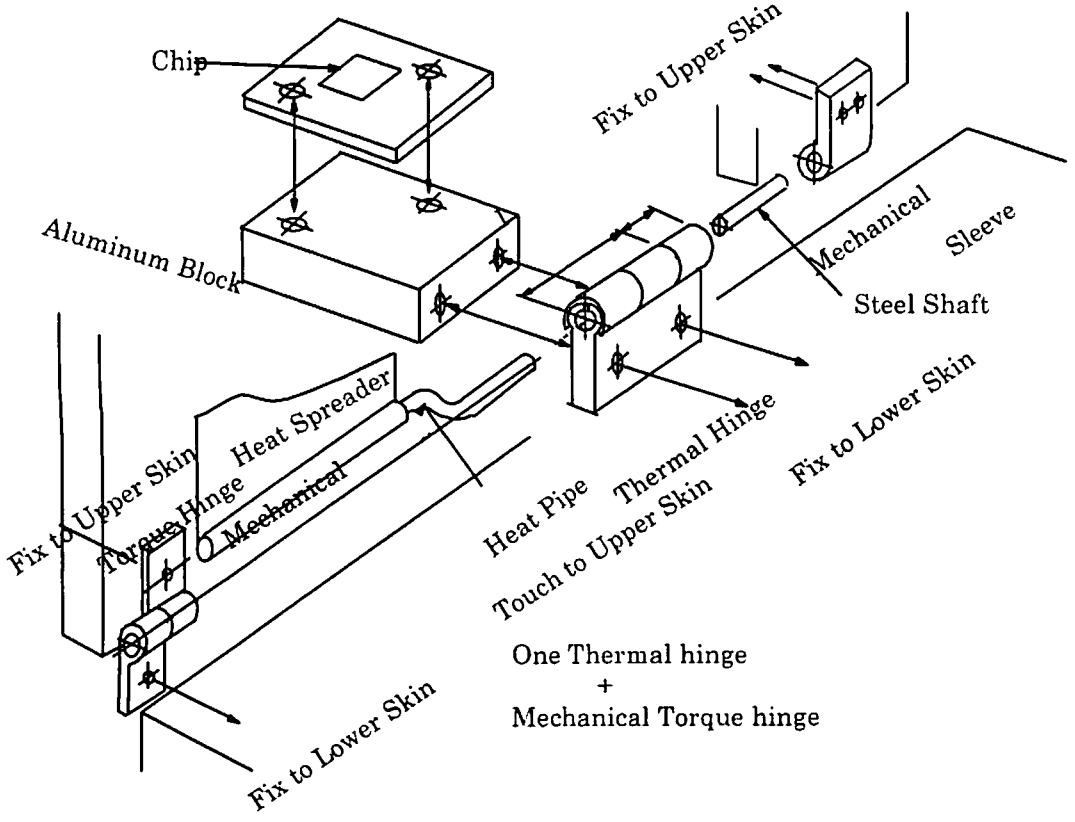

Fig. 6-11 Thermal hinge and mechanical hinge combination for practical use

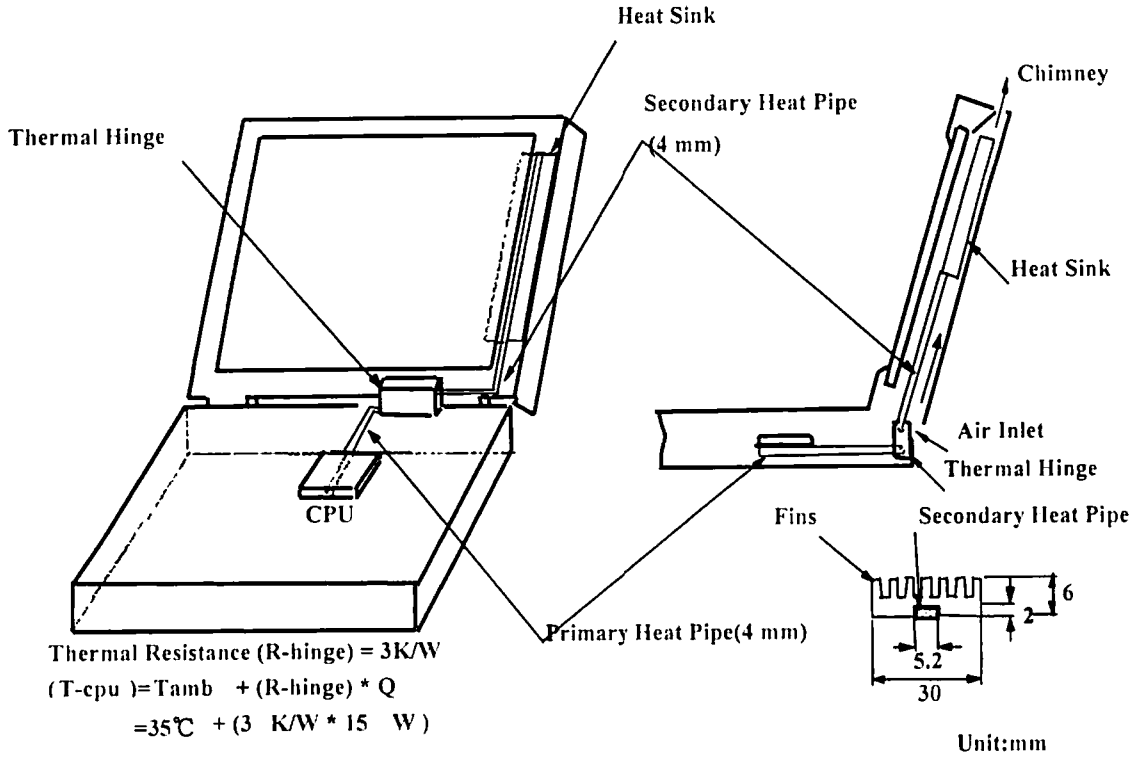

Fig. 6-12 Hinged heat pipe with chimney cooling effect

Figure 6-12 shows an example of practical use of the thermal hinge utilizing a chimney effect to get better cooling. The condenser of a secondary heat pipe installs with a heat sink by natural convection. This system is able to dissipate approximately 15 watts from CPU. Therefore, it can be used for thin laptop PC's without fans.

6.5 Mobile vapor chamber (MVC)

6.5.1 MVC sample and test setup

A vapor chamber is one type of flat heat pipe. This container can be made by stamping it with any geometry. The heat pipe has an disadvantage that it is difficult to make a small radius bending. Normal flattened heat pipe needs a bigger radius when bending so it takes up a lot of useful areas in the PC layout. The MVC can make quite a square shape which can result in us compact space. The MVC has larger width. which has the following advantages:

1) It is possible to reduce thermal resistance, especially the evaporator.
2) Bigger Q_{max}
3) Through holes of fixture bolts on the MVC are available.

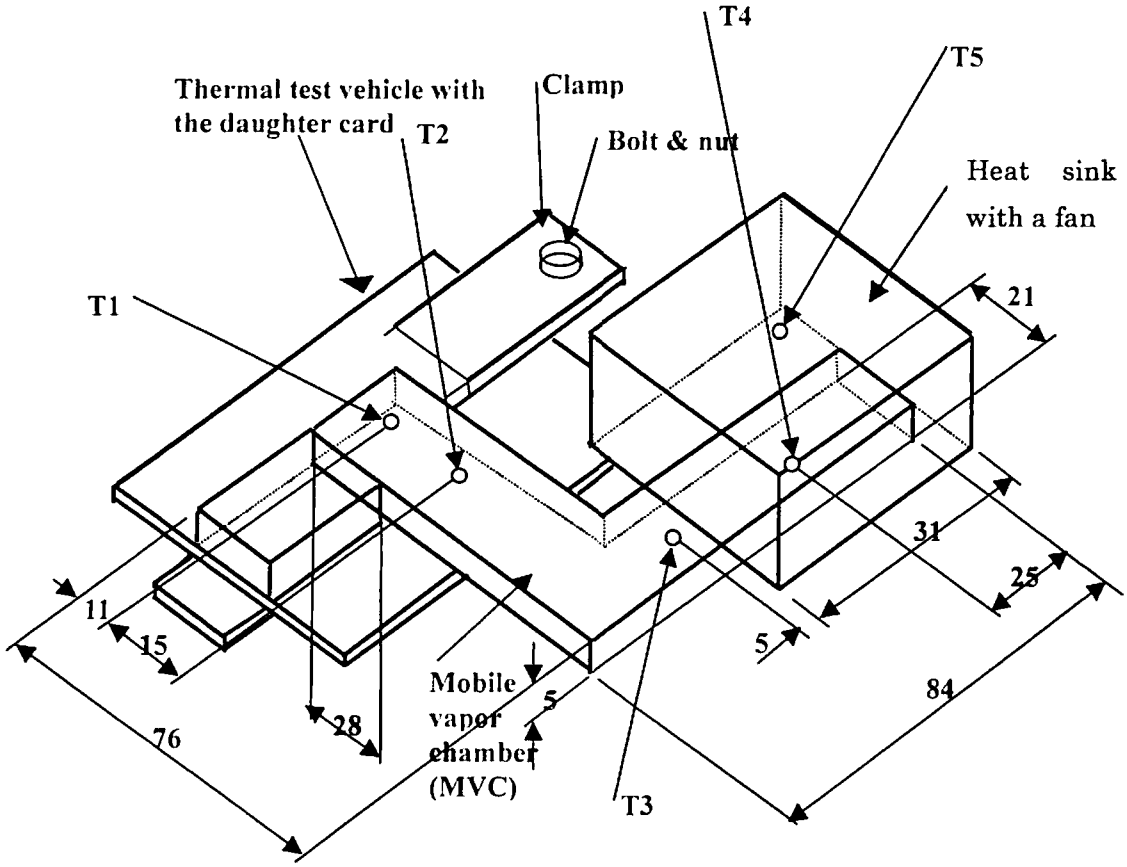

Fig. 6-13 Thermal test set up of Mobile Vapor Chamber sample

Figure 6-13 shows a sample of the L-shape MVC and its test set up. The MVC consists of a bottom copper container and a top cover made by stamping. The micro copper powder sheet of 100 μm powder and 30 to 40% as porosity is sintered inside

vapor chamber container at 900 to 1,000 ℃. The sintered columns are also inserted inside of vapor space to connect between the evaporator and the condenser. The condensed liquid can be returned to the evaporator through sintered columns. The details of vapor chamber will be discussed in chapter 7.

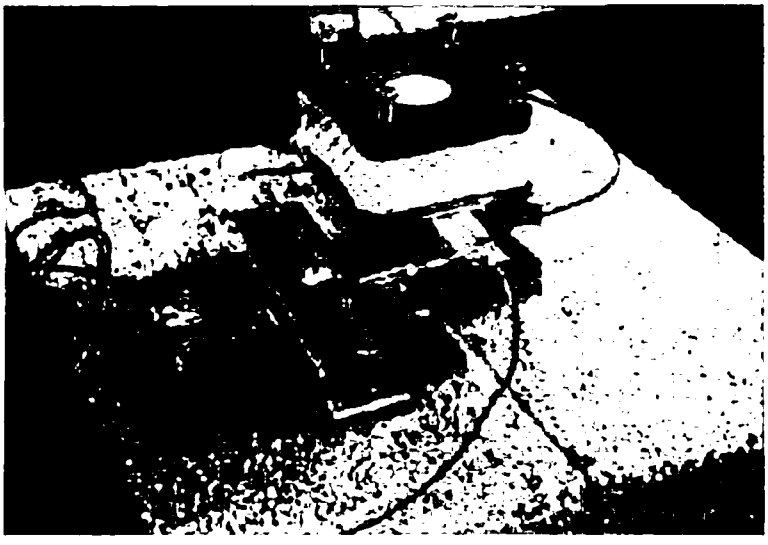

Fig. 6-14 Photo of thermal test setup of Mobile Vapor Chamber

Figure 6-14 shows the photo of the test set up for the MVC. The evaporator of the MVC was attached to the die of the thermal test vehicle which is exactly the same size as a MPU. A heat sink with a fan is mounted on the top of the MVC for cooling.

6.5.2 Test results of MVC

Table 6-2 shows test data of the MVC with three pieces of through-holes. The purpose of the through holes on the MVC is for screw attachment of MVC direct to MPU, without the need of any additional parts for attachment. Thus it gives the assembly compact and mobile. Five samples were fabricated and tested at thermal load of 20 watts and 30 watts. The thermal resistance of the MVC measured at about 0.7 to 0.9 K/W. Table 6-3 shows the same data of MVC without through-holes. The thermal resistance of the MVC with through holes is 15 to 50% than the MVC without through-holes. Figure 6-15 shows the MVC thermal solution of 30 watts consists of a high dense plate fin heat sink and horizontal fan. Figure 6-16 also shows the MVC thermal solution of 30 watts consists of folded fins direct soldered on the MVC and two vertical axial flow fans.

Table 6-2 Thermal test result of mobile vapor chamber with through holes

Vapor chamber with through holes											
Sample	Voltage	Ampere	Power	V_{core}	T_{core}	T_1	T_2	T_3	T_4	T_5	R_{1-4}
No.	(V)	(A)	(W)	(V)	(℃)	(℃)	(℃)	(℃)	(℃)	(℃)	(℃/W)
1	33.5	0.59	19.8	1.14	57.2	48.2	48.1	47.9	46.5	29.1	0.086
	42.5	0.7	29.8	1.20	73.0	58.2	56.9	56.7	56.0	28.9	0.074
2	33.5	0.59	19.8	1.15	60.7	48.1	47.7	47.6	46.5	28.9	0.081
	42.5	0.69	29.3	1.21	76.9	58.6	56.5	56.3	56.0	28.6	0.089
3	32.5	0.59	19.2	1.13	56.4	47.6	47.6	47.4	46.2	29.2	0.083
	41.5	0.72	29.9	1.19	72.2	57.7	57.7	57.6	55.7	29.3	0.077
4	30.5	0.55	16.8	1.12	54.3	44.4	44.4	44.4	43.7	28.3	0.072
	33.5	0.59	19.8	1.14	59.3	46.4	46.4	46.4	45.6	28.1	0.091
5	32.5	0.60	19.5	1.12	54.0	44.4	44.4	44.3	43.2	25.8	0.072
	41.4	0.70	29.8	1.18	69.3	53.8	53.8	53.6	51.5	25.4	0.094

Table 6-3 Thermal test result of mobile vapor chamber sample without through holes

Vapor chamber without through holes											
Sample	Voltage	Ampere	Power	V_{core}	T_{core}	T_1	T_2	T_3	T_4	T_5	R_{1-4}
No.	(V)	(A)	(W)	(V)	(℃)	(℃)	(℃)	(℃)	(℃)	(℃)	(℃/W)
1	32.5	0.59	19.2	1.14	58.8	47.6	47.3	47.2	46.5	29.3	0.057
	41.9	0.69	28.9	1.23	83.0	66.4	55.8	56.0	64.5	29.4	0.066
2	32.7	0.60	19.6	1.13	55.9	46.1	45.8	45.7	44.7	27.8	0.071
	41.0	0.72	29.5	1.18	69.0	55.7	55.3	54.9	53.4	27.6	0.078
3	33.2	0.60	19.9	1.13	56.4	46.1	46.1	45.9	45.0	27.6	0.055
	41.5	0.72	29.9	1.19	71.7	55.7	55.4	55.4	51.8	27.3	0.064
4	32.8	0.60	19.7	1.13	55.9	46.6	46.3	45.8	45.8	27.1	0.051
	41.0	0.72	29.5	1.18	69.6	56.0	55.6	54.9	54.0	26.7	0.068
5	32.9	0.60	19.7	1.13	55.9	46.4	44.4	45.5	45.5	26.8	0.051
	41.0	0.72	29.5	1.18	70.1	56.1	53.8	54.8	54.8	26.9	0.047

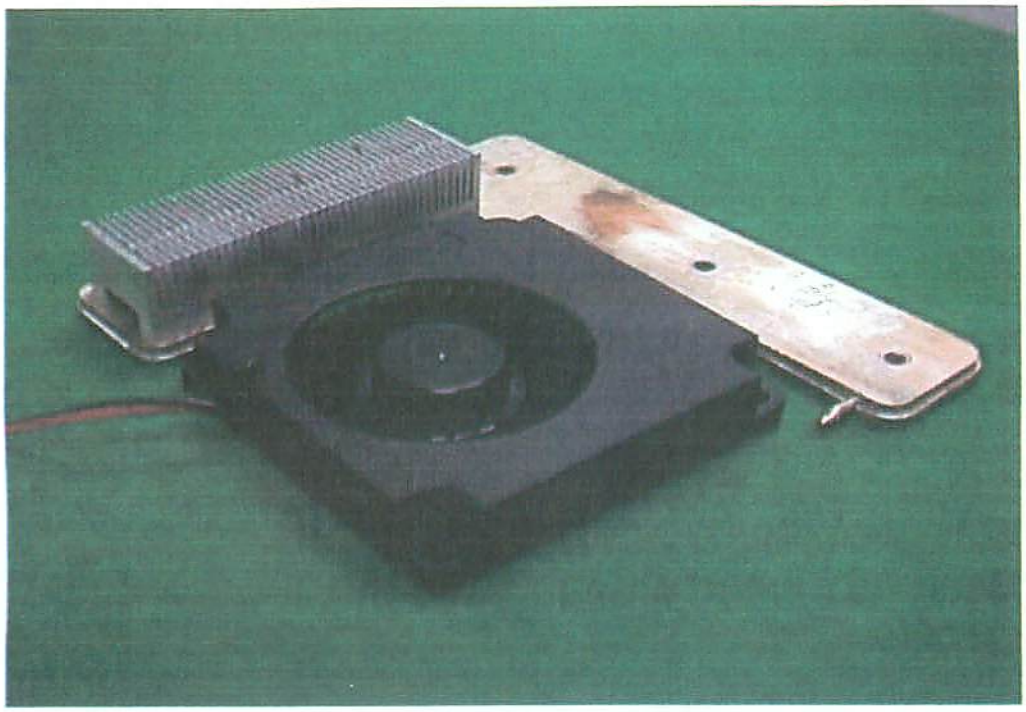

Fig. 6-15 30 watts thermal solution using MVC with a horizontal fan

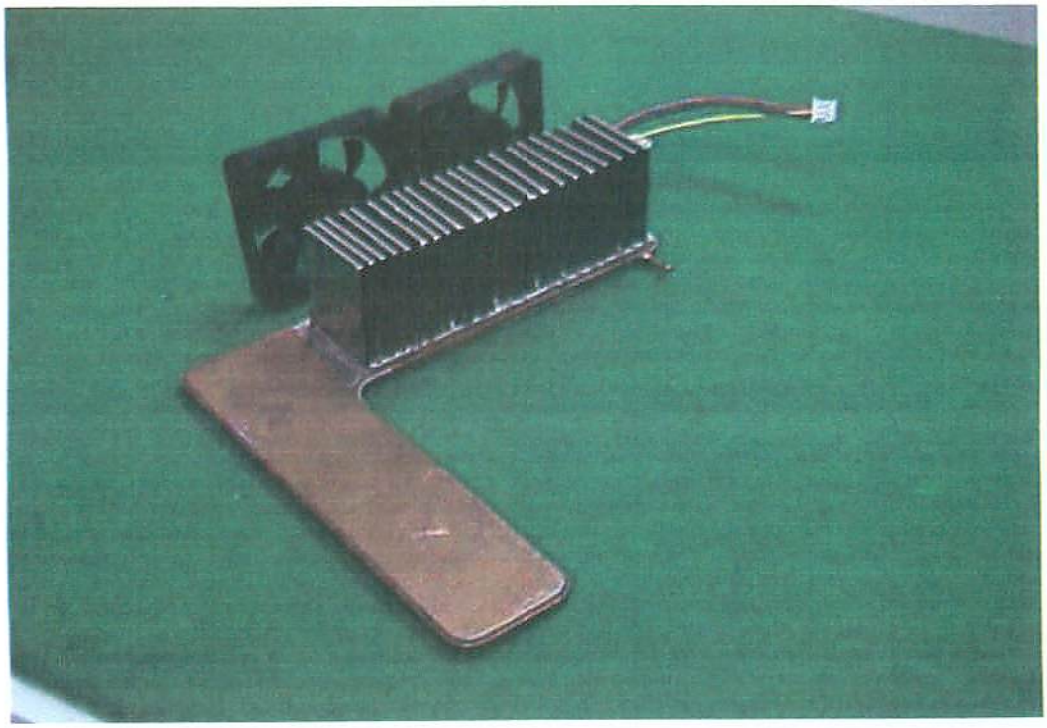

Fig. 6-16 30 watts thermal solution using MVC with axial flow fans

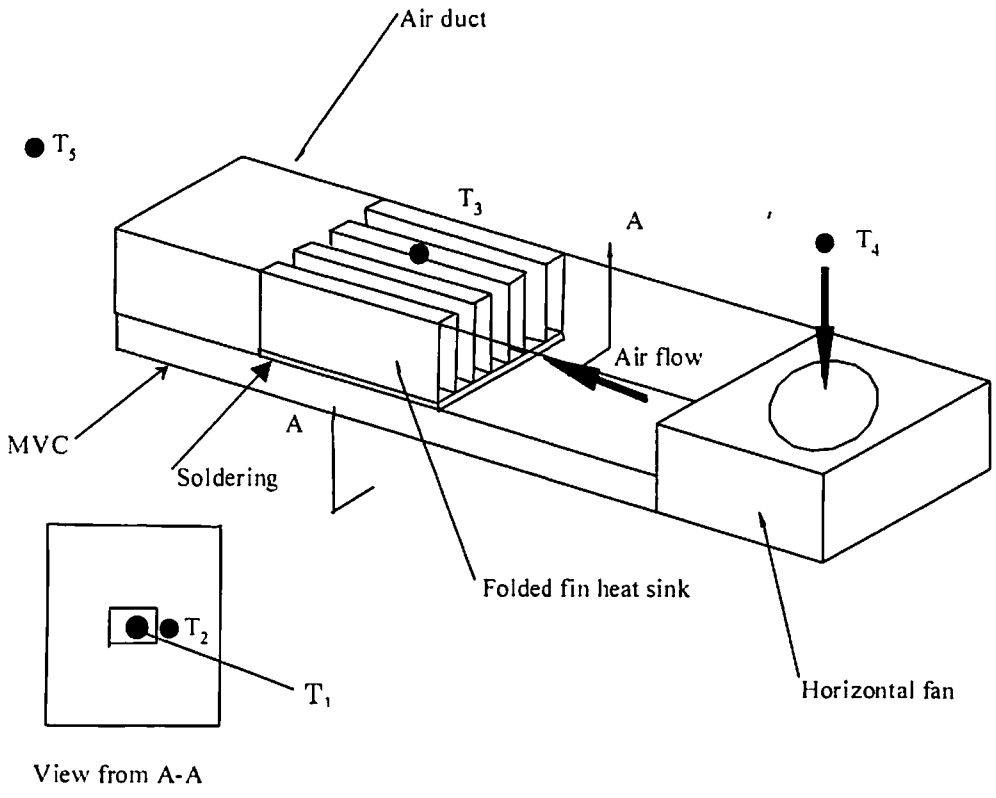

Fig. 6-17 Test sample of MVC with folded fins using thermal test vehicle

Figure 6-17 shows a test sample of a MVC with folded fins which is an accordion shape with one side directly soldered onto the MVC. A horizontal fan sits on one side of the MVC, and then the air duct is covered from fan exit to folded fins. Air comes from the top of the fan and is pushed to the inlet of the folded fins.

Table 6-4 Test data and condition of MVC with folded fins

		T_1	T_2	T_3	T_4	T_5		
Heat input (Watts)	Core voltage (Volt)	Core temp. (°C)	Base temp. (°C)	Fin top temp. (°C)	Inlet air temp. (°C)	Outlet air temp. (°C)	$R_t=(T_1-T_4)/Q$ (°C)	Fan speed (rpm)
30	1.18	69.9	56.6	44.3	25.2	48.6	1.49	6,350
40	1.23	82.8	66.6	51.0	26.0	56.1	1.49	6,400

Table 6-4 shows the test data and test conditions of a MVC with folded fins and 50mm × 50mm × 10mm thick compact fan capable of being of practical use in a PC. Total thermal resistance between T_1(core temperature of the MPU) and the ambient air was 1.49 K/W, thus the maximum heat dissipation(Q) in the system can be estimated in the following:

$Q=(80-35-15)\times 1.49$

$=44.7$ W

assuming that:

Maximum junction(core) temperature of MPU : 80℃

Ambient air temperature : 35℃

System temperature drop :15℃

This cooling system has a cooling capacity of 44.7 watts in the practical system.

6.6 How to cool 30 to 40 W of the MPU on the advanced laptop PC

Table 6-5 Total thermal design for laptop PC

		P=8 watts	P=16 watts		*Comments*
	Pcpu Psystem Ptotal	8 W 15 W 23 W	16 W 15 W 31 W		
Current Thermal Solution	HP / KBD	7 W			#Natural convection/ Radiation 25 ×20cm^2, T_s=40℃, T_a=25℃
	HP/CHASSIS	7 W			#Natural convection/ Radiation 25 ×20cm^2, T_s=40℃, T_a=25℃
	RHE	10 W			#Current RHE
	Ptotal	24W			
Future Thermal Solution	HP / KBD		7 W	7W	"Same as above"
	HP / CHASSIS		7 W	7W	"Same as above"
	RHE		20 W		#Double air flow,heat sink or ΔT inlet & outlet air
	RHE			10W	#Current RHE
	HINGED HP			10W	#Current Thermal hinged HP
	Ptotal		34W	34W	

Table 6-5 shows two examples of total thermal design on current laptop PC. For MPU power of 8 watts, the total thermal design needs 23 watts of heat dissipation due to the additional thermal load from HDD, PCMCIA, memory, and others heat generating components. For 23 watts thermal load, 7 watts can be dissipated via the key board and 7 watts through the chassis by passive and natural convection, the remaining 9 watts has to cool by RHE When the MPU power increases to 16 watts, the cooling capacity of the RHE should increase to 20 watts. 20 watts RHE is possible to install inside a thick and large-sized PC like an A-4 laptop PC. However, thinner or B-5 sized laptops do not have sufficient space to accommodate for the 20 W RHE. Therefore, a combined thermal solution which consists of 10 watts of heat dissipation by a hinged heat pipe and 10 watts by RHE is required to dissipate 34 watts.

It is challenge to consider cooling solution MPU reaching 30 to 40 watts in the year 2001-2002.

Table 6-6 Current and future thermal solution for laptop PC

Year	1998	1999	2000	2001	2002
	Current solution		Future solution		
Heat load(W)	10	16	20	30	40
R_{target}(℃/W)	5.0	3.1	2.5	1.7	1.3
R_{cpu} (℃/W)	0.5	0.5	0.5	0.5	0.5
R_{pad} (℃/W)	0.5	0.4	0.3	0.2	0.2
R_{con1} (℃/W)	0.3	0.3	0.2	0.1	0.1
R_{pipe} (℃/W)	0.5	0.4	0.2	0.2	0.2
R_{con2} (℃/W)	0.3	0.3	0.2	0.1	0.1
R_{sink} (℃/W)	2.5	1.25	1.0	0.6	0.2
R_{total} (℃/W)	4.6	3.15	2.4	1.7	1.3

Total thermal resistance (R_{total}) required as low as 1.7 to 1.3 K/W. The thermal resistance of a MPU package itself has 0.5 K/W between the die and the packing case. Therefore heat pipe thermal resistance needed to further reduce at least half, approximately heat pipe thermal resistance 0.2 K/W or below. To further reduce the overall thermal resistance, the assembling technique has changed from mechanical contact with thermal grease to direct metallic bonding by solder between the heat pipe and metal parts of the heating block and heat sink.

Heat pipe requirements:

- Maximum height 2mm, Width < 12 mm.
- Maximum heat transfer, 50 Watts.
- High evaporator heat flux, 50 W/cm^2.
- Low thermal resistance, 0.1 to 0.2 K/W (for length at least 300 mm, 10mm evaporator, 20mm condenser).
- Ability to operate at any orientation without any degradation in performance.
- No degradation in performance when subjected to bend and flatten in any direction.
- Environmental compliance (water working fluid is preferred.).
- Ease of manufacturing and low cost.

Heat sink requirements:

- L 50 mm, W 25 mm, H 15 mm (For axial fan).
- W 50 mm, L 20 mm, H 10 mm (For Blower).
- A total surface area of approximately 500 cm^2 (for example 0.2 mm fin thickness, height 10 to 15mm, gap 0.5 to 0.8 mm).

- Pressure drop, max 4 mm H_2O at for example 4 to 5 CFM(ft^3/min.)(0.113 to 0.141 m^3/min.).
- Maximum heat transfer coefficient between fins, for example >100 $W/m^2 \cdot K$ at 2 to 3 m/s. air flow.
- Light weight, preferably aluminum or other lighter materials with comparable or higher thermal conductivity.
- Ease of manufacturing and low cost .

Fan is requirements:

- Axial fan max. 25 mm × 25 mm × 10 mm.
- Blower max. 50 mm × 50 mm × 10 mm.
- Minimum air flow 6 CFM(ft^3/min.)(0.167m^3/min.), minimum pressure drop 6 mm H_2O.
- Maximum 6,000 rpm.
- Maximum 35 dBA at 1 meter distance.
- Minimum 30,000 hrs continuos operation at 60 ℃
- Low power consumption, 0.5 W.

6.7 System level thermal analysis by computer simulation

This section introduces an example of total thermal modeling for laptop a PC. There are various software readily available for simulate thermal modeling inside PC. Fir example modeling of fluid flow and heat transfer. The modeling is based on the following suumption:

1) Convection, conduction and thermal radiation are modeled.
2) The grilles at the inlet and outlet of the heat sink-fan assembly are modeled as cubic blocks.
3) Heat sink parameters: T_{fin}(Thickness of fin): 0.8mm, H_s(Width of heat sink): 20mm, H_b(Thickness of heat sink base): 2mm
4) All screws are neglected.
5) Supporting parts are assumed as equivalent cubic blocks.
6) Compact models for all the four packages are used.
7) The heat pipe is assumed to be high-conductive isotropic material with the same geometry. The heat spreaders are assumed to be made of Aluminum.
8) TIM(Thermal Interface Material) such as the chip to spreader thermal interface (TIM1), spreader to heat sink interface (TIM2) are modeled as compressed thermal resistance at the contact surface.
9) All the casing and fixing/supporting parts are assumed to be aluminum.

Table 6-7 Input parameter of thermal simulation on laptop PC

Subsystems	Size (mm)	Simulation method	Power generation (W)
Heat sink-Fan subsystem	160 × 50 × 20	Detailed heat sink-fan system	2.4
PCB	150 × 180 × 1.6	An isotropic material with equivalent thermal conductivity	0
CPU	35 × 35 × 2.19	Compact package model	25
3 other packages	35 × 35 × 2.19	Compact package model	1W each
Hard disk driver	98 × 72 × 14	Conductive block	1.3
Battery	133 × 60 × 19	Conductive block	0
Keyboards	287 × 110 × 8 with 0.8 mm thick walls	Conductive blocks	0
Computer chassis	304 × 254 × 25 with wall thickness of 0.8 mm	Conductive blocks	0
Miscellaneous: FDD, TeleJack, Mic, Sp P`P and S`P	FDD: 133 × 110 × 14, All others: 15×13×15 P` port 60 × 18 S` Port 25 × 18	Conductive blocks	0

Table 6-7 shows the input parameter of the thermal simulation for laptop PC. The MPU power is 25 watts and other parts like HDD, PCMCIA and other heat generating components are combined as one. Equivalent thermal conductivity is used in the compact model as shown in Fig. 6-18.

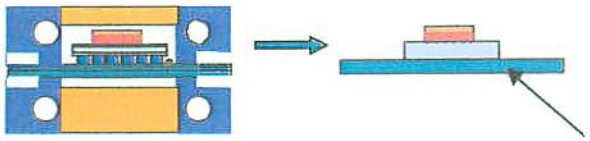

The equivalent thermal conductivity
for the block is found to be 1.34W/ m·K

Fig. 6-18 Thermal modeling

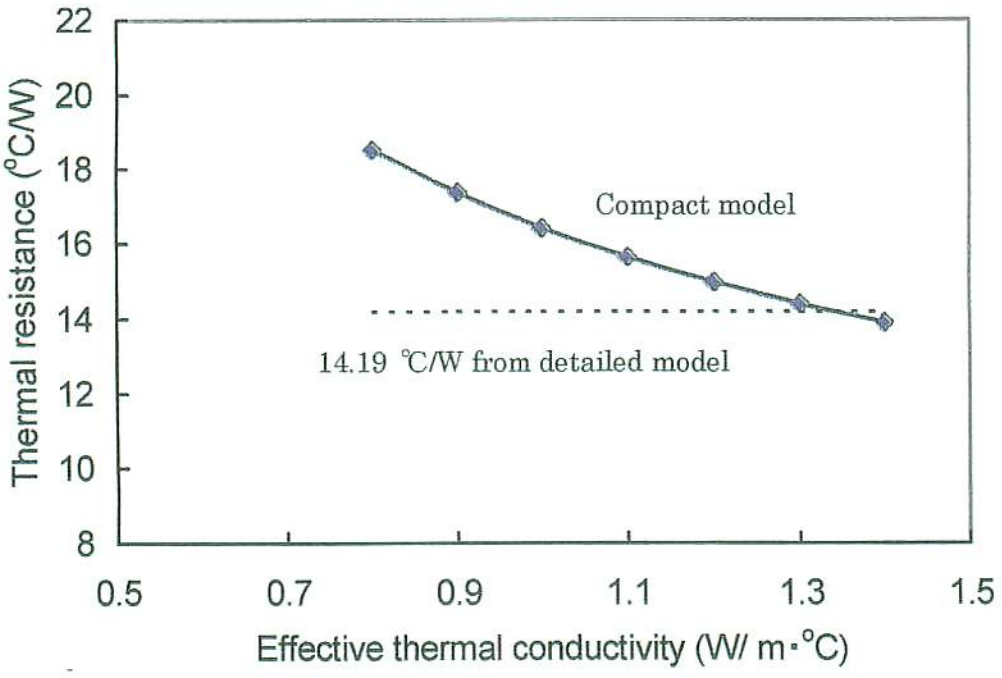

Fig. 6-19 Effective thermal conductivity

Figure 6-19 shows the effective thermal conductivity of the model shown in Fig. 6-18. The effective thermal conductivity assumed 1.34W/m.K. Figure 6-20 shows the simulation result of the fluid flow field in the plane across the bottom of the chip. Inside the chassis, the air flow is minimal, approx. 0.0014 m/s. On the other hand, air velocity is 2.2 m/s at the exhaust of the RHE. The Size of the heat pipe is 2mm thick, 8mm width, and 129 mm long. The thermal Interface Material (TIM) used between the MPU and a block is 0.323 cm^2·K/W as thermal conductivity. The PCM material of

0.129 $cm^2 \cdot K/W$ is used as TIM between both the end of heat pipe and the metal part. The effective thermal conductivity of the heat pipe is K_{HP}=10,000W/m · K. The geometry of the heat spreader of the evaporator is 49mm×49mm and the condenser spreader is 40mm × 40mm.

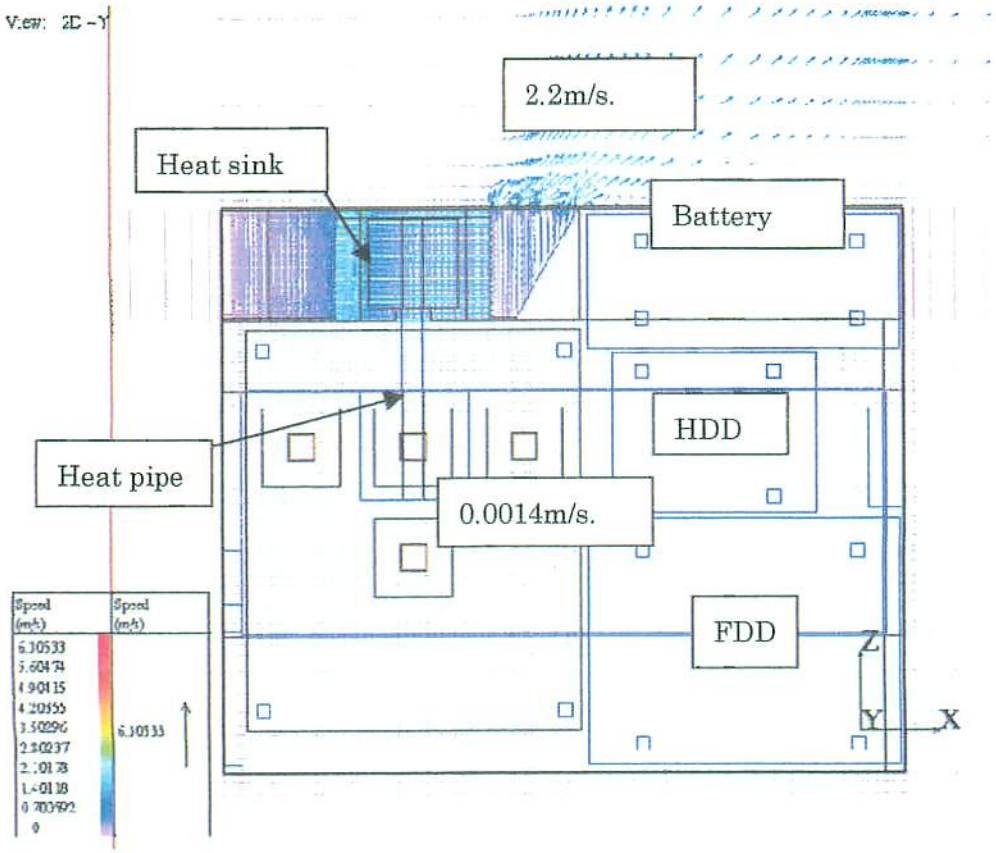

Fig. 6-20 Flow field in the plane across the bottom of chip

Figure 6-21 shows the temperature distribution inside the bottom chassis. Maximum temperature is 68.2°C at the CPU center. Figure 6-22 shows the temperature profile of heat pipe in the middle plane. The temperature difference between the evaporator and the condenser is estimated to be approximately 9.1°C.

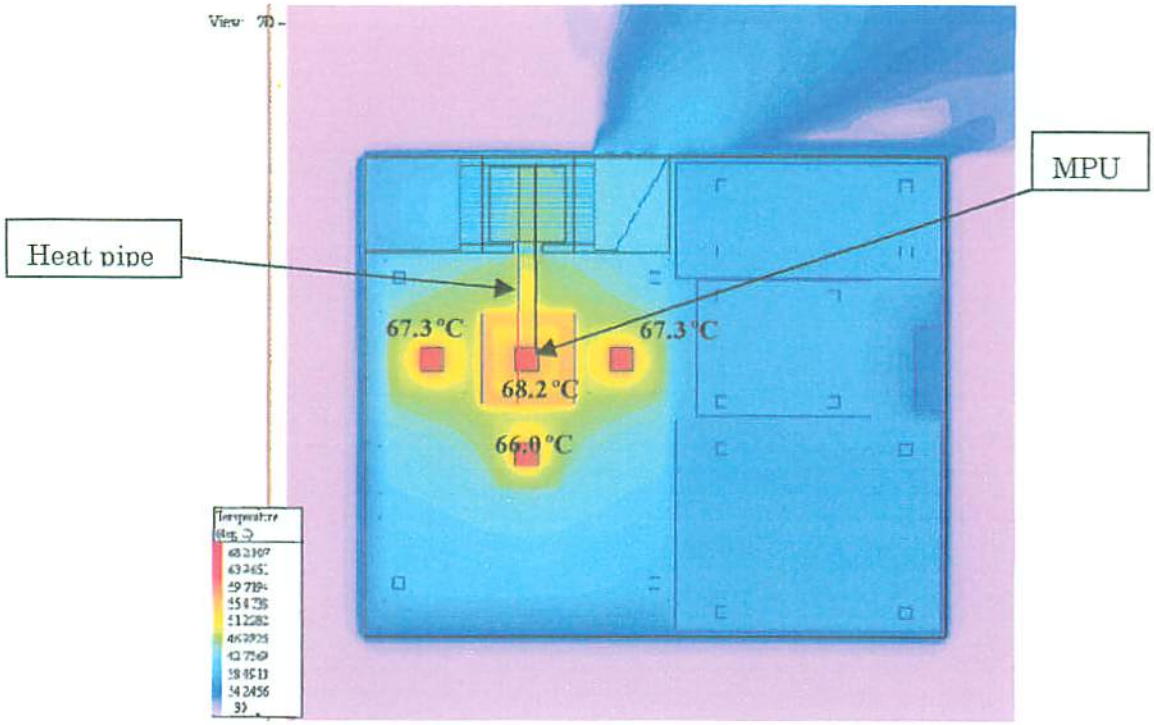

Fig. 6-21 Temperature field in the plane across the chip bottom

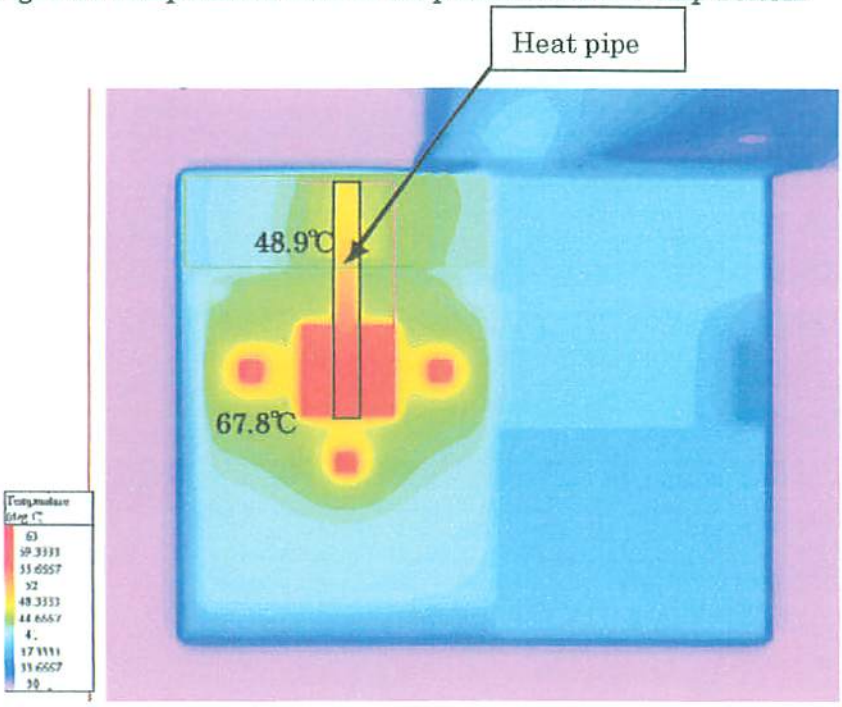

Fig. 6-22 Temperature profile of heat pipe at the middle plane

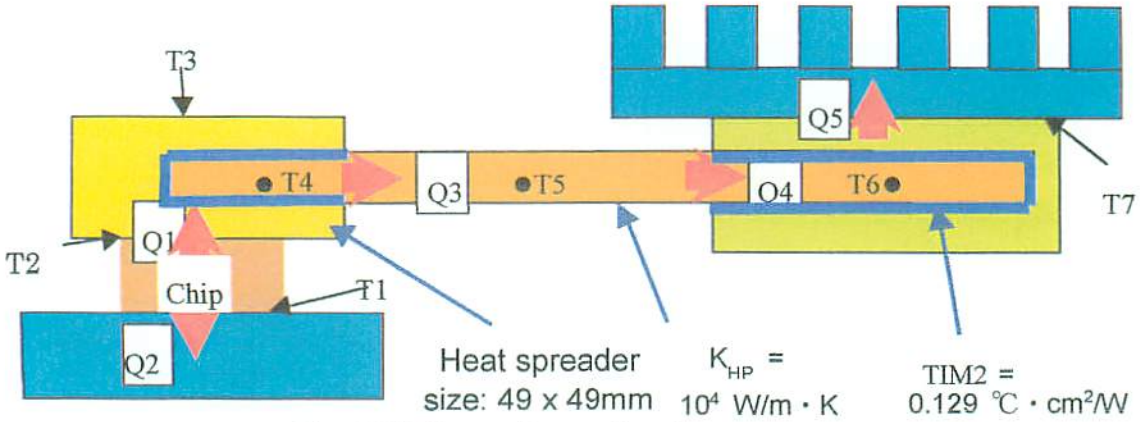

Fig. 6-23 Thermal pass of cooling system

T_1: Maximum chip temperature

T_2: Average spreader surface temperature (bottom)

T_3: Average spreader surface temperature (top)

T_4: Evaporator temperature

T_5: Temperature of middle heat pipe

T_6: Condenser temperature

T_7: Average spreader surface temperature at the top

Q_1: Heat conduction from the chip to heat spreader

Q_2: Heat conduction from the chip to substrate

Q_3: Heat conduction from the evaporator to the heat pipe

Q_4: Heat conduction from the heat pipe to the condenser

Q_5: Heat conduction from the heat spreader to heat sink

Figure 6-23 shows the thermal pass of heat pipe cooling unit. Table 6-8 shows the temperature of nodes by thermo-fluid dynamics computer simulation result.

Table 6-8 Temperature nodes by computer simulation

Measuring point	T_1	T_2	T_3	T_4	T_5	T_6	T_7
Temperature (°C)	68.2	59.4	58.9	59.1	54.2	50.1	48.3

Table 6-9 Heat flow

No. of heat	Q_1	Q_2	Q_3	Q_4	Q_5
Heat Q (W)	24.2	0.8	22.8	22.7	22.5

Table 6-9 shows the results of heat flow pattern.

The result shows that:

(1) 90% of the heat in the CPU chip is transferred through the top and to the heat sink.

(2) Approximate thermal resistance $R_{J/A}$ can be calculated in the following way:

$R_{J/A}$ = CPU temperature rise/average power

$R_{J/A}$ = 38.2°C / [0.5 × (24.2+22.5)] W=1.63 °C/W

This simulation was used in the following conditions:

Air flow rate of a fan : 2.56 CFM (ft^3/min.)(0.0724m^3/min.)

Pressure drop of heat sink : 30.7 Pa

Ambient air temperature : 30°C

Table 6-10 and 6-11 show the result of a superior heat pipe whose effective thermal conductivity was 20,000 W/m · K.

Table 6-10 Comparison result of heat flow in case of changing heat pipe thermal conductivity

Q (W)	Q_1	Q_2	Q_3	Q_4	Q_5
K=20,000W/m.k	24.3	0.7	23.3	23.2	23.1
K=10,000W/m.k	24.2	0.8	22.8	22.7	22.5

Table 6-11 Comparison result of temperature in case of changing heat pipe thermal conductivity

Temperature points	T_1	T_2	T_3	T_4	T_5	T_6	T_7
K=20,000W/mk	64.4	55.8	55.4	58.9	54.0	49.9	49.1
K= 10,000W/mk	68.2	59.4	58.9	59.1	54.2	50.1	48.3

The use of higher thermal conductivity heat pipe decreases the junction temperature rise by 10%.

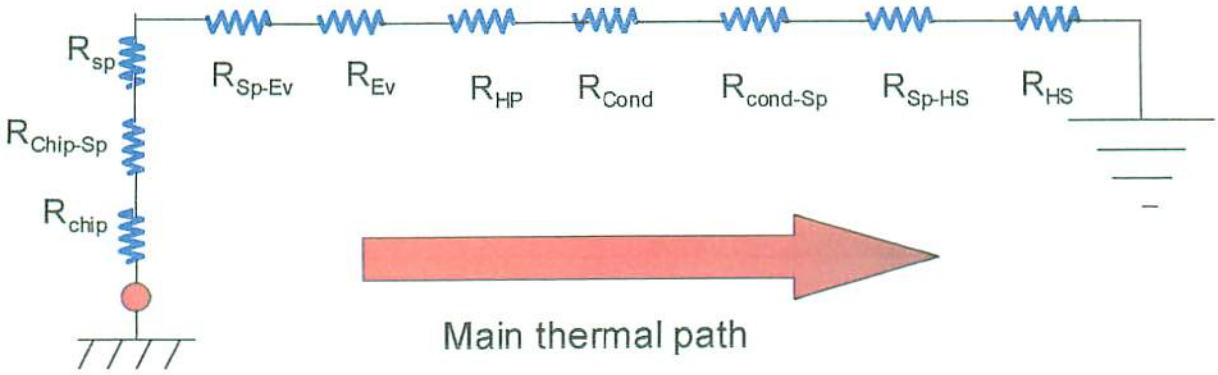

Fig. 6-24 Thermal network

Figure 6-24 shows the thermal network. Thermal resistance of each components are as follows.

- Thermal resistance from the chip bottom to the top:

  $R_{chip} = (L/K \cdot A)_{chip} = 0.65 / (100 \times 12 \times 12 \times 10^{-3}) = 0.05$ °C/W

- Thermal resistance of the TIM1

  $R_{chip\text{-}Sp} = 0.05°C.in^2.W^{-1} / (12/25.4)^2 = 0.22$ °C/W

- Thermal resistance of the aluminum heat spreader

  $R_{sp} = H/k \cdot \pi \cdot a = 0.11°C/W$

- Thermal resistance of the TIM2

  $R_{Sp\text{-}Ev} = 0.02\ °C.in^2.W^{-1} / (2 \times 49 \times 8/25.4^2) = 0.02$ °C/W

- Thermal resistance from the evaporator surface to the center of the evaporator

  $R_{Ev} = (L/k \cdot A)_{Ev} = 1 / (10{,}000 \times 2 \times 49 \times 8 \times 10^{-3}) = 0.0001$ °C/W

- Thermal resistance from the evaporator to the condenser

  $R_{HP} = (L/k \cdot A)_{HP} = 85 / (10{,}000 \times 2 \times 8 \times 10^{-3}) = 0.53$ °C/W

- Thermal resistance from the condenser center to the condenser surface

  $R_{cond} = (L/kA)_{cond} = 1/(10{,}000 \times 2 \times 40 \times 8 \times 10^{-3}) = 0.0001$ °C/W

- Thermal resistance from the condenser surface to the the heat spreader including thermal resistance of TIM2

  $R_{cond\text{-}Sp} = 0.02\ °C.in^2.W^{-1}/(2 \times 40 \times 8/25.4^2) = 0.02$ °C/W

- Thermal resistance from heat spreader to TIM1 (the heat conduction in the heat spreader is neglected)

  $R_{Sp\text{-}HS} = 0.05°C.in^2.W^{-1}/(40 \times 40/25.4^2) = 0.02$ °C/W

- Thermal resistance from the bottom of heat sink to the ambient air

  $R_{HS} = 0.8$ °C/W

Total thermal resistance of the above is calculated as below:

$R_{tot} = 0.05+0.22+0.02+0.11+0.0001+0.53+0.0001+0.02+0.02+0.8 = 1.75$ °C/W

This value is similar to the simulation result 1.63 °C/W.

6.8 Thermal interface material

Thermal interface material used between the MPU case and the heating block or heat pipe evaporator must also be of special material designed to reduce thermal resistance. The contact thermal resistance is influenced by some parameters such as surface roughness, surface flatness, contact pressure, hardness of the surface, thermal conductivity of solid material, temperature of contact surface, thermal properties of material filled between the surfaces, and interface material. There are various thermal interface materials available, for example, thermal grease, thermally conductive compounds, thermally conductive elastomers, thermally conductive adhesive tapes, phase change material (PCM), to name some. In general, grease consists of thermally conductive ceramics with silicone and hydrocarbon oils. For minimal contact thermal resistance require thin layer of thermal interface material between the mating surfaces and appropriate applied pressure. The advantages of thermal grease are best fulfill voids/gaps between the mating surfaces, no curing, lower contact thermal resistance required less applied pressure. The main disadvantage of thermal grease is dry-out problem is dry-out problems, particularly from long time use. The thickness of the thermal grease when compressed is typical in the range of 25 to 100 μm. For thermal conductive materials, it consist of thermally conductive ceramics with a cured binder. The binder forms a thin adhesive rubber layer. On assembling the material cure when applied pressure. Typical bond line thickness is about 100 μm. Silicon elastomer pads filled with conductive ceramics reinforced by woven glass are often used. This material does not need to be cured and has electrical insulation properties. However, it is necessary to add high clamping with force fasteners or springs, 100 to 500 psi. Typical bond line thickness is 0.1 to 0.5 mm. Currently Phase Change Material (PCM) has been applied as an advanced TIM. Typically a polymer/carrier filled with a thermally conductive filler, which changes from solid to a high viscosity liquid state at a certain transition temperature, is used. Bonding thickness is about 0.07 to 0.2 mm.

Table 6-12 shows a comparison of various types of thermal interface material. Two types of PCM or grease are very common materials for practical use in laptop PC's.

Table 6-12 Comparison of various type of thermal interface materials

	Typical thermal Resistance(°C/(W · m²,at 20 PSI) x 10^{-5}	Typical bond line thickness(mm)	Curing	Contact pressure	Tolerance to flatness, and warp	Re-workability	Operating temperature
Grease	1.25 to 5.16	0.02 to 0.1	No	10 to 20 PSI	Not good at high flatness variation	Possible, Messy	< 150
Thermally conductive compound	~ 6.45	0.03 to 0.1	Yes	~10 PSI	Good	Not Good	<150
Thermally conductive elastomers	6.45 to 32.2	> 0.1	No	50 to 500 PSI	Good	Good	< 150
Thermally conductive adhesive tapes	5.16 to 6.45 (phase change material base)	0.05-0.1	No	10 to 50	Good	Possible	>60
PCM	3.22	0.05 to 0.5	Online Curing	5 to 10	Medium	Good	~50 to 80
Gelwet	~6.45	0.3 to 0.5	NO	20 to 50 PSI	Good	Good	~< 150°C

References

(6-1) M. Mochizuki, T. Nguyen, K. Mashiko, Y. Saito and I. Sauciuc, *"An Advanced Heat Sink Combined with Heat Pipe for Cooling PC"*, Proceedings of the 4th JSME-KSME thermal engineering conference, pp. 2-645-648, Kobe, Japan, October 2000.

(6-2) T. Nguyen, M. Mochizuki, K. Mashiko, Y. Saito, I. Sauciuc, and R. Boggs, *"Advanced Cooling System Using Miniature Heat Pipes in Mobile PC"*, IEEE transactions on components and packaging technology, Vol. 23, No.1, pp.86-90, March 2000.

(6-3) M. Mochizuki, Y. Saito, K. Goto, T. Nguyen, P. Ho, M. Malcom, and M. Morando *"Hinged Heat Pipe for Cooling Notebook PCs"*, Proceeding of the 13th Annual IEEE Semiconductor Thermal Measurement and Management Symposium, pp.28-36, Austin, USA, January 1997.

(6-4) H. Xie, M. Aghazadeh, W. Lui and K. Haley, *"Thermal Solution to Pentium Processors in TCP in Notebooks and Sub-Notebooks"*, IEEE, Transaction on Components and Packaging and Manufacturing Technology, Part A, Vol. 19, No. 1, pp.201-210, March 1996.

(6-5) T. Nguyen, M. Mochizuki, K. Mashiko, Y. Saito and K. Goto, *"Cooling CPU Using Hinged Heat Pipe"*, Proceedings of the 5th International Heat Pipe Symposium , pp.218-222, Melbourne, Australia, Nov. 1996.

(6-6) M. Mochizuki. T. Nguyen, K. Mashiko, Y, Saito, V. Wuttijumnong, and I. Sauciuc, *"Advanced Cooling System Using Miniature Heat pipes In Mobile PC"*, Proceedings of the 6th International Heat Pipe Symposium, pp.61-64, Chiang Mai, Thailand, Nov. 2000.

(6-7) T. Nguyen, M. Mochizuki, K. Mashiko, Y. Saito, I. Sauciuc, and R. Boggs *"Advanced Cooling System Using Miniature Heat Pipes in Mobile PC"* Proceedings of the 6th ITHERM Conference, pp.507-511, Seattle, USA, May 2008.

(6-8) T. Nguyen, M. Mochizuki, K. Mashiko, Y. Saito, I. Sauciuc, and R. Boggs *"Advanced Cooling System Using Miniature Heat Pipes in Mobile PC"* IEEE Transactions on Components and Packaging Technology, Vol.23, No.1, pp.86-90, March 2000.

7. Heat sink combined with heat pipe for desktop and server

7.1 Cooling system requirement on desktop and server

Prior year 2000, the desktop PC, server, and workstation did not face significant thermal challenge because heat generation from the MPU is not as high, and also the space available for cooling is sufficient. For typical cooling of desktop PC either passive or active cooling, in active cooling a heat sink with a fan on top of heat sink, and cooling unit directly attached to the MPU, whereas in passive cooling a heat sink without fan mounted on the MPU. In the later case there is a system fan for pulling cooling air through the system as well as through the heat sink. As shown in Figs. 1.3 and 1.4, operating frequency of the MPU has reached to 1 GHz and the heat of a MPU has also reached 70 to 100 watts. While the MPU's frequency and heat dissipation increased, but the die size has not been improved and worse still it reduced in size. The wiring width of the MPU circuit was also changed from 0.25 μm to 0.18 μm. The size of heat sink required for cooling depends on the heat generation of the MPU. The size of the die, where heat generated, is significant smaller compared to the size of the base of the heat sink, therefore the cooling efficient of the heat sink is very low to the high temperature gradient existed from die to the surrounding areas. A high aspect ratio heat sink and vapor chamber are key features to achieve high performance cooling solution for a server and workstation as well as the desktop PC. The high aspect ratio heat sink has fin thickness and fin gap smaller, and fin height taller than the traditional extrusion heat sink, resulting in more surface areas for cooling and thus it is more efficient. For the high aspect ratio heat sink, it is important to consider the method of attachment of the Ins to the base. If no good attachment, heat sink performance will be significant reduced due to the high thermal contact resistance between fins and base. The heat sink called "Modified Die-Cast" (MDC) or folded fin with vapor chamber are examples of high performance cooling solution are detailing in the following.

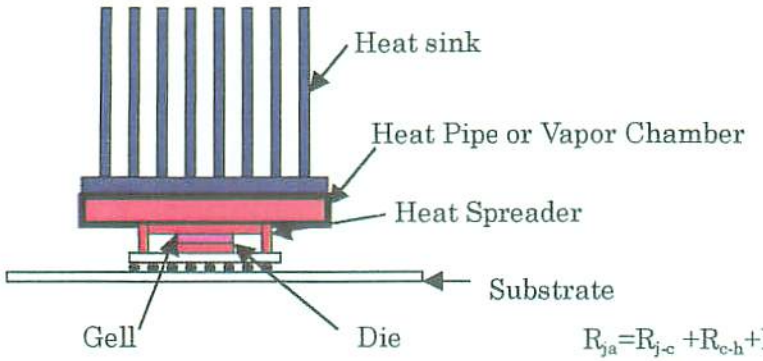

T_{system}: Increasing temperature by other components

Fig. 7-1 Structure of heat sink

Figure 7-1 shows the structure of the heat sink with the MPU. The earlier MPU does not have any heat spreader on the die but the current model has a heat spreader plate to enhance the heat transfer from processor's die. The heat spreader plate is made of copper or copper/ tungsten composition. Even with a copper heat spreader, high temperature gradient still exist on the surface of spreader plate. This problem can be eliminated if a heat pipe thermal spreader used.

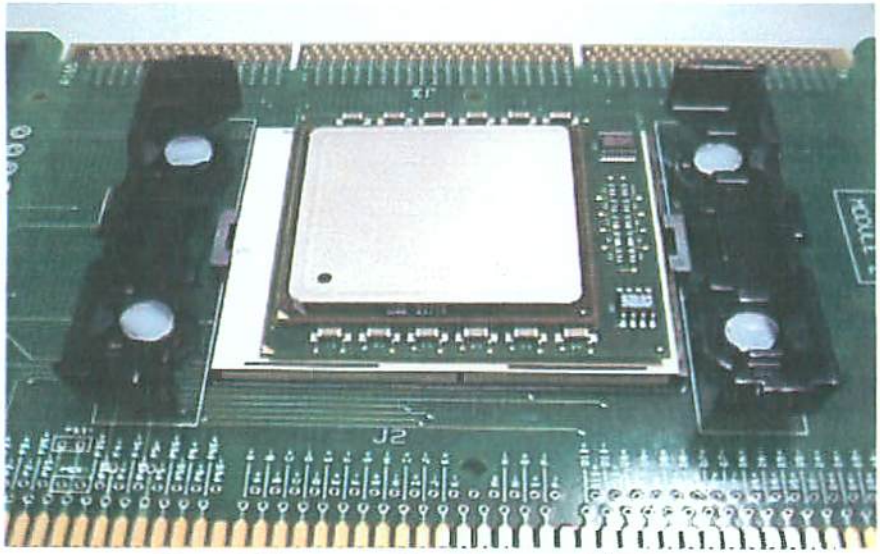

Fig. 7-2 Heat spreader of current MPU

Figure 7-2 shows the overall view of the current MPU. A die is placing on the board with the MPU smaller board fits to the MPU socket by FCPGA (Flip Chip Pin Grid Array). The processor's die is less than 1 cm^2 in size. A heat sink can be fitted directly on the spreader plate with retention mechanism and spring-clip mechanism to hold the heat sink firmly to spreader plate.

7.2 Vapor chamber heat sink[7-4 - 7-9]

7.2.1 Structure of vapor chamber heat sink

The schematic structure of the vapor chamber heat sink is shown in Fig.7-3. The shape of the copper-water vapor chamber is flat and rectangular, and the condensing surface is larger than the evaporating surface. The fin base bonded to the condensing surface of vapor chamber. The wicks of the vapor chamber is a fine porous copper powders coated by plasma spray technique where used on the surface of evaporator as nucleate boiling surface and wicks for capillary force. The configuration of Fig. 7-3 shows that the tapered shape enhance the gravity effect to assist the condensed liquid returning to the evaporator.

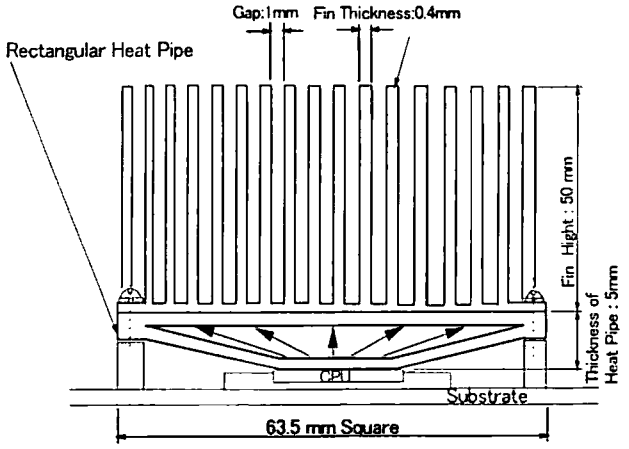

Fig. 7-3 The schematic of high aspect ratio fins with vapor chamber

7.2.2 Thermal test of vapor chamber heat sink

In testing of the vapor chamber, a 1 inch square electric heater simulated as a heat source, was attached to the bottom of the evaporator of the vapor chamber. Heat sink attached directly on the top of the vapor chamber, and the unit tested in fully air flow. At first, the vapor chamber was examined in the condition of the bottom heat mode arrangement (inclined angle = 0 degree). Thermal resistance R_t (K/W) of vapor chamber was calculated by equation (7-1).

$$R_t = (T_{hpe} - T_{ain}) / Q \quad (7\text{-}1)$$

Where, T_{hpe}: Temperature of evaporating surface of vapor chamber (°C)

T_{ain} : Inlet temperature of cooling air (°C)

Q : Heat input (W)

Figure 7-4 shows the test results of the thermal resistance of the vapor chamber heat sink at various heat input, up to 160 watts. The result showed that for heat input of 20 to 160 watts, the thermal resistance of the vapor chamber heat sink

remained almost constant at 0.2 and 0.25 K/W at cooling air velocity of 1 m/s. Thermal resistance are the same when tested at different orientation. Also shown in Fig. 7-4. the comparison of the thermal resistance when the vapor chamber base was replaced with solid copper or aluminum base of the same geometry. The result clearly indicated that the vapor chamber heat sink is 2.5 to 3 times better than the solidl base heat sink.

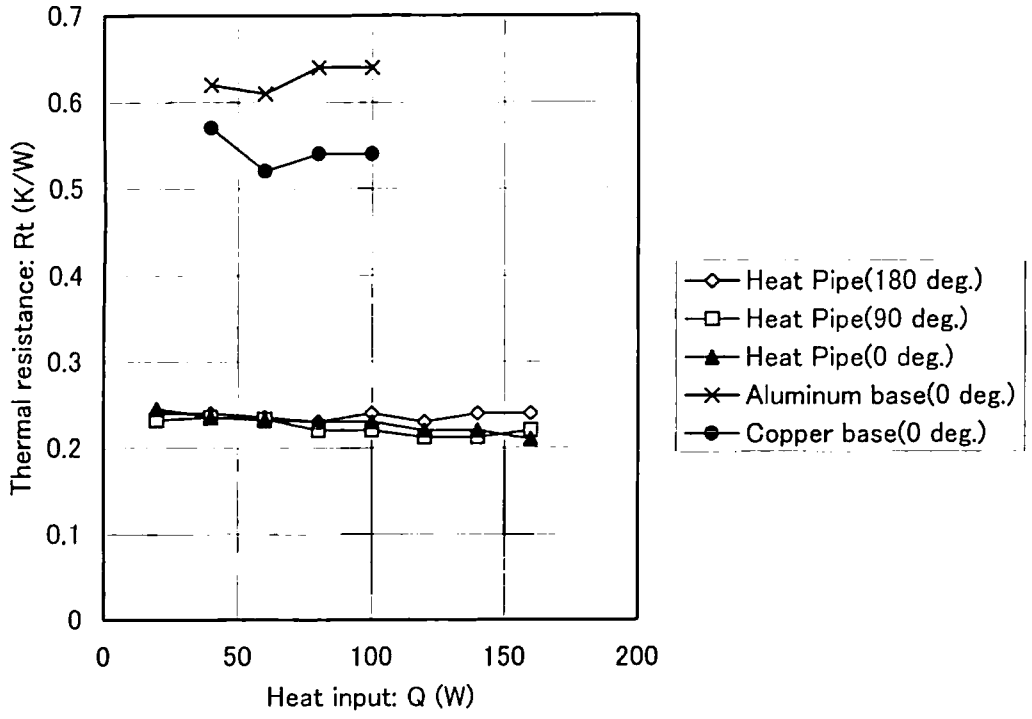

Fig. 7-4 Thermal resistance of vapor chamber heat sink in comparison with metal base heat sink (Vair=1m/s)

Figure 7-5 shows the test results of the thermal resistance of the vapor chamber heat sink and cooling air pressure drop air at various inlet velocity 1 to 3 m/s. at the front. The results showed that the thermal resistance is about 0.5 K/W to 0.3 K/W at air inlet velocity approximately 1 and 2 m/s. respectively. In the current demand for cooling specifications. 2 m/s of inlet air velocity is acceptable and sufficient for cooling 40 to 100 watts. Higher air velocity may cause unacceptable acoustic noise.

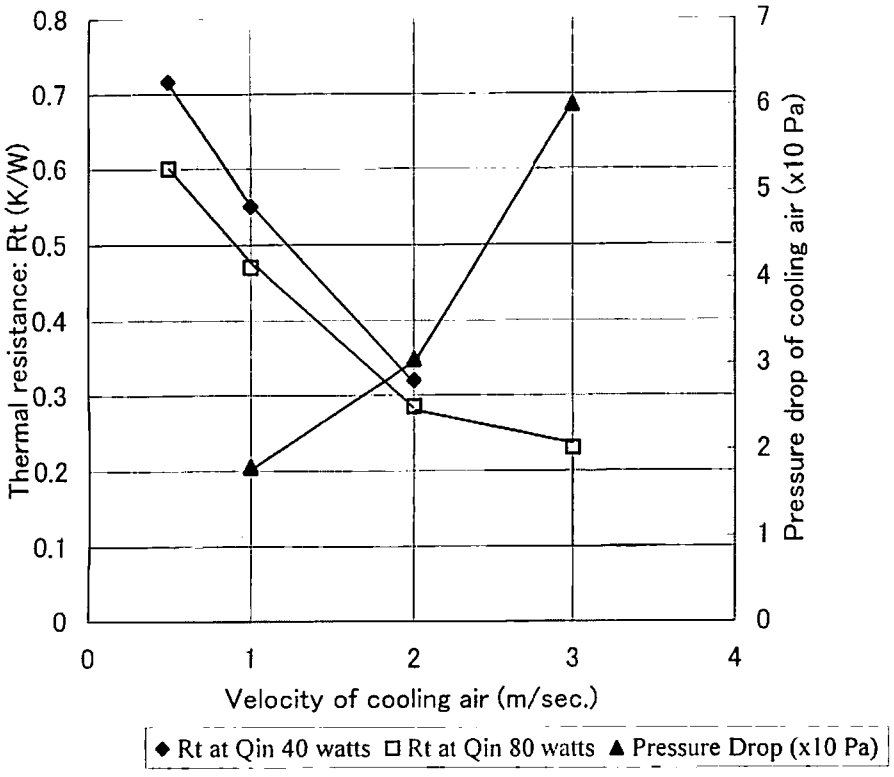

Fig. 7-5 Thermal resistance and pressure drop vs. air cooling velocity

7.3 The optimum working fluids ratio for vapor chamber[7-7]

7.3.1 Background of the development

The vapor chamber (or flat plate heat pipe) has been developed for use as the base of the heat sink for cooling high heat flux electronic devices. Many papers have investigated the internal structures of vapor chambers to determine the parameters for high performance. The working fluids ratio is one of parameter that can affect the performance of vapor chambers. The objectives of this experimental study were to see the effects of the working fluids ratio, and to find the optimum working fluids ratio to vapor chambers used in electronics cooling. In this study, two types of vapor chambers were used (A-Type and B-Type vapor chambers have different dimensions, and internal porous wick structures). All tests were conducted under identical conditions with varying working fluids ratios (relative to the calculated internal volume of each vapor chamber), and varying power inputs.

Seri Lee[7-1] proposed a correlation for calculating the spreading resistance of heat sink base. He showed that when the size of the heat sink base is larger than the heat source, or that the heat source is located at the end of the heat sink, the spreading

resistance of the heat sink base increased. Mashiko et al.[7-2] proposed the combination between the heat sink and vapor chamber used in an advanced cooling system. By considering the contact resistance (R_c=0.5 × 10^{-4} m^2 °C/W) between vapor chamber and heat sink, and the heat transfer coefficient (30.000W/m^2°C) between the evaporator and condenser of the vapor chamber. they indicated that when the ratio of heat sink base area to heat source area is about 5 times. the total resistance of the heat sink with vapor chamber was smaller than that of only the heat sink with the same thickness. Z. Jon Zuo and Mark T.North[7-3] proposed the improvement for vapor chamber performance by using graded wick structure. Theoretical models were developed to calculate liquid pressure profiles within the grading wick structures for both 1D and 2D configuration. By comparing the graded and uniform wick structures, they proposed that the graded wick structures are capable of improving heat pipe capillary limits. The working fluids ratio was one of several parameters that contribute to vapor chamber performance, not just to avoid dry-out. The objectives of this experimental study were to see the effects of the working fluids ratio on the performance of vapor chambers, and to determine the optimum working fluids ratio for the minimal thermal resistance.

7.3.2 Vapor chambers

Vapor chambers which function in the same manner as conventional tubular heat pipes whose main difference is the type of the wick which assist liquid to distribute over a large surface area. The main characteristic of this form of heat pipe is its ability to produce a very small temperature gradient across the surface. The nearly isothermal surface characteristic of the vapor chamber helps to spread the heat and reduce hot spots produced by the heat source. By attaching a number of heat generating components to the vapor chamber base, they can be operated at similar temperatures due to the in-built equalization process resulting from the fact that the vapor space will be at a fixed uniform temperature.

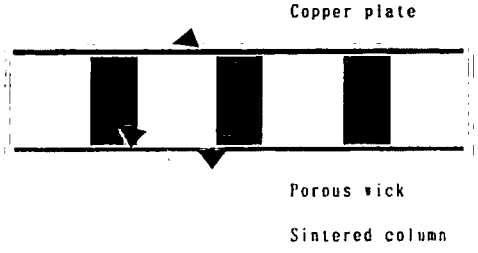

Fig. 7-6 The internal structure of a vapor chamber

Figure 7-6 shows the internal structure of a vapor chamber. Copper is used for the container, with 0.5mm sintered wicks attached to the internal surfaces of the container. The fine porous sintered powder wicks provide high capillary force to maintain liquid circulating from the condenser to the evaporator in the vapor chamber. Sintered columns, of the same porous size and material as the wicks, are used to ensure that liquid can be returned to and distributed over the top surface of the plate in cases where the operation is against gravity.

7.3.3 Experimental setup

Two types of vapor chambers (different in dimensions as shown in Table 7-1) were fabricated and tested for comparison. All tests were conducted under identical conditions with varying working fluids ratios (relative to the calculated internal volume of each vapor chamber), and varying power inputs. The test setup is shown in Fig.7-7. The size of the heater block was 20 × 20mm, located at the center of the vapor chamber. The heat sink was cooled by air velocity at 3 m/s in a fully ducted flow. The power input to the heater block was varied from 40W to 180W in 20W increments. Temperatures were recorded at thermocouple locations shown in Fig. 7-8. After that, we calculated the thermal resistance of the vapor chamber. In this experimental study, we considered the thermal resistance from the heat sink to the ambient air as:

$$R_{pipe} = (T_{sinkbase} - T_{ambient}) / \text{Power} \qquad (7\text{-}2)$$

Table 7-1 Dimensions of vapor chambers

Dimensions	A-Type	B-Type
Overall Length (mm)	89.0	106.0
Overall Width (mm)	76.0	47.0
Overall Height (mm)	4.6	6.7
Internal volume (cm^3)	1.0	1.5

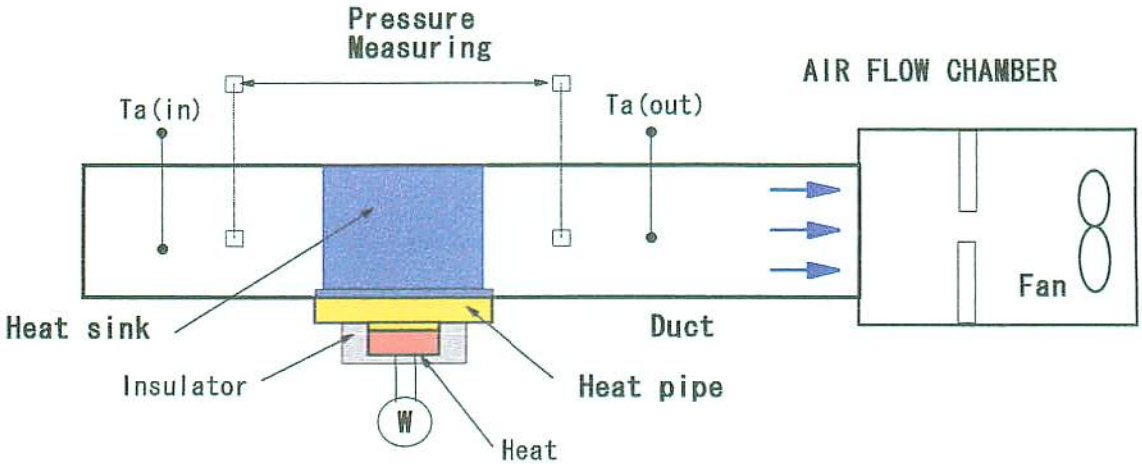

Fig. 7-7 Test setup

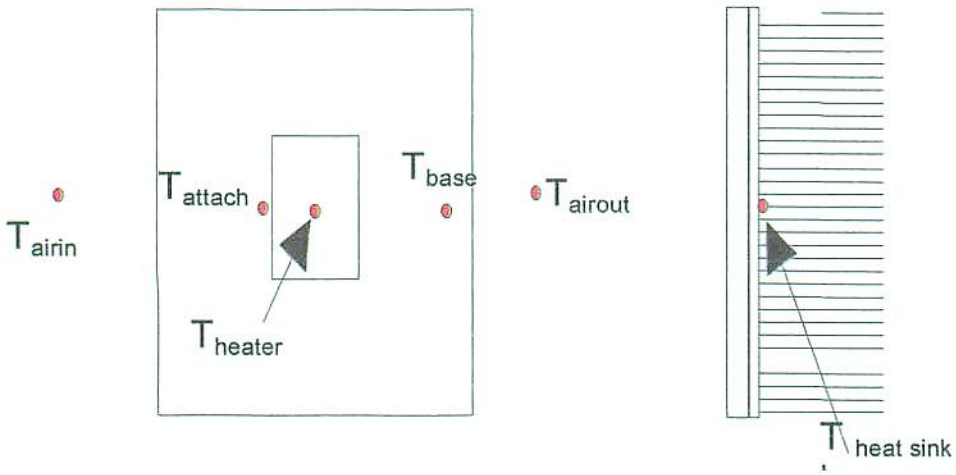

Fig. 7-8 Thermocouple locations

7.3.4 Test results and discussion

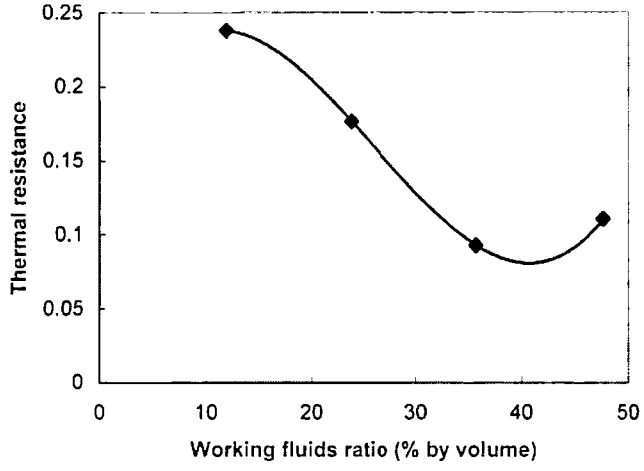

Fig. 7-9Effect of working fluids ratio on the thermal resistance for A-Type vapor chamber.

Figure 7-9 shows the results of the A-Type vapor chamber. When the working fluids ratio was increased from 20% to 40%, the thermal resistance of the vapor chamber was decreased from 0.2°C/W to 0.08°C/W. The thermal resistance of the vapor chamber increased with the working fluids ratio above 40%. It can be concluded that the optimum working fluids ratio for the A-Type vapor chamber is 40% of the internal volume, a minimum thermal resistance being 0.08°C/W.

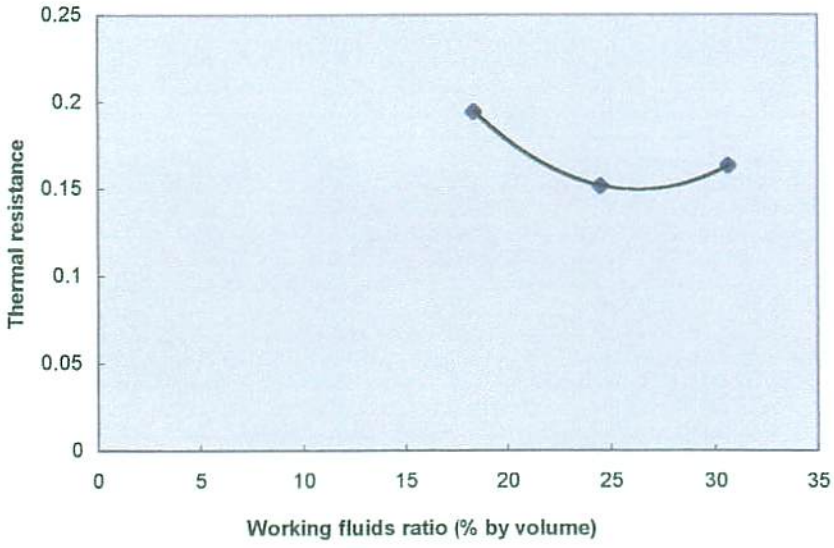

Fig. 7-10 Effect of working fluids ratio on the thermal resistance for B-Type vapor chamber.

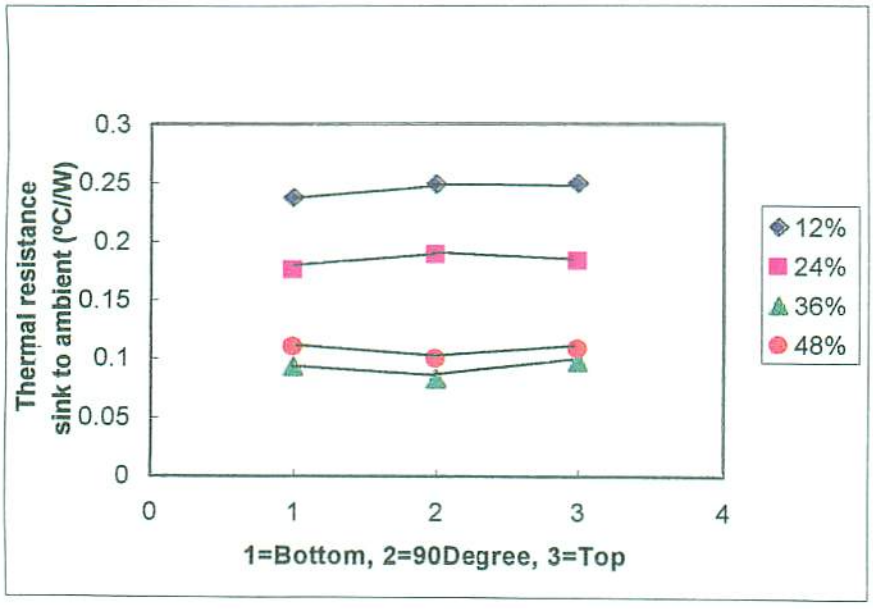

Fig. 7-11 Effect of orientation on thermal resistance of A-Type vapor chamber

Figure 7-10 shows the result of thermal resistance when the working fluid ratio is changed, in the case of the B-type vapor chamber. When the working fluids ratio was

increased from 15% to 25%, the thermal resistance of the vapor chamber decreased from 0.2°C/W to 0.15°C/W. The thermal resistance of the vapor chamber increased with the working fluids ratio above 25%. It can be concluded that the optimum working fluids ratio for the B-Type vapor chamber is 25% of internal volume at a minimum thermal resistance of 0.15°C/W.

Figure 7-11 shows the thermal resistance of the A-Type vapor chamber when changed orientation. It can be seen that the thermal performance of the vapor chamber is insensitive to orientation. This is due to the sintered columns inside the vapor chamber which assist the return of the working fluid to the evaporating surface when in top heat mode. Similar results were observed for the B-Type vapor chamber. It can be concluded that for a vapor chamber with internal sintered columns, the orientation of the vapor chamber did not affect the thermal resistance.

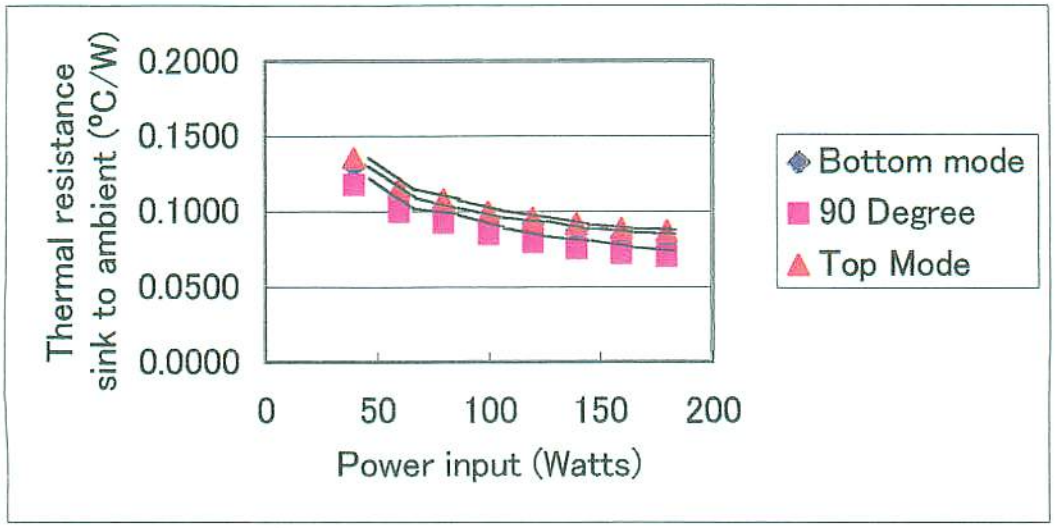

Fig 7-12 Effect of power input to thermal resistance of A –type vapor chamber.

Fig 7-12 shows the effect of power input on the thermal resistance of the A-Type vapor chamber at 36% working fluids ratio. When the power input increased from 80W to 100W, the thermal resistance of the vapor chamber decreased from 0.11 K/W to 0.1 K/W. Similar results were observed for the B-Type vapor chamber. It can be concluded that the thermal resistance decreases as the power input increases.

Conclusions of this test:

1)For the A-Type vapor chamber the optimum working fluids ratio was 40% of internal volume, with the minimum vapor chamber thermal resistance of 0.08°C/W.

2)For the B-Type vapor chamber the minimum working fluids ratio was 25% of internal volume, with the minimum vapor chamber thermal resistance of 0.15°C/W.

3)The working fluids ratio affects the thermal resistance of vapor chambers.

4)The orientation of the vapor chamber does not affect the thermal resistance of vapor chambers with internal sintered columns.

5)Thermal resistance decreases as power input increases.

7.4 Evaluation of vapor chamber effectiveness

Equations (7-3) and (7-4) show the thermal spreading resistance of a heat sink base which was presented by Seri Lee. [7-1]

$$R_c = \frac{\sqrt{A_p} - \sqrt{A_s}}{k\sqrt{\pi A_p A_s}} \times \frac{\lambda k A_p R_o + \tanh(\lambda t)}{1 + \lambda k A_p R_o \tanh(\lambda t)} \qquad (7\text{-}3)$$

$$\lambda = \frac{\pi^{3/2}}{\sqrt{A_p}} + \frac{1}{\sqrt{A_s}} \qquad (7\text{-}4)$$

Where,

A_p = Footprint area of the heat sink-base plate (m^2)

A_s = Footprint or contact area of the heat source (m^2)

k = Thermal conductivity of the heat sink base-plate (W/m °C)

R_c = Spreading thermal resistance of heat sink-base plate (°C/W)

R_o = Average heat sink thermal resistance (°C/W)

t = Thickness of the heat sink-base plate (m)

On the other hand, the thermal spreading resistance of a vapor chamber can be approximated in the equation (7-5).

$$R_{hp} = 1 / (h_e \cdot A_e) + 1 / (h_c \cdot A_c) \qquad (7\text{-}5)$$

where,

R_{hp}: Thermal spreading resistance of vapor chamber (℃ / W)

h_e : Heat transfer coefficient of evaporator (30,000 W/m^2 · ℃)

A_e: Heat transfer area of evaporator, assumed that A_e equals to the contact area of the heat source A_s

h_c : Heat transfer coefficient of condenser (30,000 W/m^2 · ℃)

A_c: Heat transfer area of condenser, assumed that A_c equals to the base plate of the heat sink A_p

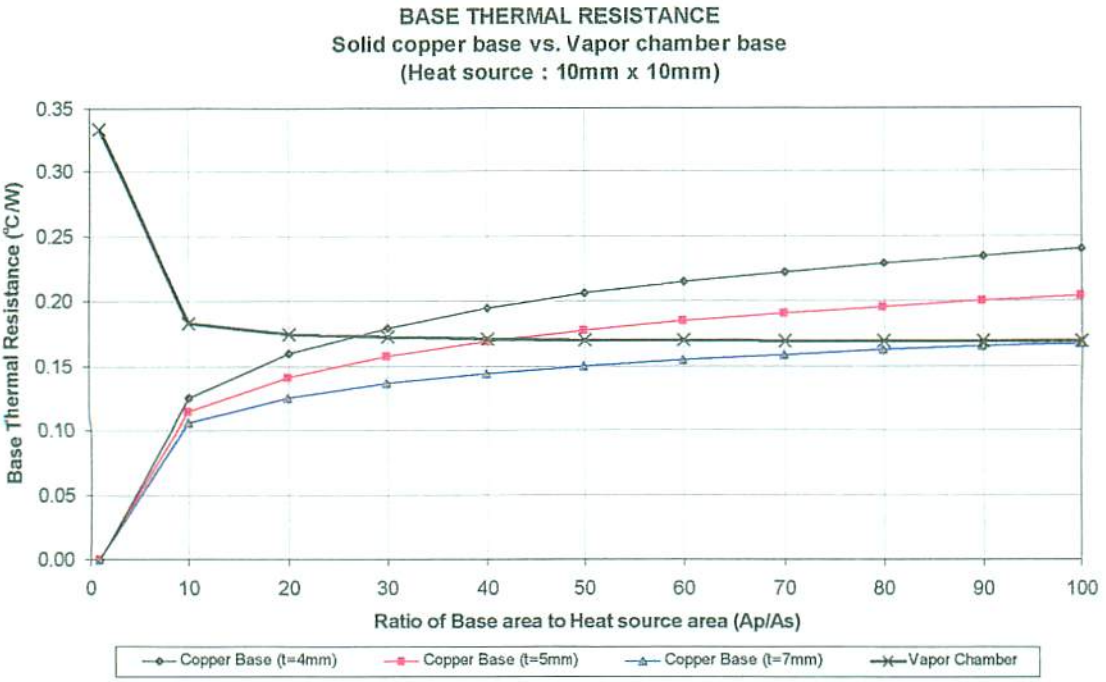

Fig. 7-13 Thermal spreading resistance of vapor chamber vs normal heat sink in case of 10mm × 10mm heat source

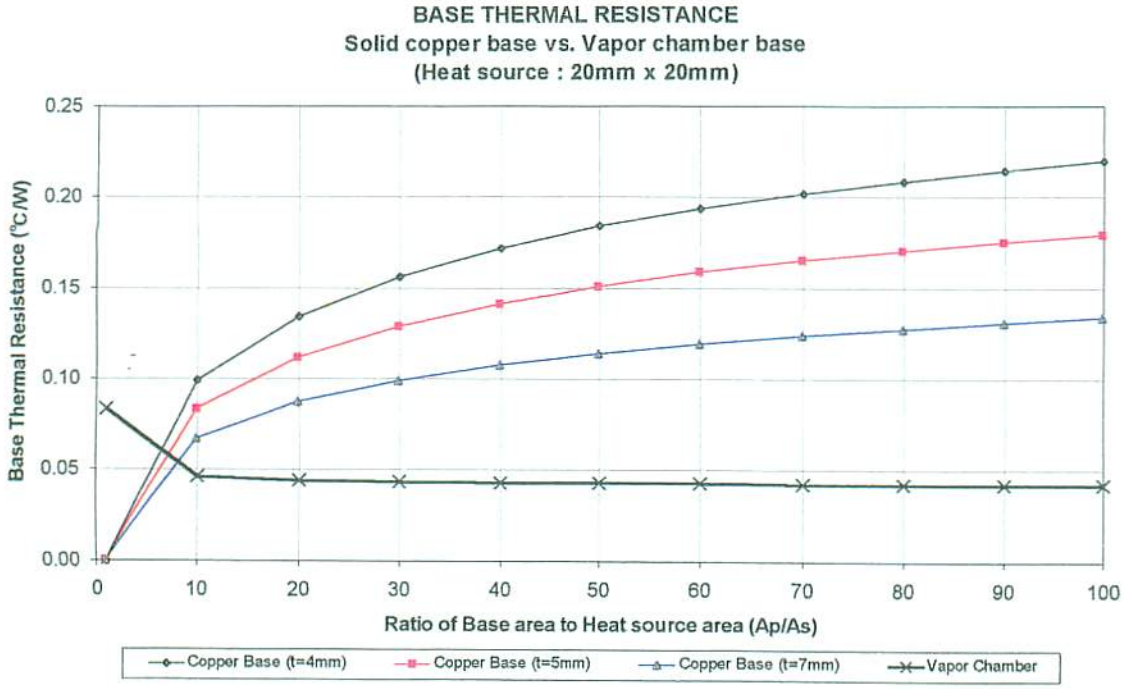

Fig. 7-14 Thermal spreading resistance of vapor chamber vs normal heat sink in case of 20mm × 20mm heat source

Figures 7-13 and 7-14 show the calculation result of heat spreading resistance of a traditional heat sink of solid base and vapor chamber. The spreading resistance of the traditional heat sink increases as the ratio of A_p/A_s increases, and on the other hand, the VC has constant resistance. In the case of a 20mm × 20mm die or heat spreader, the VC can become thermally effective when the ratio of A_p/A_s is larger than 5. This means that if a heat sink base is larger than 2,000 mm^2, i.e., bigger than 40mm × 50mm, vapor chambers help to reduce the thermal resistance.

7.5 Example of vapor chamber heat sink for practical use

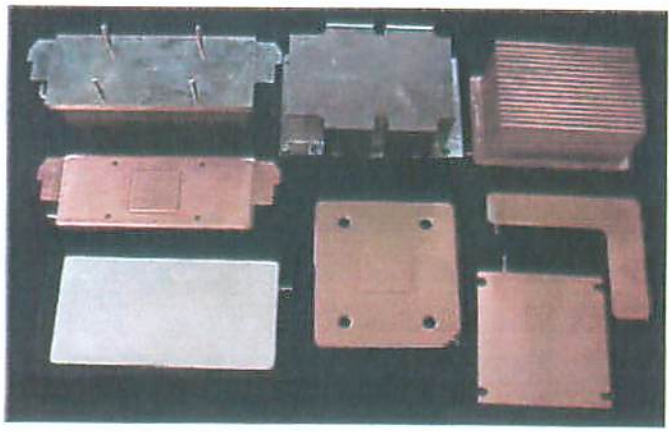

Fig. 7-15 Various types of vapor chamber and heat sink

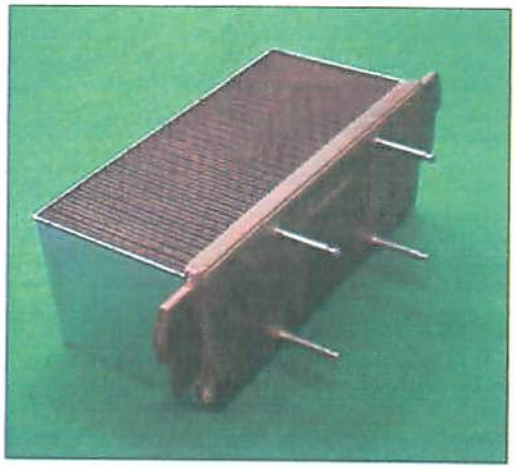

Fig. 7-16 Vapor chamber heat sink

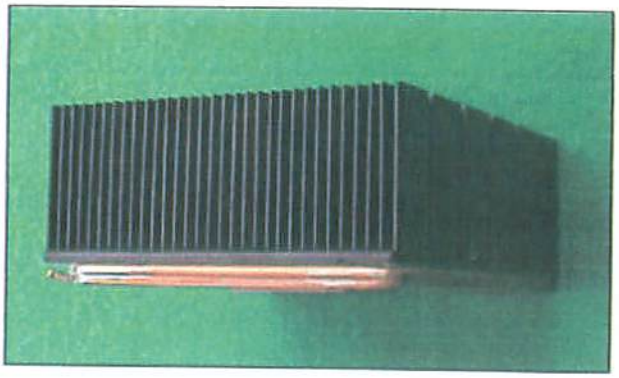

Fig. 7-17 Vapor chamber heat sink

Figure 7-15 shows various types of vapor chambers and heat sinks which have been applied to practical use. Figure 7-16 shows a folded fin heat sink metallic soldered on the copper vapor chamber. This heat sink base is very wide, so that the vapor chamber can reduce the spreading resistance in this direction. An example shown in Fig. 7-17 consists of a cold forged heat sink bonded to vapor chamber by hard cure thermal epoxy.

7.6 Heat sink with traditional heat pipe application

Fig.7-18 shows a design that has a 1 inch OD vertical heat pipe with stacked fins. This type is very common and efficient for use in large enclosure server due to its low air impedance characteristics.

Fig. 7-18 Tower heat pipe heat sink

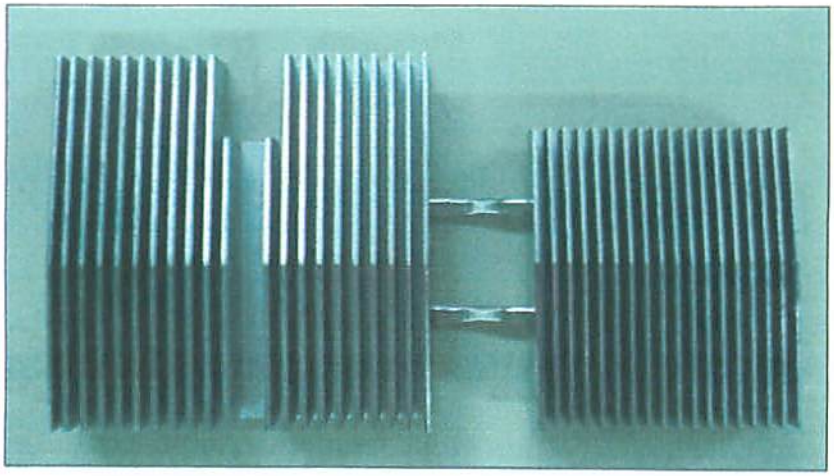

Fig. 7-19 Heat sink with remote heat pipe heat exchanger

Fig. 7-19 shows compact remote heat exchanger which consisted of heat pipe and heat sink. These types have been used in 1U server (38.1mm height chassis) which is a low height enclosure, that has space constant to install bigger heat sink on the MPU. Heat pipe can be used to transfer the heat from the MPU area where space is restricted and to a remote areas where larger space for cooling is available.

References

(7-1) Seri Lee, *"Calculating Spreading Resistance in Heat Sinks"*, Electronics Cooling, Volume 4, No.1, pp.30-33, January, 1998.

(7-2) Koichi Mashiko, Masataka Mochizuki, Yuji Saito, Thang Nguyen, Rex Boggs and Ioan Sauciuc, *"Advanced Cooling System Combined with Heat Sink and Heat Pipe for Cooling PC "*, Proceedings of 11th International Heat Pipe Conference, Japan, pp. 464-468, Tokyo Japan, September 1999.

(7-3) Z. Jun Zuo and Mark T. North, "*Improved Heat Pipe Performance Using Graded Wick Structures"*, 11th International Heat Pipe Conference, Japan, pp. 80-84, 1999

(7-4) K. Mashiko, M. Mochizuki, Y. Saito, and M. Nagata, *" Cactus Type Heat Pipe for Cooling CPU"*, 33rd National Heat Transfer Symposium of Japan, pp.787-788, Niigata Japan, May 1996.

(7-5) The Heat Transfer Engineering Data Book, (the 4th edition revision), J.S.M.E., pp.46

(7-6) A. D. Kraus, and A. B. Cohen, *"Design and Analysis of Heat Sinks"*, John Wiley & Sons Inc., pp.273-278

(7-7) V. Wuttijumnong, M.Mochizuki, K.Mashiko, I. Sauciuc, and T. Nguyen, *" The Optimum Working Fluids Ratio for Vapor Chamber"*, Proceedings of the 6th International Heat Pipe Symposium, pp.159-163, Chiang Mai Thailand, November 2000.

(7-8)T. Nguyen, M. Mochizuki, K. Mashiko, and Y. Saito, *"Use of Heat Pipe Heat Sink for Thermal Management of High Performance CPUs"*, Proceedings of 16th Annual IEEE Semiconductor Thermal Measurement and Management Symposium, pp.76-79, San Jose, CA USA, March 2000.

(7-9) M. Mochizuki, K. Mashiko, K. Goto, Y. Saito, M. Nagata, K. Eguchi, T. Nguyen, and P.Ho, *"Cactus-Type Heat Pipe for Cooling CPU"*, Proceedings of the 5th International Heat Pipe Symposium, pp.194-198, Melbourne Australia, November 1996.

8. Innovative and advanced cooling system for cooling PC [8-1]

Finally, I would want to propose an innovative and advance cooling system for cooling of higher power MPU for future research. In the current cooling technology, fan heat sink air cooling system is the most common and practical use due to its readily available, low cost and low maintenance. The heat transfer capacity is the product of mass flow and temperature difference between the heated surface and cooling air ($Q=m \cdot Cp \cdot \Delta T$). Fan is just to provide air flow, and obviously the higher air flow, but the higher air flow associated with higher acoustic noise. The forced sir cooling system will soon reach its limit when the air flow has reach its limit level where the acoustic noise is not acceptable for human comfort. It would not be acceptable if fan operating like an airplane turbine inside a PC. A better approach is to find a way to reduce the temperature rather than increase the air flow. For example, using air conditioning system to reduce the ambient temperature and thus increase the heat transfer. The advance cooling system proposed here is an opened air Brayton cooler. This system is only at the initial stage of development so the structure is complex and size is relatively large. It is believe that the design could be refine to compact size and manufacture-able for use of PC in near future.

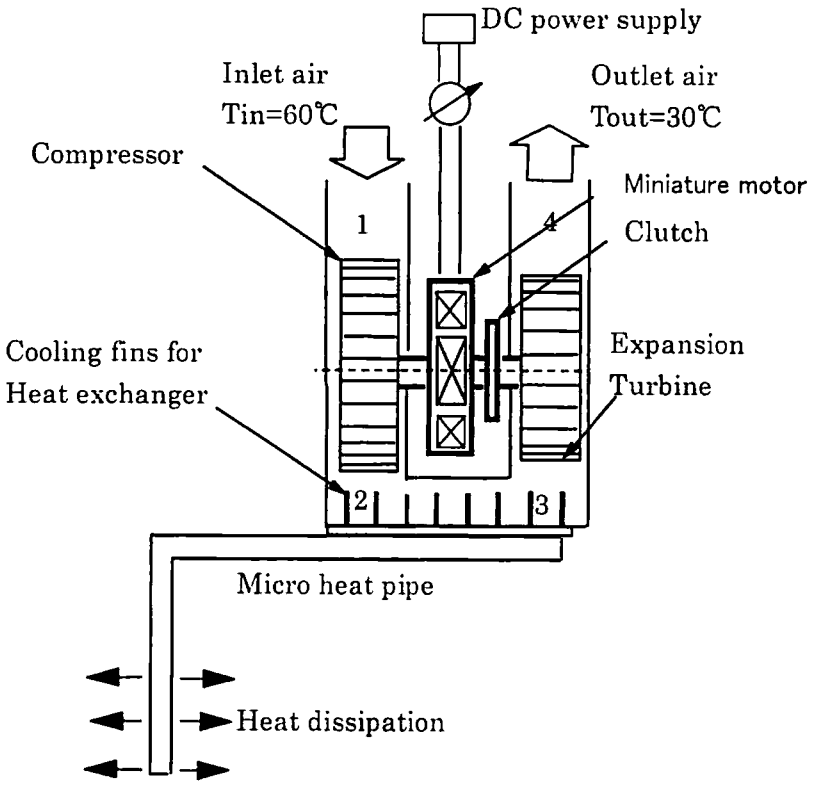

Fig. 8-1 Conceptual schematic of opened Brayton air cooler

Figure 8-1 shows the conceptual schematic of opened Brayton air cooler. A hot air

is compressed to higher pressure, maybe 1.3 atoms by a compressor and cooled by a heat pipe heat exchanger. Compressed air is expanded by an expansion turbine or a nozzle. The exhaust air temperature can be chilled. The chilled air is applied to cooling chips. As a turbine and an expander are located on the co-shaft, the expansion turbine can recover the energy from expansion air. This can become energy conservation. When chip does not need to cool by chilled air, a compressor has just simple task such as a common fan after power transmission is cut off by the clutch.

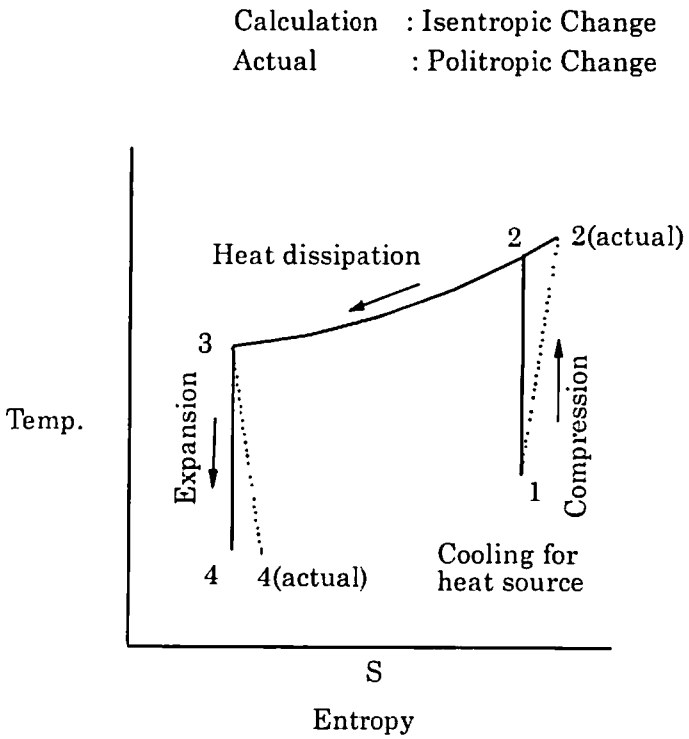

Fig. 8-2 T-S Diagram of opened air Bayton cooler

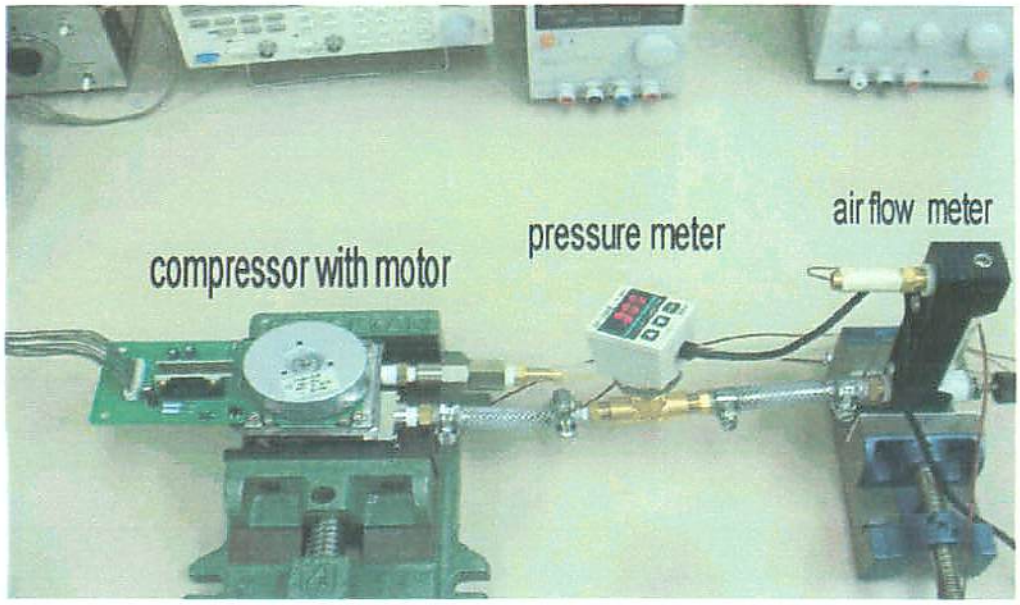

Fig. 8-3 Testing setup of Brayton cooler

Figure 8-2 shows the T-S diagram of the Brayton cooler. The thermo-dynamic cycle consists of three process of compression, cooling, and expansion. Figure 8-3 shows the fundamental setup to test the cycle. It will be introduced in detail at next opportunity.

Reference

(8-1) J. Sutanto, A. Akbarzadeh, M. Mochizuki, T. Nguyen, and H. Imura, *"Brayton Cycle Cooling Sytem"*, Proceedings of 6th International Heat Pipe Symposium, pp.456-460, Chiang Mai Thailand, November 2000.

9. Conclusion

In the demand for increasing higher performance PC, the MPU has to run at higher speed and that caused increase in heat dissipation. As a result, there has been active development on advance cooling system to cope with this high performance and high heat dissipation MPU. In particular, the MPU for the laptop PC needs an advanced cooling system with a passive or semi-passive solution that used miniature heat pipe of 3 to 6 mm diameters were developed and had been actively put into practical use. First, this paper discussed and provided the requirement of the thermal performance for cooling PC and the performance of the MHP. There are various types of wick structure in heat pipes such as fiber wicks, sintered powder, screen mesh and axially grooved. This research covered the optimization of wick design, maximum heat transfer of the MHP, thermal resistance and the influence of the heat pipe to orientation through experiment. For practical use, most heat pipes are fabricated into a flattened shape of 2 mm thickness and several bends to suit the apace constraints in the PC. Investigation on the variation of heat transfer characteristics of heat pipe after it had been flatten and bent vs. original round heat pipes also presented. A MHP has a small quantity of optimum filling charge of working fluid. The amount of fluid about in the 0.1 gram level due to the small internal volume of heat pipe. Therefore, it is very important to maintain accurate filling error within $\pm 5\%$ against total volume. To achieve this accuracy required state of the art process, techniques and equipment. There has been a trend in using thin laptop PC's of A-4 and B-5 size particularly in Japan. Thermal performance of thinner heat pipe of 2.0mm and 1.5mm was investigated. Research and tests have been performed to improve the thermal performance of heat pipe by improving the wetability of the heat pipe's internal surface and wick material. Additionally, super fine fiber wick heat pipe and a sintered wire heat pipe have been developed to achieve lower thermal resistance and higher maximum heat transfer rate.

This paper has investigated methods by which a reasonable cooling system using MHPs for laptop PC's can be achieved. In 1994 or earlier, the cooling system in laptop PC was by ventilation, natural convection cooling using a small heat sink or an aluminum spreader plate since the MPU heat generation was lower than 3 watts. When the Pentium processors were introduced, the heat generation of the MPU sharply increased, so the use of heat pipe with a thermal spreader plate for cooling is most efficient and favorable solution to put into practical use. The thermal resistance between the temperature of the chip junction to the ambient air was approximately 6 to 10 K/W. It was required that the thermal resistance of heat pipe to be less than 1K/W.

Preferably as low as possible to compensate for thermal resistance of other components like the spreading plate, contact thermal resistance between a heat pipe and mating parts, and heat sink to ambient. The use of metallic soldering, thermal epoxy between the mating surface will help to minimize the contact resistance. Thermal interface materials such as silicon or boron-nitride base thermal pad, thermal grease and phase change material are often use to reduce the contact resistance between the MPU and cooling units.

A forced air cooling system called a Remote Heat Exchanger (RHE) was developed in 1998 to act against increasing MPU heat over 10 watts. A RHE consists of a block to attach the MPU, a heat pipe to carry the heat, and a heat exchanger with a miniature fan to exhaust heat to the ambient air. The paper described the design concept and its experimental study on the thermal issues.

There has been active development on the passive solution even for high performance MPU. Passive solution conserved energy on the battery so the laptop PC van run longer hours when it is operated in battery mode. Therefore, a hinged heat pipe cooling system developed as a passive cooling system. Basically, the hinged heat pipe cooling system consisted of a primary heat pipe that transfers heat from the MPU to hinged parts. A secondary heat pipe takes over to transfer the heat to the back panel of the Liquid Crystal Display where the temperature is the lowest because of the smaller heat-generating parts than the bottom skin area of the laptop PC. The LCD is an excellent area for heat dissipation because of the large surface available and vertical orientation. The thermal hinge has thermal resistance less than 1 K/W. Reliability tests of opening/closing was carried out on thermal hinge for 30,000 cycles, and results showed no degradation on the thermal hinge performance.

Since the MPU power has still been increasing and there are many other parts which generated heat such as HDD, memory, PCMCIA, and others heat generated components, a cooling system design must take into account of all these heat generated components. This paper also described a system level thermal design using a computer aided thermo-fluid dynamics modeling.

For the desktop PC, server and workstation. There is need and demand for advance heat pipe cooling technology. The current and widely used cooling technology for desktop PC consisted of a fan mounted direct on the heat sink. For server and work station, in most cases, the fan was not mounted direct on the heat sink, but instead of a bigger fan used in the system to provide the air flow through the heat sink as well as the whole system. The MPU continued and rapidly increased operating frequency and well pasted 1 GHz. The correspondence heat dissipation in the range 70 to 100 watts.

The heat dissipation of the MPU was exponentially increased. but the die size of the MPU remained the same or even reduced in size. As a results a significant increased in the heat density of the MPU. and that created further challenge to solve the thermal problem. The size of wiring width has been decreased from 0.25 μ m to 0.18 μ m. and expected to reduce further to cope with the everlasting demand of more faster performance MPU. The MPU heat dissipation significantly increased. but the space available for cooling remained the same or increased lightly. It is therefore crucial that the cooling solution has to be optimized in anyway possible. One of the main parameter can be optimized is the heat spreading resistance in the base of the heat sink. The die size is significant small compare to the size of the base of the heat sink. Therefore a large temperature gradients existed from the die to the surrounding areas. To minimize the heat spreading resistance in the base of the heat sink, flat heat pipe or vapor chamber is used to isothermalize the base. The basic requirements of the Vapor Chamber (VC) are that the thermal resistance less than 0.1 K/W, preferably as low as possible heat flux of 50 W/cm^2 and the thickness less than 5mm thick. The basic structure of the VC consisted of copper container, copper powder for wicks and working fluid is water. A VC should work at any orientation without capillary limitation. The paper described a fundamental tests of a filling ratio and thermal performance of VC by experiment. The VC is not ultimate solution for any design. Estimation also presented in this paper to provide design guideline whether VC is effective or not for any particular cooling solution.

In the final chapter a proposal of innovative and advanced cooling system for future research. It is called opened sir Brayton cooler. similar to refrigeration system. Also future research to make improvement on the heat pipe thermal performance. that is heat pipe has as high heat transfer, and as low thermal resistance as possible.

Acknowledgement

The author wishes to express sincere appreciation to Professor Hideaki Imura. supervised and provided guidance to my research and the completion of this paper and also acknowledge with Professor H. Ohba, Professor M. Sadatomi and Professor Y. Ohno at Kumamoto University.

Also acknowledgement is expressed to all of my colleagues at Fujikura Ltd., particularly Mr. R. Okiai. Dr. M. Takaoka, Dr. S. Yoshida. Dr. N. Shiseki. Mr. K. Mashiko, Dr. Y. Saito. Dr. Thang Nguyen. Dr. I. Sauciuc. Mr. Tien Nguyen and Mr.V. Wuttijumnong. They provided many helps with sample, test data, and great suggestion. Professor A. Akbarzadeh at RMIT University in Australia gave me essential suggestions.